Algebraic & Geometric Topology 17 (2017) 1445–1525

Heegaard Floer homology of spatial graphs

SHELLY HARVEY
DANIELLE O'DONNOL

We extend the theory of combinatorial link Floer homology to a class of oriented spatial graphs called transverse spatial graphs. To do this, we define the notion of a grid diagram representing a transverse spatial graph, which we call a graph grid diagram. We prove that two graph grid diagrams representing the same transverse spatial graph are related by a sequence of graph grid moves, generalizing the work of Cromwell for links. For a graph grid diagram representing a transverse spatial graph $f\colon G \to S^3$, we define a relatively bigraded chain complex (which is a module over a multivariable polynomial ring) and show that its homology is preserved under the graph grid moves; hence it is an invariant of the transverse spatial graph. In fact, we define both a minus and hat version. Taking the graded Euler characteristic of the homology of the hat version gives an Alexander type polynomial for the transverse spatial graph. Specifically, for each transverse spatial graph f, we define a balanced sutured manifold $(S^3 \setminus f(G), \gamma(f))$. We show that the graded Euler characteristic is the same as the torsion of $(S^3 \setminus f(G), \gamma(f))$ defined by S Friedl, A Juhász, and J Rasmussen.

57M15; 05C10

In memory of Tim Cochran

1 Introduction

Knot Floer homology, introduced by P Ozsváth and Z Szabó [18], and independently by J Rasmussen [20], is an invariant of knots in S^3 that categorifies the Alexander polynomial. Knot Floer homology is widely studied because of its many applications in low-dimensional topology. For example, it detects the unknot (Ozsváth and Szabó [17]), whether a knot is fibered (P Ghiggini [5] and Y Ni [15]) and the genus of a knot [17]. The theory was generalized to links by Ozsváth and Szabó [19]. The primary goal of this paper is to extend link Floer homology to a class of oriented spatial graphs in S^3, called transverse spatial graphs.

Originally, knot Floer homology was defined as the homology of a chain complex obtained by counting certain holomorphic disks in a $2g$–dimensional symplectic manifold

Published: 17 July 2017 DOI: 10.2140/agt.2017.17.1445

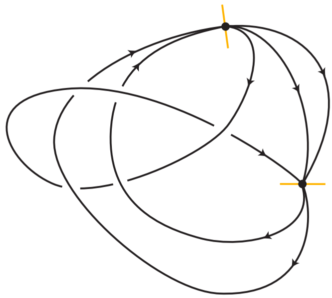

Figure 1: Example of a diagram of a transverse spatial graph; the lines at each vertex indicate the grouping of the incoming and outgoing edges.

with some boundary conditions that arose from a (doubly pointed) Heegaard diagram for S^3 compatible with the knot. As such, the chain *groups* were combinatorial but one could not, a priori, compute the boundary map. However, Sucharit Sarkar discovered a criterion that would ensure that the count of said holomorphic disks is combinatorial. This crucial idea was used by C Manolescu, P Ozsváth and S Sarkar [11] to give a combinatorial description of link Floer homology using grid diagrams. Using this description, C Manolescu, P Ozsváth, Z Szabó and D Thurston [12] gave a combinatorial proof that link Floer homology is an invariant. In this paper, we generalize the combinatorial description of Heegaard Floer homology and proof in [11; 12] to transverse spatial graphs. Specifically, we define a relatively bigraded chain complex (a combinatorial minus version) which is a module over $\mathbb{F}[U_1, \dots, U_V]$, where V is the number of vertices of the transverse spatial graph and $\mathbb{F} = \mathbb{Z}/2\mathbb{Z}$ is the field with two elements. We then show that it is well defined up to quasi-isomorphism. We note that, independently, Y Bao [1] defined a (noncombinatorial version of) Heegaard Floer homology for balanced bipartite spatial graphs with a balanced orientation; see Section 6 for the relationship to our theory.

Informally, a transverse spatial graph is an oriented spatial graph where the incoming (respectively outgoing) edges are grouped at each vertex and any ambient isotopy must preserve this grouping. See Figure 1 for an example. Details can be found in Section 2. To define the chain complex, we first introduce the notion of a graph grid diagram representing a transverse spatial graph in Section 3. Roughly, a graph grid diagram is an $n \times n$ grid of squares each of which is decorated with an X, an O (sometimes decorated with $*$) or is empty, and satisfies the following conditions. Like for links, there is precisely one O per row and column. There are no restrictions on the X's but if an O shares a row or column with multiple (or no) X's then it must be decorated with $*$. Moreover, each *connected component* must contain an O decorated with $*$. See Section 3.1 for a precise definition and Figure 2 for an example.

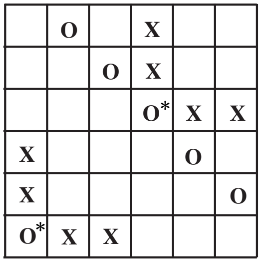

Figure 2: Example of a graph grid diagram

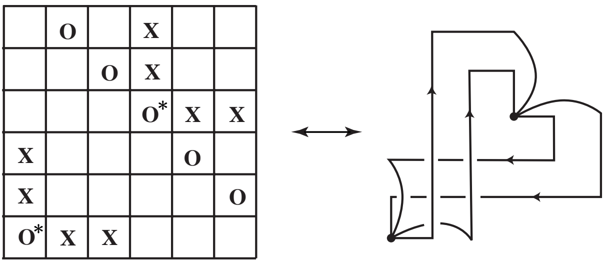

Figure 3: Associating a transverse spatial graph to a graph grid diagram

To each graph grid diagram we associate a transverse spatial graph by connecting the X's to the O's vertically and the O's to the X's horizontally with the convention that the vertical strands go over the horizontal strands. See Section 3.2 for more details and Figure 3 for an example.

We prove that every transverse spatial graph can be represented by a graph grid diagram.

Proposition 3.3 *Let $f\colon G \to S^3$ be a transverse spatial graph. Then there is a graph grid diagram g representing f.*

However, this representative is not unique. We define a set of moves on graph grid diagrams (cyclic permutation, commutation$'$, and stabilization$'$), called graph grid moves, generalizing the grid moves for links. See Section 3.2 for their definitions. We prove that any two representatives for the same transverse spatial graph are related by a sequence of graph grid moves.

Theorem 3.6 *If g and g' are two graph grid diagrams representing the same transverse spatial graph, then g and g' are related by a finite sequence of graph grid moves.*

In Section 4, to each (saturated) graph grid diagram g, we assign a chain complex $(C^-(g), \partial^-)$. Saturated means that there is at least one X per row and column, and these graph grid diagrams correspond to transverse spatial graphs where the underlying graphs have neither sinks nor sources. We need this technical condition to show that $\partial^- \circ \partial^- = 0$. The chain group consists of bigraded free $\mathbb{F}[U_1, \dots, U_V]$–modules, where V is the number of O's decorated with $*$. Like in link Floer homology, the generators of the chain groups are unordered tuples of intersection points between the horizontal and vertical line segments in the grid, with exactly one point on each horizontal and vertical line segment. The Maslov grading is defined exactly as in [12]. Note that this is possible since it only depends on the set of O's on the grid. For links, the Alexander grading lives in $\mathbb{Z}^m$. For transverse spatial graphs, we define an Alexander grading that has values in $H_1(S^3 \setminus f(G))$, where $f\colon G \to S^3$ is the transverse spatial graph associated to g. To compute this, for each point in the lattice of the grid, we define an element of $H_1(S^3 \setminus f(G))$, called the generalized winding number. It is defined so that if you can get from one point to another by passing an edge of the projection of $f(G)$ coming from g, then the difference between their values is (plus or minus) the homology class of the meridian of that edge. The Alexander grading of a generator is obtained by taking the sum of the generalized winding numbers of the points of the generator. Each U_i is associated with an O, and we define the Alexander grading so that multiplication by U_i corresponds to lowering the Alexander grading by the element of $H_1(S^3 \setminus f(G))$ represented by the meridian of the O. See Section 4.3 for more details. The ∂^- map is defined by counting empty rectangles in the (toroidal) grid that do not contain X's. We show in Section 4 that $\partial^- \circ \partial^- = 0$ and so the homology of $(C^-(g), \partial^-)$ gives a well-defined invariant for each saturated graph grid diagram.

For a given transverse spatial graph, there are infinitely many graph grid diagrams representing it. In Section 5, we show that the homology of the bigraded chain complex is independent of the choice of saturated graph grid diagram. To prove this, we show that the quasi-isomorphism type of the chain complex is preserved under the three graph grid moves.

Theorem 4.22 *If g_1 and g_2 are saturated graph grid diagrams representing the same transverse spatial graph $f\colon G \to S^3$ then $(C^-(g_1), \partial^-)$ is quasi-isomorphic to $(C^-(g_2), \partial^-)$ as relatively absolutely $(H_1(E(f)), \mathbb{Z})$–bigraded $\mathbb{F}[U_1, \dots, U_V]$–modules. In particular, $\mathrm{HFG}^-(g_1)$ is isomorphic to $\mathrm{HFG}^-(g_2)$ as relatively absolutely $(H_1(E(f)), \mathbb{Z})$–bigraded $\mathbb{F}[U_1, \dots, U_V]$–modules.*

Thus, we can define the *graph Floer homology* of the sinkless and sourceless transverse spatial graph f, denoted $\mathrm{HFG}^-(f)$, to be $\mathrm{HFG}^-(g)$ for any saturated grid diagram g representing f. We also define a hat variant, $\widehat{\mathrm{HFG}}(f)$ by taking the homology of the chain complex obtained by setting $U_1, \dots, U_V$ to zero. See Sections 4.2–4.4 for more details.

As far as the authors are aware, there have been no papers in the past that have defined an Alexander polynomial for an arbitrary spatial graph that do not just depend on the fundamental group of the exterior. Kinoshita [9] defines the Alexander polynomial of an oriented spatial graph as the Alexander polynomial of its exterior. In contrast, Litherland [10] defined the Alexander polynomial of a spatial graph where the underlying graph is a theta graph and his definition does not depend solely on the exterior of the embedding. At the same time as this paper was being written, Bao [1] independently defined an Alexander polynomial of a balanced bipartite spatial graphs with a balanced orientation and produces a state sum formula for the polynomial. Bao's invariant is essentially the same as ours; see Section 6 for more details.

In Section 6, we define an Alexander polynomial for any transverse spatial graph $f\colon G \to S^3$. To do this, we associate a balanced sutured manifold $(S^3 \setminus f(G), \gamma(f))$ to f. We then define the Alexander polynomial of f, $\Delta_f \in \mathbb{Z}[H_1(S^3 \setminus f(G))]$, to be the torsion invariant associated to balanced sutured manifold $(S^3 \setminus f(G), \gamma(f))$ defined by S Friedl, A Juhász, and J Rasmussen [4]. We show that the graded Euler characteristic of $\widehat{\mathrm{HFG}}(f)$ is essentially Δ_f. Note that $\bar{\Delta}_f$ is the image of Δ_f under the mapping that sends each element of $H_1(S^3 \setminus f(G))$ to its inverse.

Corollary 6.8 *If $f\colon G \to S^3$ is a sinkless and sourceless transverse spatial graph where G has no cut edges, then*

$$\chi(\widehat{\mathrm{HFG}}(f)) \doteq \bar{\Delta}_f.$$

That is, they are the same up to multiplication by units in $\mathbb{Z}[H_1(S^3 \setminus f(G))]$.

To prove this, we first prove the stronger result that the hat version of our graph Floer homology is essentially the same as the sutured Floer homology of $(S^3 \setminus f(G), \gamma(f))$. We say $\mathrm{rSHF}(E(f), \gamma(f))$ to mean $\mathrm{SFH}(E(f), \gamma(f))$ considered as a bigraded $(H_1(E(f)), \mathbb{Z}_2)$–module but with the $H_1(S^3 \setminus f(G))$ Alexander grading changed by a negative sign.

Theorem 6.6 *Let $f\colon G \to S^3$ be a sinkless and sourceless transverse spatial graph where G has no cut edges. Then*

$$\widehat{\mathrm{HFG}}(f) \cong \mathrm{rSHF}(E(f), \gamma(f))$$

as relatively $(H_1(E(f)), \mathbb{Z}_2)$–bigraded $\mathbb{F}$–vector spaces.

To complete the proof of Corollary 6.8, we use the theorem of S Friedl, A Juhász and J Rasmussen stating that the decategorification of sutured Floer homology is their torsion invariant [4].

Acknowledgements We would like to thank Sucharit Sarkar, András Juhász, Eamonn Tweedy, Tim Cochran, Katherine Vance, Adam Levine, Ciprian Manolescu, Matt Hedden, Robert Lipshitz, and Dylan Thurston for helpful conversations. We would also like to thank the referee for helpful comments.

Harvey was partially supported by National Science Foundation grants DMS-0748458 and DMS-1309070 and by grant #304538 from the Simons Foundation. O'Donnol was partially supported by National Science Foundation grants DMS-1406481 and DMS-1600365 and by an AMS-Simons travel grant.

2 Transverse disk spatial graphs

Graph Floer homology is a version of Heegaard Floer homology defined for transverse spatial graphs. In this section we will define the term *transverse spatial graph* and the notion of equivalence of transverse spatial graphs. We will also discuss their diagrams and Reidemeister moves.

We will work in the PL category. A *graph* Y is a 1–dimensional complex, consisting of a finite set of vertices (0–simplices) and edges (1–simplices) between them. A *spatial graph* $f\colon Y \to S^3$ is an embedding of a graph Y in S^3. A *diagram* of a spatial graph is a projection of $f(Y)$ to S^2 with only transverse double points away from vertices, where the over and under crossings are indicated. Two spatial graphs f_1 and f_2 are *equivalent* if there is an ambient isotopy between them. Notice that the ambient isotopy gives a map $h\colon S^3 \to S^3$ which sends $f_1(Y)$ to $f_2(Y)$ sending edges to edges and vertices to vertices.

Theorem 2.1 (Kauffman [8]) *Let f_1 and f_2 be spatial graphs. Then f_1 is ambient isotopic to f_2 if and only if any diagram of f_2 can be obtained from any diagram of f_1 by a finite number of graph Reidemeister moves (shown in Figure 4) and planar isotopy.*

An *oriented graph* is a graph together with orientations given on each of the edges. Let $\mathcal{D}$ be the 2–complex obtained by gluing three copies of the 2–simplex $[e_0, e_1, e_2]$ together so that their union is a disk and with all three of the e_0's identified to a single point in the interior of $\mathcal{D}$. Note that e_0 is the unique vertex in the interior of $\mathcal{D}$. We say that $\mathcal{D}$ is a *standard disk* and e_0 is the *vertex associated to* $\mathcal{D}$. An *oriented disk graph* G is a 2–complex constructed as follows. Start with an oriented graph Y. Then, for each vertex v of Y, glue a standard disk $\mathcal{D}$ to Y by identifying the vertex associated to $\mathcal{D}$ with v. We note that Y is a subset of the oriented disk graph, which we call the *underlying oriented graph* of the oriented disk graph (or the *underlying graph* of G if we do not want to consider the orientations). We say that a vertex of an oriented disk

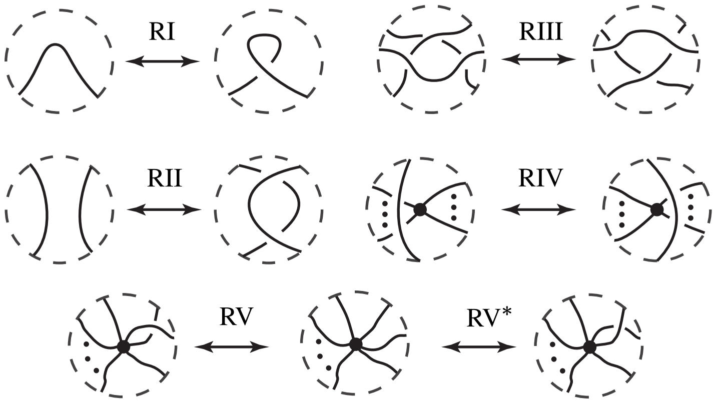

Figure 4: The graph Reidemeister moves. Reidemeister moves RI, RII, and RIII are the same as those for knots and links. Reidemeister move RIV moves an edge past a vertex, either over or under (over is pictured here). Reidemeister move RV swaps two of the edges next to the vertex.

graph is a *graph vertex* (respectively *graph edge*) if it is a vertex (respectively edge) of its underlying oriented graph. When it is clear, we will just refer to them as vertices and edges of the oriented disk graph (and will not refer to the other 0 and 1–simplices of the oriented disk graph as vertices or edges). For an oriented disk graph G and a given graph vertex v of G, the set of graph edges of G with orientation going towards v are called the *incoming edges* of v and the set of edges with the orientation going away from v are called the *outgoing edges* of v.

Definition 2.2 A *transverse spatial graph* is an embedding $f\colon G \to S^3$ of an oriented disk graph G into S^3 where each vertex of the graph locally looks like Figure 5, each standard disk of G lies in a plane, and locally the disk separates the incoming and outgoing edges of the given vertex. We call the image of each of the standard disks of G a *disk* of f, and the embedding of the underlying graph of G the *underlying spatial graph* of f. Two transverse spatial graphs are *equivalent* if there is an ambient isotopy between them.

Note that in a transverse spatial graph the incoming and outgoing edges are each grouped together. In the ambient isotopy, at each vertex, both the set of incoming and the set of outgoing edges can move freely. However, in an ambient isotopy, the incoming and outgoing sets cannot intermingle, because the disk separates the edges.

Definition 2.3 A *regular projection* of a transverse spatial graph $f\colon G \to S^3$ is a projection that satisfies the following two conditions: (1) For each point p in the

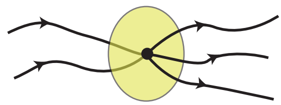

Figure 5: A vertex of a transverse spatial graph shown with the disk

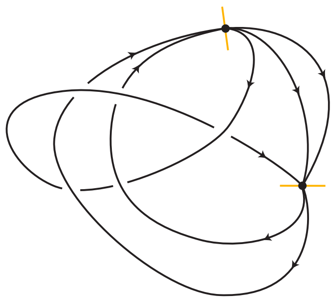

Figure 6: A diagram of a transverse spatial graph; the projections of the disks, transverse to the plane of projection, are indicated by the straight yellow line segments.

image of the underlying graph of G, $f^{-1}(p)$ contains no more than two points and if $f^{-1}(p)$ contains two points then neither is a graph vertex. (2) All of the standard disks of f are perpendicular to the plane of projection. A *diagram* for a transverse spatial graph $f\colon G \to S^3$ is a regular projection of f where all the over and under crossings are indicated.

In Figure 6, a diagram of a transverse spatial graph is shown, where the disks are also shown in the projection. Notice that the incoming edges and outgoing edges are grouped in the projection. We will from here forward not indicate disks in diagrams, because the position of the disk is already clear from the diagram.

The Reidemeister moves for transverse spatial graphs are the same as the Reidemeister moves for graphs shown in Figure 4, with the restriction that RV may *only* be made between pairs of incoming edges or pairs of outgoing edges. For clarity, we will say $\mathrm{R}\overline{\mathrm{V}}$ for this restriction of RV.

Theorem 2.4 *Every transverse spatial graph has a diagram. If two transverse spatial graphs are ambient isotopic, then any two diagrams of them are related by a finite sequence of the Reidemeister moves* RI–RIV, $\mathrm{R}\overline{\mathrm{V}}$ *and planar isotopy.*

Proof We first show that every transverse spatial graph has a diagram. Let $f\colon G \to S^3$ be a transverse spatial graph. A regular projection for the transverse spatial graph is a

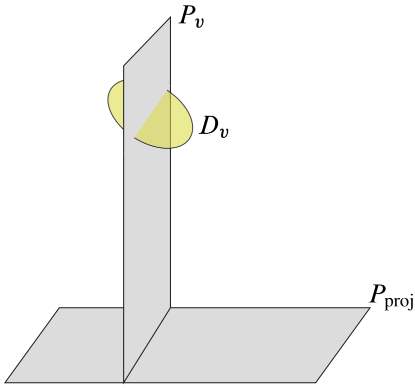

Figure 7: The plane of projection P_{proj} together with a disk D_v of the vertex v and P_v; the plane P_v is the plane perpendicular to P_{proj} meeting D_v in the line parallel to P_{proj}.

projection of $f(G)$ which is a regular projection of the underlying spatial graph of f. That is, the projection only has transverse double points and these are away from the vertices. We will first obtain a regular projection for the transverse spatial graph, and next find a representative in the ambient isotopy class where the disks are transverse to P_{proj}, where P_{proj} denotes the plane of projection for the regular projection. A regular projection for a spatial graph is obtained in the usual way: a point projection of a representative of the ambient isotopy class is obtained via ϵ–perturbations of the graph. To have the disks perpendicular to P_{proj}, a similar process is used. If the disk is transverse to P_{proj}, we will see that there is a unique way to move it via an ambient isotopy of f to a position where it is perpendicular to P_{proj}. So we need only have all of the disks transverse to P_{proj}. For an arbitrary vertex v with disk D_v, let $\mathbf{x}$ be the vector that is perpendicular to D and pointing in the direction of the outgoing edges. If v remains in the same place and the neighborhood around it is allowed to rotate, there is a full sphere of directions in which $\mathbf{x}$ can be pointing. Only two of these directions will result in D_v being parallel to P_{proj}. By dimensionality arguments having the disks transverse to P_{proj} is generic. If any of the disks are not transverse, an ϵ–perturbation is done. For each vertex v, let P_v be the plane that is perpendicular to P_{proj} and meets D_v in the line through v and parallel to P_{proj}. For each disk transverse to P_{proj} there is a unique map via rotation through the acute angle between D_v and P_v, moving D_v into the plane P_v, so that it is perpendicular to P_{proj}; see Figure 7.

For (topological) spatial graphs, any ambient isotopy is made up of elementary moves. Recall that an elementary move of a spatial graph replaces a linear segment of an edge $[e_i, e_j]$ by two new linear segments $[e_i, e_k]$ and $[e_k, e_j]$ that, together with $[e_i, e_j]$, bound a 2–simplex which intersects the original spatial graph only in $[e_i, e_j]$, or is

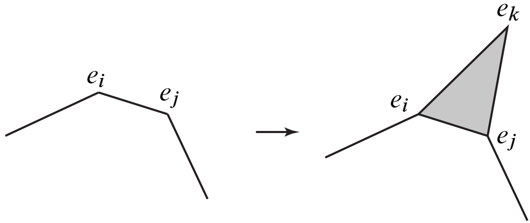

Figure 8: An elementary move

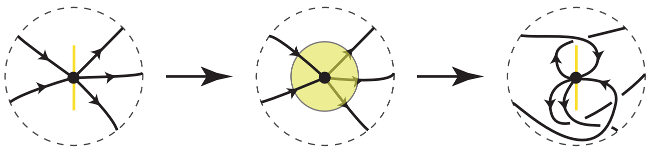

Figure 9: An example of what can happen when a disk flips over, moving through a position parallel to P_{proj}

the reverse of this move; see Figure 8. Kauffman [8] showed that any elementary move for a spatial graph can be obtained by a sequence of the Reidemeister moves shown in Figure 4. Now we consider transverse spatial graphs. An elementary move of a transverse spatial graph $f\colon G \to S^3$ replaces a linear segment of an edge of the underlying graph $[e_i, e_j]$ by two new linear segments $[e_i, e_k]$ and $[e_k, e_j]$ that, together with $[e_i, e_j]$, bound a 2–simplex T which intersects $f(G)$ in $[e_i, e_j]$, or is the reverse of this move; see Figure 8. We note that T must miss all the transverse disks. We will show that any ambient isotopy of transverse spatial graphs is made of elementary moves of a transverse spatial graph. First note that Reidemeister moves RI–RIV preserve the isotopy class of a transverse spatial graph. In addition, one can still interchange a pair of neighboring incoming edges or a pair of neighboring outgoing edges in RV. However, if one tried to interchange an incoming with a neighboring outgoing edge at the vertex v, the disk from the elementary move that would result in RV would intersect the transverse disk D_v. So Reidemeister move RV is restricted to R$\overline{\text{V}}$. Recall that R$\overline{\text{V}}$ is the move RV where only neighboring incoming (respectively outgoing) edges are interchanged.

We claim that one needs only Reidemeister moves RI–RIV and R$\overline{\text{V}}$ to get all ambient isotopies. One might be concerned that this is incomplete because of the danger of a vertex flipping over (ie moving through a position where the disk is parallel to the plane of projection) resulting in a change in the diagram like that shown in Figure 9. However, this move and any move like it can be obtained with the set of Reidemeister moves RI–RIV, and R$\overline{\text{V}}$. To discuss this we will introduce another type of graph. A *flat vertex graph* or *rigid vertex graph* is a spatial graph where the vertices are flat disks or polygons with edges attached along the boundary of the vertex at fixed places. The set of Reidemeister moves for flat vertex graphs is RI–RIV as before, and the move RV* [8]. Reidemeister

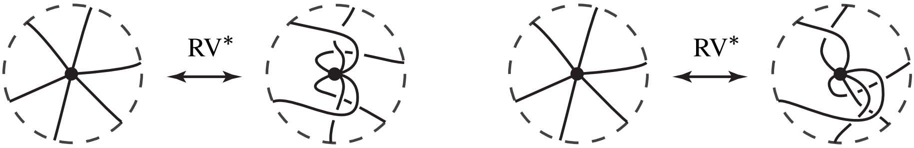

Figure 10: Two different RV* moves for flat vertex graphs

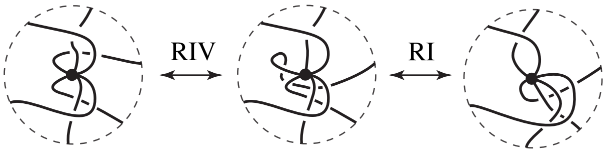

Figure 11: How to move between the two different RV* moves shown in Figure 10; thus only one RV* move is needed for each valence of vertices

Figure 12: This shows how many R$\overline{\text{V}}$ moves will give a RV* move

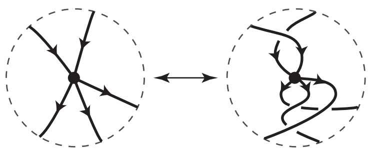

Figure 13: The RV* move that is a result of many R$\overline{\text{V}}$ moves

move RV* is the flipping over of a flat vertex by 180°; see Figure 10. For the move RV* a choice is made of how many edges are on each side when the vertex is flipped, but only one of these moves is need together with Reidemeister moves RI–RIV to do any of the other ones [8]; see Figure 11. In the case of transverse spatial graphs repeated use of R$\overline{\text{V}}$ will result in what looks like a RV* move, shown in Figures 12 and 13. Thus flipping the vertex over can be accomplished by Reidemeister moves RI–RIV and R$\overline{\text{V}}$. □

3 Graph grid diagrams

In this section, we define the notion of graph grid diagrams and explain their relationship to transverse spatial graphs. To each graph grid diagram we associate a unique transverse spatial graph. On the other hand, we show that every transverse spatial graph can be represented by a nonunique graph grid diagram. As with grid diagrams for knots and links, we define a set of moves on graph grid diagrams (cyclic permutation, commutation$'$, and stabilization$'$) that we call graph grid moves. Finally, we prove that any two graph grid diagrams representing the same transverse spatial graph are related by a sequence of graph grid moves.

3.1 Graph grid diagrams

We will assume that the reader is familiar with grid diagrams for knots and links; see [11; 12]. Recall that a (planar) grid diagram for a link is an $n \times n$ grid of squares in the plane where each square is decorated with an X, an O or nothing, and such that every row (respectively column) contains exactly one X and exactly one O. Here we are using the notation of [12]. To each grid diagram, one can associate a planar link diagram by drawing horizontal line segments from the O's to the X's in each row, and vertical line segments from the X's to the O's in each column with the convention at the crossings that a vertical segment always goes over a horizontal segment. We will define a more general class of grid diagrams that will represent transverse spatial graphs. Before defining a grid diagram we need a technical definition.

Definition 3.1 Suppose D is an n by n grid where each square is decorated with an X, an O or is empty. We let $\mathbb{X}$ be the set of X's and $\mathbb{O}$ be the set of O's. We say that two elements $p, q \in \mathbb{X} \cup \mathbb{O}$ are *related* if p and q share a row or column. Let $\sim$ be the equivalence relation generated by this relation. We define the *connected components* of D to be the equivalence classes of $\sim$.

Definition 3.2 A *graph grid diagram* g is an n by n grid where each square is decorated with an X, O or is empty, a subset of the O's are decorated with $*$, and that satisfies the following conditions. There is exactly one O in each row and column. Each connected component contains at least one O decorated with $*$. If a row or column does not contain exactly one X then the O in that row or column must be decorated with $*$. The total number of rows (equivalently columns) n is called the *grid number* of g. The O's decorated with $*$ are called *vertex* O*'s*, the number of which will be denoted V. We will say that an O is *standard* if the O has exactly one X in its row and exactly one X in its column; otherwise we say it is *nonstandard*. Often, it will be convenient to number the O's and X's by $\{\mathrm{O}_i\}_{i=1}^n$ and $\{\mathrm{X}_i\}_{i=1}^m$. When numbering, we always assume that $\mathrm{O}_1, \dots, \mathrm{O}_V$ correspond to the vertex O's.

For convenience, we may sometimes omit the $*$ from a figure when it is clear which O's should have $*$, ie the nonstandard ones. It will also be convenient to think of the grid as the set $[0, n] \times [0, n]$ in the plane, with vertical and horizontal grid lines of the form

$\{i\}\times[0,n]$ and $[0,n]\times\{i\}$, where i is an integer from 0 to n, and the X's and O's are at half-integer coordinates.

As in [11; 12], our chain complex is obtained from a graph grid diagram, with the main difference being the definition of the Alexander grading. To define this, it is sometimes necessary to consider toroidal graph grid diagrams instead of (planar) graph grid diagrams. A *toroidal graph grid diagram* is a graph grid diagram that is considered as being on a torus by identifying the top and bottom edges of the grid and identifying the left and right edges of the grid. We denote the toroidal graph grid diagram by $\mathcal{T}$. We view the torus as being oriented and the orientation being inherited from the plane. When the context is clear, we will just call it a graph grid diagram. In a toroidal graph grid diagram, the horizontal and vertical grid lines, become circles. We denote the horizontal circles by $\alpha_1,\dots,\alpha_n$, the vertical circles $\beta_1,\dots,\beta_n$ and we let $\boldsymbol{\alpha}=\{\alpha_1,\dots,\alpha_n\}$ and $\boldsymbol{\beta}=\{\beta_1,\dots,\beta_n\}$. When the grid is drawn on a plane, by convention, we will order the horizontal (respectively vertical) circles from bottom to top (respectively left to right) so that the leftmost circle is β_1 and the bottommost circle is α_1. Note that to get a (planar) diagram from a toroidal diagram, one takes a *fundamental domain* for the torus and cuts along a horizontal and vertical grid circle and identifies it with $[0,n)\times[0,n)$.

3.2 Graph grid diagram to transverse spatial graphs and their diagrams

Let g be a graph grid diagram. We can associate a transverse spatial f to g as follows. First put a vertex at each of the O's that are decorated with $*$. Let O_i be an O in g lying in row r_i and column c_i. For each X_j in row r_i, connect O_i to X_j with an arc inside of the row (oriented from O_i to X_j) so that it is disjoint from all the X's and O's and so that all the arcs in row r_i are disjoint from one another. We will call these horizontal arcs. Now push the interior of the arcs in row r_i slightly upwards, above the plane. For each X_j in column c_i, connect X_j to O_i with an arc inside of the column (oriented from X_j to O_i) so that it is disjoint from all the X's and O's and so that all the arcs in row c_i are disjoint from one another. We will call these vertical arcs. Now push the interior of the arcs in column c_i slightly downward, below the plane. Put a disk in the squares containing O's decorated with $*$ and the vertex at the disks center. In this case we say that the graph grid diagram g *represents* the spatial graph f. Any choice of arcs gives the same transverse spatial graph.

Note that the aforementioned procedure will actually give us a (nonunique) projection of the transverse spatial graph. However, this will not be a diagram of f since the transverse disks will be parallel to the plane of projection. It will be convenient for us to define a class of grid diagrams that give a well-defined diagram of a transverse spatial graph when following this procedure.

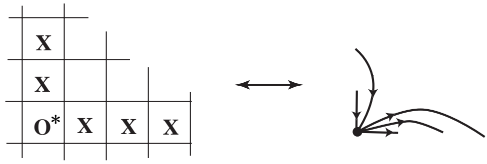

Figure 14: A graph grid diagram of a nonstandard O with the flock in L–formation (left), and the diagram of the associated vertex for this portion of the graph grid diagram, showing the order in which the edges appear around the vertex (right)

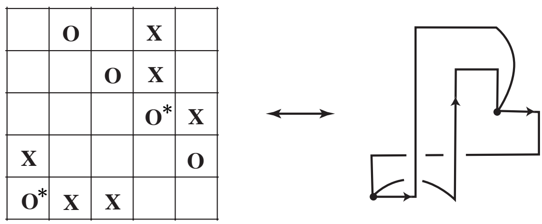

Figure 15: A preferred grid diagram (left), and the diagram of the transverse spatial graph associated with this graph grid diagram (right)

Consider a graph grid diagram. For a nonstandard O, let the set of X's that appear in a row or column with this O be called its *flock*. If the X's in the flock of an O are all adjacent to the O or adjacent to other X's that are adjacent to the O, then the flock is said to be *clustered*. A flock is in *L–formation*, if the X's are all to the right and above the O. It should be noted that the choice of having the X's above and to the right of the O is arbitrary; any pair of below and to the right, above and to the left, or below and to the left will work similarly. A *preferred* graph grid diagram is a graph grid diagram where all nonstandard O's (with more than one X in it's flock) have their flocks in L–formation.

Now suppose that g is a preferred graph grid diagram. We follow the procedure in the first paragraph of this section except that now we put the transverse disks perpendicular to the plane so that they divide the horizontal and vertical arcs. Moreover, to get a unique diagram D, the ordering of the edges around the vertex for nonstandard O's is given by the convention illustrated in Figure 14. In this case we say that the *graph grid diagram g represents the diagram of the transverse spatial graph*, D. We note that the transverse spatial graph associated to this diagram is equivalent to the transverse spatial graph obtained by following the procedure in the first paragraph of this section.

3.3 Graph embedding to preferred graph grid diagram

We have shown that to each graph grid diagram, we can associate a transverse spatial graph. We now show that for each transverse spatial graph, there is a (preferred) graph grid diagram representing it.

Proposition 3.3 *Let $f\colon G \to S^3$ be a transverse spatial graph. Then there is a preferred graph grid diagram g representing f. Moreover, for each diagram of a transverse spatial graph, D, there is a preferred graph grid diagram g representing D.*

Proof Choose a diagram D of the transverse spatial graph f. We construct a graph grid diagram g, representing D, by the following procedure. At the vertices, the edges are partitioned into two sets: incoming edges and outgoing edges, as D is a diagram of a transverse spatial graph. Move the edges around each vertex (and perhaps the disk) by planar isotopy so that all outgoing edges are to the right of the vertex and all incoming edges are above the vertex, as shown in Figure 14. Away from vertices the process is the same as that for knots or links. The arcs of the edges are made "square". All crossings are made so that the horizontal arc goes under the vertical arc; see Figure 16. Then the diagram is moved via a planar isotopy so that no vertical arcs or vertices with their incoming edge arcs are in the same vertical line, and similarly for horizontal arcs and vertices with their outgoing edge arcs. A vertex along with its incoming edge arcs are associated with a single column, and the vertex together with its outgoing edge arcs are associated with a single row; see Figure 14. Each of the vertical and horizontal arcs are also associated with a column and row of the grid, respectively. This will result in an equal number of rows and columns. Each vertex will add a row and a column. Each vertical arc that is not next to a vertex will add a column. Each vertical arc can be paired with the following horizontal arc that is not next to a vertex, which will add a row. A graph grid representation is then given by placing X's and O's on the n by n grid. At each vertex a single O^* is placed, then an X is placed in the same row at the corner of each of the outgoing edges and an X is placed in the same column at the corner for each of the incoming edge, this is done as shown in Figure 14. Next X's and O's are placed along the edges at the corners consistent with the orientation: arcs go from X's to O's in columns and from O's to X's in rows. □

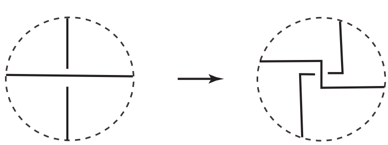

Figure 16: How to change a horizontal over-crossing to a vertical over-crossing without changing the embedded graph

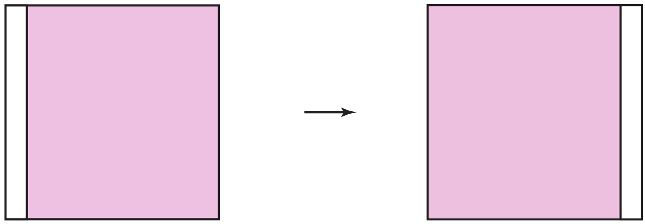

Figure 17: An example of cyclic permutation of columns

3.4 Grid moves

Following Cromwell [2] and Dynnikov [3], any two grid diagrams of the same link are related by a finite sequence of grid moves:

Cyclic permutation The rows and columns can be cyclically permuted; see Figure 17.

Commutation Pairs of adjacent columns (respectively rows) may be exchanged when the following conditions are satisfied. For columns, the four X's and O's in the adjacent columns must lie in distinct rows, and the vertical line segments connecting O and X in each column must be either disjoint or nested (one contained in the other) when projected to a single vertical line. There is an obvious analogous condition for rows; see Figure 18.

Stabilization/destabilization Let g be an $(n-1)\times(n-1)$ graph grid diagram with decorations $\{\mathrm{O}_i\}_{i=1}^{n-1}$ and $\{\mathrm{X}_j\}_{j=1}^{n-1}$. Then $\bar{g}$, an $n\times n$ graph grid diagram, is a stabilization of g if it is obtained from g as follows. Suppose there is a row of g that contains O_i and X_j. In $\bar{g}$, we replace this one row with two new rows and add one new column. We place O_i into one of the new rows (and in the same column as before) and X_j into the other new row (and in the same column as before). We place decorations O_n and X_n into the new column so that O_n occupies the same row as X_j and X_n occupies the same row as O_i. See Figure 19 for an example. There is a similar move with the roles of columns and rows interchanged. A destabilization is the reverse of a stabilization.

For the graph grid moves there are two differences. We will replace the usual commutation with a slightly more general commutation$'$ to include exchanging neighboring columns which have entries in the same row (or rows with entries in the same columns) and to include exchanges of rows and columns that have more than a single X in them (or no X's). We will also restrict the stabilization/destabilization move to only occur along edges (which we explain below).

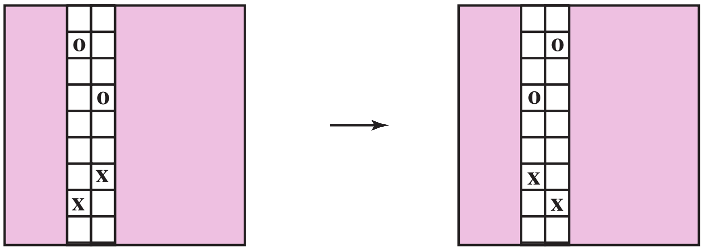

Figure 18: An example of commutation of columns

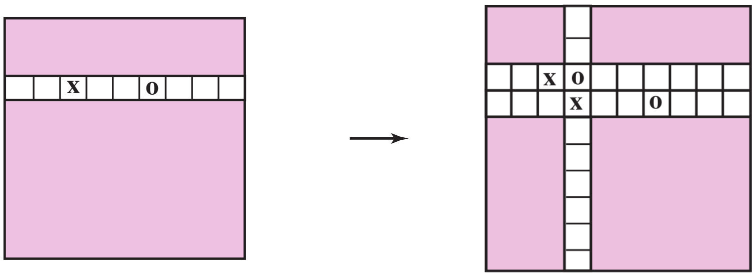

Figure 19: An example of stabilization

The graph grid moves

Cyclic permutation is unchanged.

Cyclic permutation The rows and columns can be cyclically permuted; see Figure 17.

Commutation will be replaced with the more general commutation$'$.

Commutation$'$ Pairs of adjacent columns may be exchanged when the following conditions are satisfied. There are vertical line segments LS_1 and LS_2 on the torus such that (1) $\mathrm{LS}_1 \cup \mathrm{LS}_2$ contain all the X's and O's in the two adjacent columns, (2) the projection of $\mathrm{LS}_1 \cup \mathrm{LS}_2$ to a single vertical circle β_i is β_i, and (3) the projection of their endpoints, $\partial(\mathrm{LS}_1) \cup \partial(\mathrm{LS}_2)$, to a single β_i is precisely two points. Here we are thinking of $\mathbb{X}$ and $\mathbb{O}$ as a collection of points in the grid with half-integer coordinates. There is an obvious analogous condition for rows; see Figure 20.

We define a generalization of stabilization, called stabilization$'$. This move will add a jog or a nugatory crossing to the edge of the projection of the associated transverse spatial graph.

Stabilization$'$/destabilization$'$ Let g be an $(n-1)\times(n-1)$ graph grid diagram with decorations $\{\mathrm{O}_i\}_{i=1}^{n-1}$ and $\{\mathrm{X}_j\}_{j=1}^{m-1}$. Then $\bar{g}$, an $n \times n$ graph grid diagram,

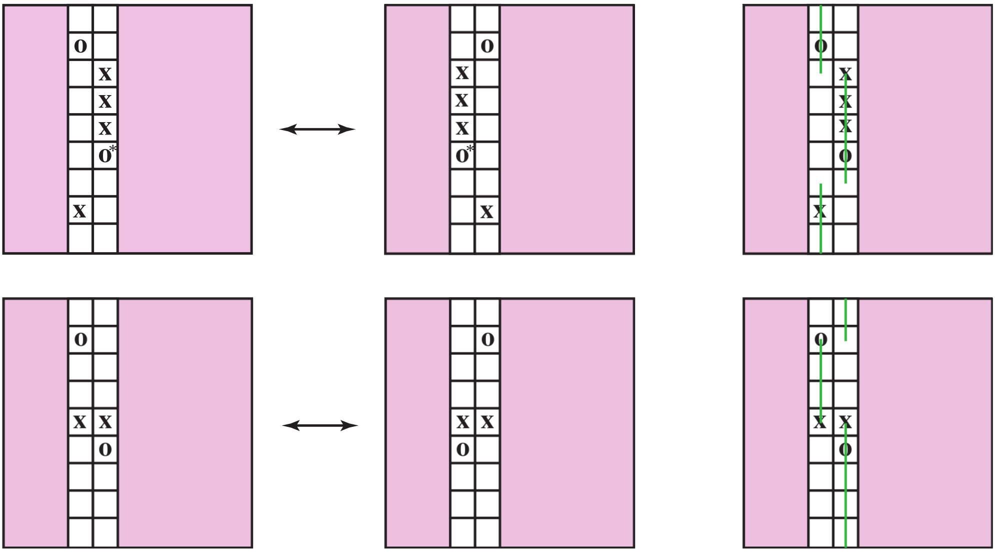

Figure 20: Two examples of commutation′ moves of columns

is a row stabilization′ of g if it is obtained from g as follows. Suppose there is a row of g that contains the decorations $\mathrm{O}_k, \mathrm{X}_{j_1}, \dots \mathrm{X}_{j_l}$ with $l \geq 1$. In $\bar{g}$, we replace this one row with two new rows and add one new column. We place $\mathrm{O}_k, \mathrm{X}_{j_2}, \dots, \mathrm{X}_{j_l}$ into one of the new rows (and in the same column as before) and X_{j_1} into the other new row (and in the same column as before). We place decorations O_n and X_m into the new column so that O_n occupies the same row as X_{j_1} and X_m occupies the same row as O_k. See Figure 21 for an example. A column stabilization′ is a row stabilization′ where one reverses the roles of rows and columns. We say that $\bar{g}$ is obtained from g by a *stabilization′* if it is obtained by a row or column stabilization′. A destabilization′ is the reverse of a stabilization′.

Note that O_n will not be associated to a vertex so will not be decorated with $*$. Also, if any O_i is decorated with $*$ (including O_k) in g then it will also be decorated with $*$ in $\bar{g}$. We do not allow stabilization′ of rows with no X's in them.

Remark 3.4 If $\bar{g}$ is obtained as row stabilization′ on the graph grid diagram g then one can use multiple commutation′ moves to change $\bar{g}$ into a row stabilization′ obtained from g, where $\mathrm{X}_{j_1}, \mathrm{X}_m, \mathrm{O}_n$ share a corner, X_{j_1} is directly to the left of O_n, and O_n is directly above X_m (as in Figure 21). Note that by using only commutation, like in [12], one can only assume that $\mathrm{X}_{j_1}, \mathrm{X}_m, \mathrm{O}_n$ share a corner, which leaves four cases instead of one. This will allow us to simplify the proof of stabilization′. There is a similar statement for column stabilization′.

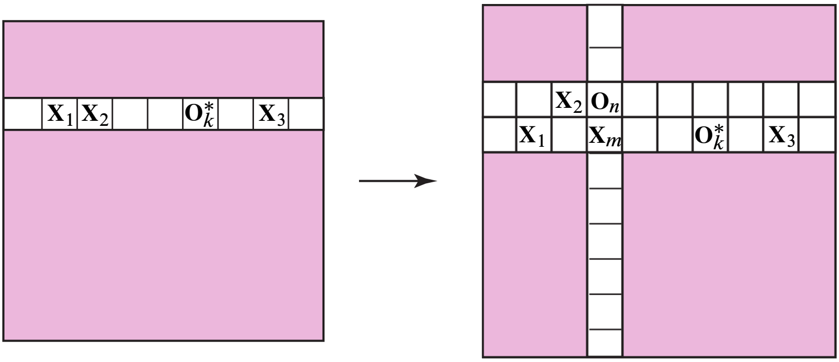

Figure 21: An example of stabilization′

3.5 The graph grid theorem

Before the main theorem of this section we need a lemma. To each diagram of a transverse spatial graph f there are an infinite number of different graph grid diagrams representing f that can be constructed using the procedure described in the proof of Proposition 3.3. This procedure produces a preferred grid diagram. However, doing a graph grid move on a preferred graph grid diagram will result in diagrams that are not necessarily in preferred form. Moreover, if one chooses a random graph grid diagram representing a transverse spatial, it will not necessarily be in preferred form. Indeed, in practice, one can often reduce the size of the grid number by moving it out of preferred form.

Lemma 3.5 *Every graph grid diagram g representing a transverse spatial graph f is related to a preferred graph grid diagram representing f by a finite sequence of graph grid moves.*

Proof Recall that a preferred grid diagram is one in which all of the nonstandard O's have their flocks in L–formation. Given a graph grid diagram, choose a nonstandard O that is not in L–formation. We will explain an algorithm to move this O into L–formation, but first we must separate this flock from any of the other flocks that are in L–formation. If there are any X's in the flock with this O that are also in a flock of another O that is in L–formation, then the other L–formation flock will need to be moved. If our nonstandard O of interest is in a column with an X that is in L–formation with another nonstandard O, we use the following procedure to move the flock out of the way. An example of this is shown in Figure 22. We do a row stabilization′ at said X; the new row is placed below the L–formation flock. Now the nonstandard O's no longer share an X, but if there were any X's to the right of the previously shared X,

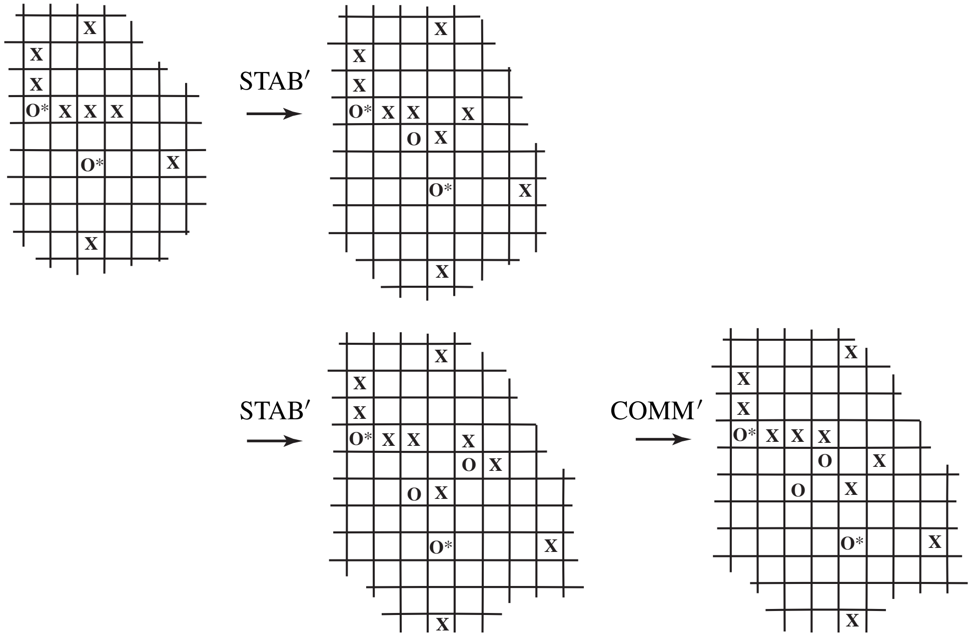

Figure 22: An example of the moves needed to separate the flocks of two O^* and move the upper most flock back into L–formation

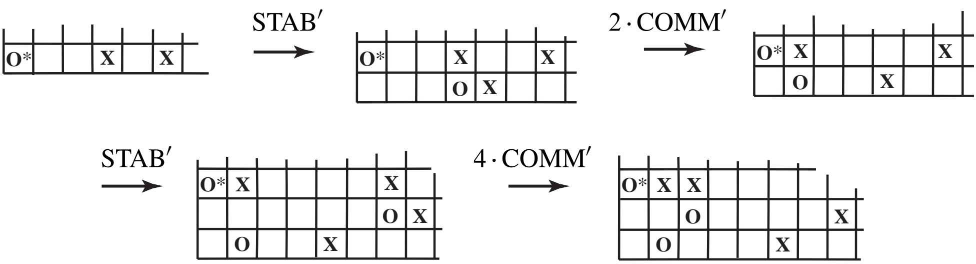

Figure 23: An example of the moves needed to move the X in the row into L–formation

the flock was split by the stabilization′ move and so it is no longer in L–formation. To move the flock back into L–formation a stabilization′ move is done at each of the X's to the right of the split (going from left to right), each time adding a row below the flock. After the stabilization′ moves are done, the columns containing an X in the flock can be moved by commutation′ moves to be next to the other X's in the flock. This is done with all of the X's, so the flock is in L–formation again. If the X shares a row with our O and a column with a different nonstandard O that is in L–formation, a similar procedure is done with the roles of the rows and columns switched.

Suppose there is no X in the flock that is already in L–formation with a different O. Use cyclic permutation to put the O at the lower left corner of the grid. Then, a row stabilization$'$ is done on the rightmost X that is in the row with the O, adding a row to the bottom of the diagram and adding an X and O next to each other in the new column. Commutation$'$ can be used to move the new column next to the nonstandard O, or next to X's that are next to the O; see Figure 23. This is repeated until all of the X's in the row are adjacent to the O. A similar process is done with the X's in the column of the O, bringing the O into L–formation. This process can be repeated until all of the O's are in L–formation.

This will increase the number of nonstandard O's in L–formation, because no other flock is moved out of L–formation. We continue until all flocks are in L–formation. □

For the following proof, we need a few more definitions. If an O^* is associated with a vertex v and is in L–formation, then all of the columns that contain an X in the flock are called *v–columns*, similarly those rows containing the flock are called *v–rows*. We will give a name to certain sequences of the graph grid moves, which will be called (column or row) *vertex stabilization* (and *destabilization*). A column (or row) *vertex stabilization* introduces a stabilization to the left of (or below) all of the X's in the column (or in the row) with a nonstandard O, as shown in Figure 24. The row vertex stabilization is a combination of a number of stabilization$'$s and commutation$'$s. For a nonstandard O, first a row stabilization$'$ is done, where the rightmost X is placed into the lower new row by itself, the new column is placed to the left and the new X and O are added. Next, the second from the right X is moved by commutation$'$ so that it is in the rightmost position. A stabilization$'$ move is done in the same way. Then commutation$'$ moves are done on the rows, moving the newest row directly below the flock, below the rows created in the stabilization$'$s that happened before. Finally, the X in the flock is moved back to the original place in the flock via commutation$'$. Follow the same procedure for all of the X's in the row.

Theorem 3.6 *If g and g' are two graph grid diagrams representing the same transverse spatial graph, then g and g' are related by a finite sequence of graph grid moves.*

Proof First, using Section 3.5 we move both g and g' to preferred graph grid diagrams. We know that the diagrams of two isotopic transverse spatial graphs are related by a finite sequence of the graph Reidemeister moves, RI–RIV and R$\overline{\text{V}}$, shown in Figure 4, together with planar isotopy. So we need only show that preferred graph grid diagrams that result from embeddings that differ by a single Reidemeister move (or planar isotopy) can be related by a finite sequence of graph grid moves.

Due to the work of Cromwell [2] and Dynnikov [3], it is known that any two grid diagrams of the same link are related by a finite sequence of grid moves, cyclic

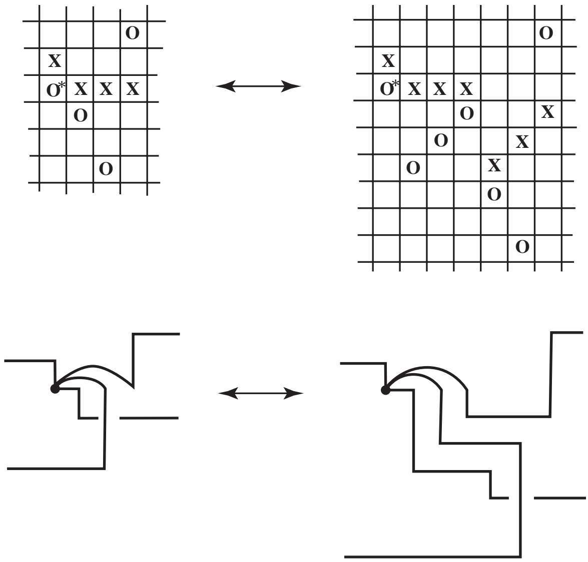

Figure 24: An example of a row vertex stabilization

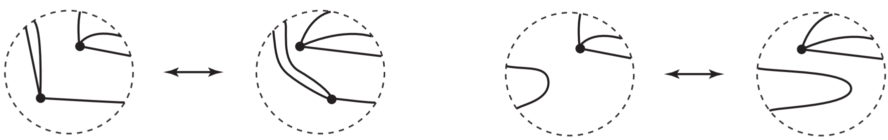

Figure 25: Examples of the two planar isotopies that can occur which contain vertices: two vertices are moved parallel to each other (left), and an arc and a vertex move parallel to each other (right)

permutation, commutation, and stabilization/destabilization. The Reidemeister moves are local moves. In the grid diagram there is a set of columns and or rows that will be moved to accomplish any one of RI–RIII. Because the first three Reidemeister moves do not involve vertices and we are working with preferred diagrams, the rows and columns that are moved will not contain an O^*. It could however contain rows or columns that contain X's that are in a flock with an O^*. In this case, first a vertex stabilization is done, so that the flock is not disrupted and the graph grid stays in preferred formation. Thus we need only show that any two preferred graph grid diagrams that come from the same embedding and differ as a result of a single Reidemeister move or planar isotopy which involves vertices can be related by a finite sequence of graph grid moves.

There are two moves and three planar isotopies with vertices to be considered: RIV, $\mathrm{R}\overline{\mathrm{V}}$, a planar isotopy in which a valence two-vertex is moved along the arc of the edges, a planar isotopy in which two vertices are moved parallel to each other, and a planar

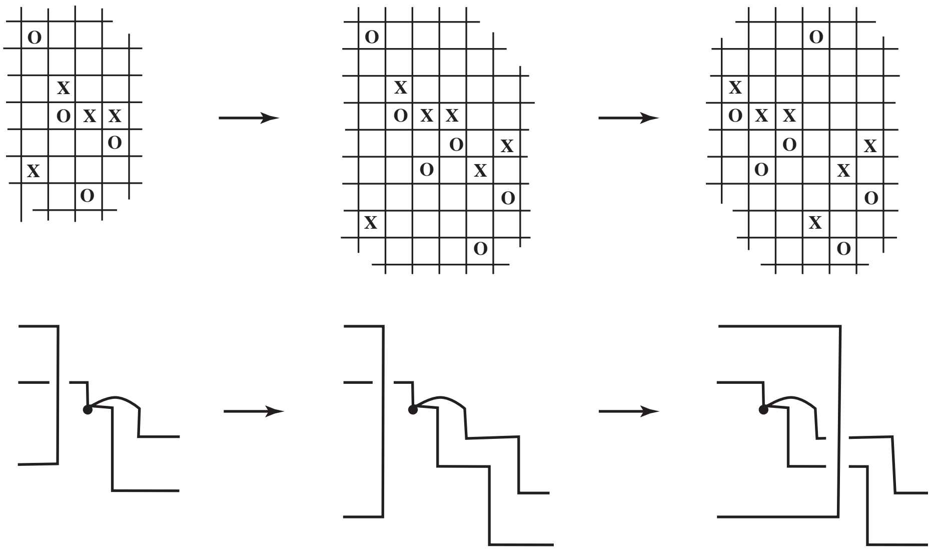

Figure 26: An example of a vertex stabilization move followed by three commutation′ moves, resulting in a RIV move in the associated graph

isotopy in which an arc and a vertex move parallel to each other, shown in Figure 25. For the figures of the graph grid diagrams in this proof we will only place $*$ on an O if it is not obvious from the grid that it is an O^*.

RIV move The move RIV moves an arc from one side of a vertex to the other, either over or under the vertex. Up to planar isotopy we can assume that the edge is next to the vertex that it will pass over (or under). An example of RIV is shown in Figure 26, here a row vertex stabilization is done followed by three column commutation′ moves. In general, RIV can be obtained via the following: first a vertex stabilization move, if needed, then a number of commutation′ moves between the v–columns (resp. v–rows) and other column (resp. row) that is associated with an appropriate arc.

R$\overline{\mathbf{V}}$ move The R$\overline{\mathrm{V}}$ move corresponds to switching the order of the edges in the projection next to the vertex, which introduces a crossing between these edges. See the leftmost move in Figure 12 for reference. Since we are working with transverse spatial graphs, such a move can only occur between pairs of incoming edges and outgoing edges. We will look at the graph grid moves needed for an R$\overline{\mathrm{V}}$ move between two outgoing edges. The proof is similar for two incoming edges.

In general, a commutation′ move between columns or rows that contain X's in the same flock will result in a R$\overline{\mathrm{V}}$ move between the two associated edges involved. In order to be able to iterate such moves, we present the follow processes. In an R$\overline{\mathrm{V}}$ move, two edges are switched next to a vertex. Let's call one of them the left edge and one

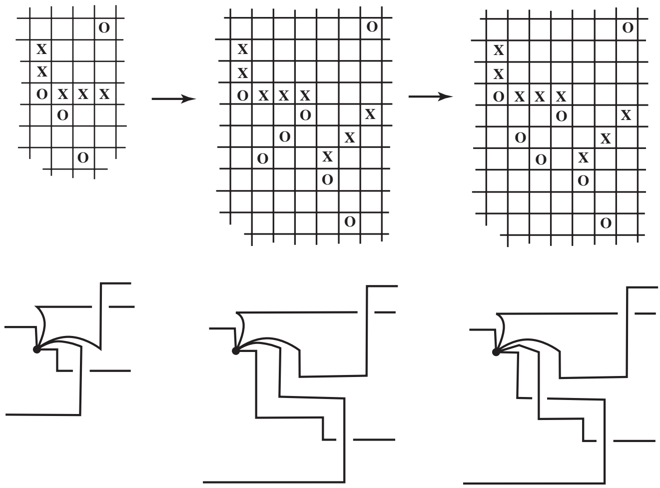

Figure 27: A row vertex stabilization move, followed by a commutation$'$ move in the grids, producing a $R\overline{V}$ move in the associated spatial graph

the right edge. There are two possibilities with a $R\overline{V}$ move: the right edge either goes under or over the left edge.

In Figure 27, we show an example of $R\overline{V}$ where the right edge goes under the left between the two leftmost outgoing edges. In general, to have the right edge go under the left edge between two outgoing edges, first a row vertex stabilization move is done, followed by a commutation$'$ move between the columns containing the X's associated with the edges involved.

In Figure 28, we show an example of $R\overline{V}$ where the right edge goes over the left between the two leftmost outgoing edges. Let X_1 and X_2, from left to right, be the X's in the flock that are associated with the edges that will be interchanged next to the vertex. In general to have the right edge go over the left edge, a row vertex stabilization move is done, if needed. Next a row stabilization$'$ move is done on the row that contains the standard O that is in the same column as X_2. Call this O O_i. The column that is added in the stabilization$'$ is placed immediately to the right of the flock. Then a commutation$'$ move is done to move the row containing O_i below the row containing the standard O that is in the same column as X_1. Finally a commutation$'$ move is done between the columns containing X_1 and X_2. To do $R\overline{V}$ for the incoming edges, one needs only switch the role of the row and column.

Movement of a valence-two vertex The movement of a valence-two vertex is equivalent to moving an O^* with a single X in both its row and column to the position of a standard O that is on one of the incident edges. This could be thought of as choosing

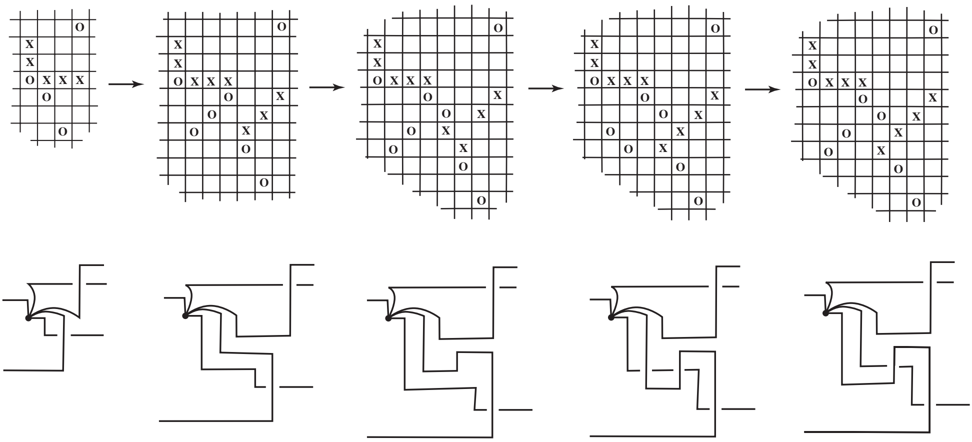

Figure 28: A row vertex stabilization move, followed by a row stabilization′ move, a row commutation′ move and a column commutation′ move in the grids, producing a R$\overline{\text{V}}$ move in the associated spatial graph

a different O on the edge to be special, and was first addressed for grid diagrams in [12, Lemma 2.12]. A proof of the independence of which O is special is given in [21, Lemma 4.1]. Since this is a local change, the same diagrammatic proof works in the graph case. We outline the proof here.

We will describe in words the moves needed to do this. However, the reader may just choose to look at the moves done in Figure 29. To move a valence-two vertex along an edge, we move the associated O^* to the position of a standard O on an adjacent edge. First a row stabilization′ is done at one of the neighboring X's, between the X and the O^*. The new column containing the new X and O are moved by commutation′ next to O^*, shown in the second image in Figure 29. Then the row containing O^* can be moved by commutation′ moves to the X in the column with the O^*. Then the column containing O^* can be moved by commutation′ to the O in the column with the X that is next to O^*. Now O^* is left and the O and X can be moved in their row by commutation′ to the X that is in the O's column. These X and O can then be removed by a column destabilization′.

Two vertices pass each other The planar isotopy where one vertex v passes another vertex w can be obtained via first vertex stabilization moves if needed, and then a number of commutation′ moves between the v–columns and the w–columns. In Figure 30, we show an example where only a single stabilization′ move is needed before the commutation′ moves, switching the order of the v–columns and the w–columns. To have the vertices move passed each other vertically rather than horizontally, the roles of the rows and columns are interchanged.

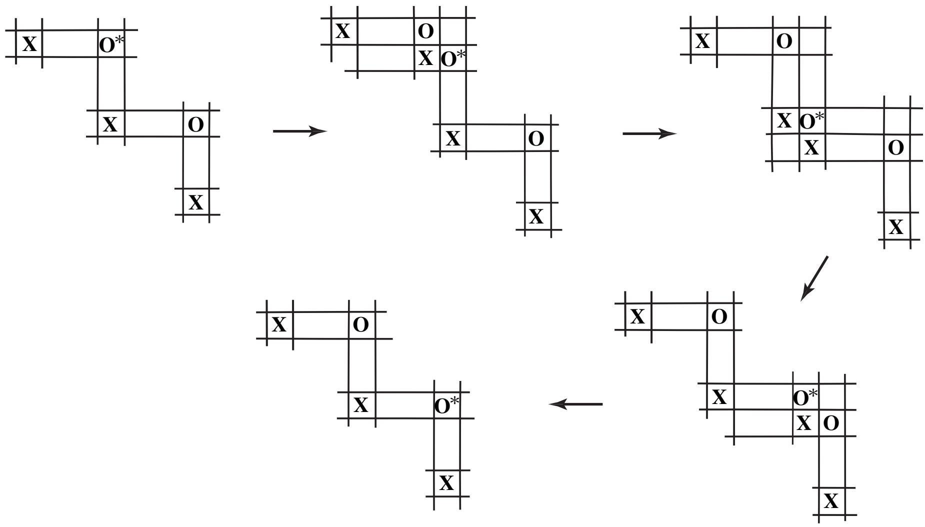

Figure 29: The graph grid moves needed to move a standard O* to the position of an O

A vertex and arc pass each other The planar isotopy where an arc and a vertex move passed each other can be obtained via first vertex stabilization moves if needed and then commutation$'$ moves between a set of v–columns (resp. v–rows) and another column (resp. row) that is associated with an appropriate arc; see Figure 31. □

This shows that even though there are numerous different graph grid diagrams that will represent the same transverse spatial graph, all such grids are related by a sequence of the graph grid moves.

4 Graph Floer homology

In this section, we will define the main invariant of this paper, which we call the graph Floer homology of a spatial graph. This will take the form of the homology of a bigraded chain complex that is a module over a polynomial ring (or more generally, the quasi-isomorphism type of the chain complex). One of the gradings is the homological grading (also called the Maslov grading) and the other grading is called the Alexander grading, and will take values in the first homology of the exterior of the transverse spatial graph. Our definitions will generalize those given in [11] and [12] except that we only get a (relatively) bigraded object instead of a filtered object. In particular, when the spatial graph is a knot or link, we recover the associated graded objects from [12] (but with a relative Alexander grading). In this section and throughout the rest of the paper, we assume that the reader is familiar with the material of [12, Sections 1–3].

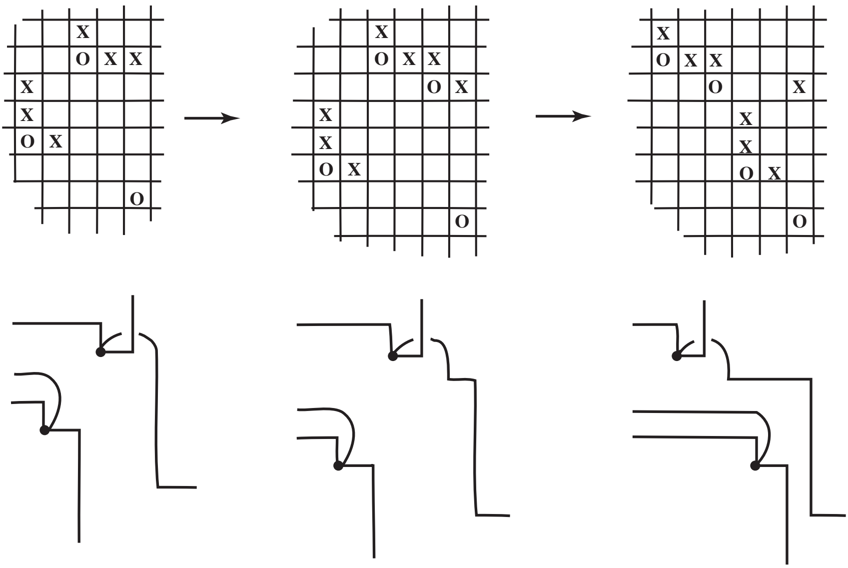

Figure 30: An example illustrating the two steps to construct a planar isotopy in which one vertex passes another vertex in the diagram of the associated transverse spatial graph. First a stabilization′ move was done then a number of the commutation′ moves were done.

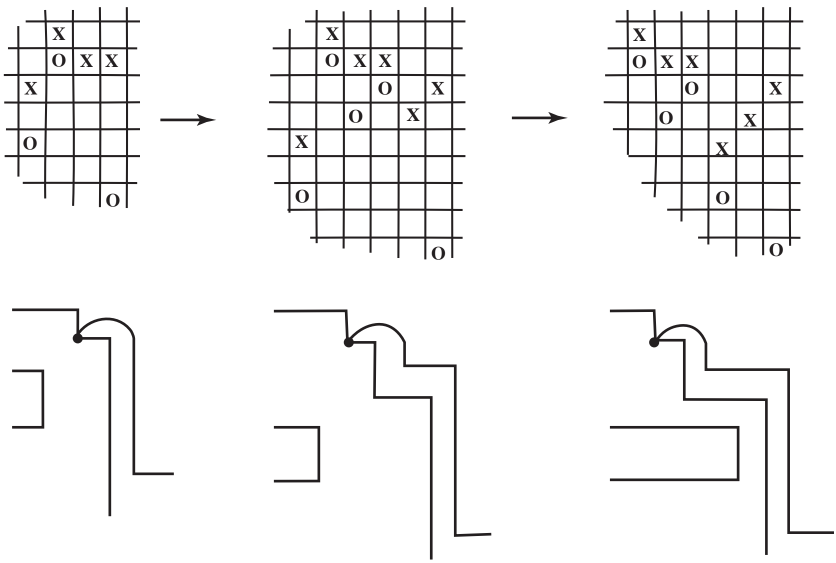

Figure 31: An example illustrating the two steps to construct a planar isotopy where a vertex passes an arc in the diagram of the associated transverse spatial graph. First a row vertex stabilization move was done then a number of the commutation′ moves were done.

4.1 Algebraic terminology

We start with some algebraic preliminaries. The reader can skip this section upon first reading and refer back to it as needed. Many of these definitions are similar to those of [12, Section 2.1].

Let C be a vector space over $\mathbb{F}$, where $\mathbb{F}$ is the field with 2 elements and let $\mathbb{G}$, $\mathbb{G}_1$ and $\mathbb{G}_2$ be abelian groups. Recall that a $\mathbb{G}$*–grading on* C (also called an *absolute* $\mathbb{G}$*–grading*) is a decomposition $C = \bigoplus_{g\in\mathbb{G}} C_g$, where $C_g \subseteq C$ is a vector subspace of C for each g. In this case we say that C is *graded over* $\mathbb{G}$ or is *graded*. A linear map $\phi\colon C \to C'$ between two graded vector spaces is *a graded map of degree* h if $\phi(C_g) \subseteq C'_{g+h}$ for all $g \in \mathbb{G}$. A *relative* $\mathbb{G}$*–grading on* C is a $\mathbb{G}$–grading that is well defined up to a shift in $\mathbb{G}$. That is, $C = \bigoplus_{g\in\mathbb{G}} C_g$ and $C = \bigoplus_{g\in\mathbb{G}} C'_g$ give the same relative $\mathbb{G}$–gradings if there exists an $a \in \mathbb{G}$ such that $C_g = C'_{g+a}$ for all $g \in \mathbb{G}$. Thus if $C = \bigoplus_{g\in\mathbb{G}} C_g$ has a well-defined relative grading and $x \in C_{g_1}$ and $y \in C_{g_2}$, then the difference between their gradings $g_1 - g_2$ is well-defined and independent of the choice of direct sum decomposition. In this case, we say that C is *relatively graded over* $\mathbb{G}$ or is *relatively graded*. A linear map $\phi\colon C \to C'$ between two relatively graded vector spaces is a *graded map* if there exists an $h \in \mathbb{G}$ such that $\phi(C_g) \subseteq C'_{g+h}$ for all $g \in \mathbb{G}$. Note that it does not make sense to talk about the degree of this map since we can shift the subgroups and get a different value for h. In this paper, we will be interested in relatively *bigraded* vector spaces over $H_1(E(f))$ and $\mathbb{Z}$, where $E(f)$ is the complement of a transverse spatial graph in S^3.

Definition 4.1 A $(\mathbb{G}_1, \mathbb{G}_2)$*–bigrading* on C is a $\mathbb{G}_1 \oplus \mathbb{G}_2$–grading on C. In this case we say that C is *bigraded* over $\mathbb{G}_1$ and $\mathbb{G}_2$, or is *graded*. We may also refer to a bigrading as an *absolute bigrading* when convenient. A linear map $\phi\colon C \to C'$ between two bigraded vector spaces is a *bigraded map of degree* (h_1, h_2) if $\phi(C_{(g_1,g_2)}) \subseteq C'_{(g_1+h_1,g_2+h_2)}$ for all $(g_1, g_2) \in \mathbb{G}_1 \oplus \mathbb{G}_2$. A *relative bigrading* on C over $\mathbb{G}_1$ and $\mathbb{G}_2$ is a relative $\mathbb{G}_1 \oplus \mathbb{G}_2$–grading on C. In this case we say that C is *relatively bigraded over* $\mathbb{G}_1$ *and* $\mathbb{G}_2$ or is *relatively graded*. A linear map $\phi\colon C \to C'$ between two relatively graded vector spaces is a *bigraded map* if there exists an $(h_1, h_2) \in \mathbb{G}_1 \oplus \mathbb{G}_2$ such that $\phi(C_{(g_1,g_2)}) \subseteq C'_{(g_1+h_1,g_2+h_2)}$ for all $(g_1, g_2) \in \mathbb{G}_1 \oplus \mathbb{G}_2$.

Note that a (relative) bigrading of C over $\mathbb{G}_1$ and $\mathbb{G}_2$ gives a well-defined (relative) grading over $\mathbb{G}_i$ for $i = 1, 2$ in the obvious way:

$$C = \bigoplus_{g_1\in\mathbb{G}_1} C_{(g_1,g_2)}\Bigg(\bigoplus_{g_2\in\mathbb{G}_2} C_{(g_1,g_2)}\Bigg) \quad \text{and} \quad C = \bigoplus_{g_2\in\mathbb{G}_2} C_{(g_1,g_2)}\Bigg(\bigoplus_{g_1\in\mathbb{G}_1} C_{(g_1,g_2)}\Bigg).$$

Our main invariant will turn out to be graded over two groups, one of which will be relatively graded and one of which will be (absolutely) graded. In the following definition, RA stands for relative absolute or relatively absolutely.

Definition 4.2 Let $\mathbb{G}_1$ and $\mathbb{G}_2$ be abelian groups and C be a vector space. An *RA* $(\mathbb{G}_1, \mathbb{G}_2)$*–bigrading* on C is a $\mathbb{G}_1 \oplus \mathbb{G}_2$–grading that is well defined up to a shift in $\mathbb{G}_1 \oplus \{0\}$. That is, $C = \bigoplus_{g \in \mathbb{G}} C_g$ and $C = \bigoplus_{g \in \mathbb{G}} C'_g$ give the same RA $(\mathbb{G}_1, \mathbb{G}_2)$–bigradings if there exists some $(g_1, 0) \in \mathbb{G}$ such that $C_g = C'_{g+(g_1,0)}$ for all $g \in \mathbb{G}$. In this case, we say that C is *RA bigraded* over $\mathbb{G}_1$ and $\mathbb{G}_2$, or, simply, is *RA bigraded*. A linear map $\phi\colon C \to C'$ between two RA bigraded vector spaces is a *bigraded map of degree* $(*, h_2)$ if there exists an $h_1 \in \mathbb{G}_1$ such that $\phi(C_{(g_1,g_2)}) \subseteq C'_{(g_1+h_1, g_2+h_2)}$ for all $(g_1, g_2) \in \mathbb{G}_1 \oplus \mathbb{G}_2$. A linear map $\phi\colon C \to C'$ between two RA bigraded vector spaces is a *bigraded map* if it is a bigraded map of some degree.

Note that an RA $(\mathbb{G}_1, \mathbb{G}_2)$–bigrading of C gives a well-defined relative grading over $\mathbb{G}_1$ and a well-defined (absolute) grading over $\mathbb{G}_2$. We will also need to define bigraded chain complexes and their equivalences.

Definition 4.3 A $(\mathbb{G}, \mathbb{Z})$*–bigraded chain complex* is a $(\mathbb{G}, \mathbb{Z})$–bigraded vector space C and bigraded map $\partial\colon C \to C$ of degree $(0, -1)$ such that $\partial^2 = 0$. For $g \in \mathbb{G}$ and $i \in \mathbb{Z}$, a linear map $\phi\colon C \to C'$ between $\mathbb{G} \oplus \mathbb{Z}$–bigraded chain complexes is a *bigraded chain map of degree* (g, i) if it is a chain map, ie $\partial \circ \phi = \phi \circ \partial$, and it a bigraded map of degree (g, i). We say that ϕ is a *bigraded chain map* if it is a bigraded chain map of some degree.

Note that if $C = \bigoplus_{g \in \mathbb{G}} C_g$ has a relative $\mathbb{G}$–grading then it makes sense to talk about a *graded map* $\phi\colon C \to C$ *of degree* h as one that satisfies $\phi(C_g) \subset C_{g+h}$ for all $g \in \mathbb{G}$. For, suppose $a \in \mathbb{G}$ and $C = \bigoplus_{g \in \mathbb{G}} C'_g$ are such that for all $g \in \mathbb{G}$, $C_g = C'_{g+a}$. Then $\phi(C'_g) = \phi(C_{g-a}) \subset C_{g-a+h} = C'_{g+h}$ for all $g \in \mathbb{G}$. Similarly, we can define a bigraded map of degree (g_1, g_2) between a relatively (or RA) bigraded vector space and itself. We say a linear map (between absolutely, relatively or RA bigraded vector spaces) is a *bigraded* map if it is a bigraded map of some degree.

Definition 4.4 A *relative* (respectively *RA*) $(\mathbb{G}, \mathbb{Z})$*–bigraded chain complex* is a relative (respectively RA) $(\mathbb{G}, \mathbb{Z})$–bigraded vector space C and bigraded map $\partial\colon C \to C$ of degree $(0, -1)$ such that $\partial^2 = 0$. A linear map $\phi\colon C \to C'$ between relative (respectively RA) $\mathbb{G} \oplus \mathbb{Z}$–bigraded chain complexes is a *bigraded chain map* if it is a chain map, ie $\partial \circ \phi = \phi \circ \partial$, and it is a bigraded map.

Similarly, we can define $(\mathbb{G}, \mathbb{Z}_2)$*–bigraded*, *relatively bigraded*, and *RA bigraded chain complexes*. This will be used in the last section of the paper when we compare our invariant to sutured Floer homology.

The primary invariant will be a chain complex that also takes the form of a module over a multivariable polynomial ring. Recall that a $\mathbb{G}$*–graded ring* is a commutative ring R with a direct sum decomposition as abelian groups $R=\bigoplus_{g\in\mathbb{G}} R_g$, where R_g is a subgroup of R and $R_{g_1}R_{g_2}\subset R_{g_1+g_2}$ for all $g_i\in\mathbb{G}$. If R is a $\mathbb{G}$–graded ring, a $\mathbb{G}$*–graded (left) R–module* is a (left) R–module with a direct sum decomposition as abelian groups $M=\bigoplus_{g\in\mathbb{G}} M_g$, where M_g is a subgroup of M and $R_{g_1}M_{g_2}\subset M_{g_1+g_2}$ for all $g_i\in\mathbb{G}$. A *graded R–module homomorphism of degree h* is a graded map $\phi\colon C\to C'$ (of degree h) between $\mathbb{G}$–graded R–modules that is also an R–module homomorphism. We can similarly define *relatively graded, bigraded, relatively bigraded, and relatively absolutely bigraded R–modules* and graded module homomorphisms in these cases.

Definition 4.5 A $(\mathbb{G},\mathbb{Z})$*–bigraded (left) R–module chain complex* is a $(\mathbb{G},\mathbb{Z})$–bigraded (left) R–module C and bigraded R–module homomorphism $\partial\colon C\to C$ of degree $(0,-1)$ such that $\partial^2=0$. For $g\in\mathbb{G}$ and $i\in\mathbb{Z}$, an R–module homomorphism $\phi\colon C\to C'$ between $\mathbb{G}\oplus\mathbb{Z}$–bigraded R–module chain complexes is a *bigraded R–module chain map of degree* (g,i) if $\partial\circ\phi=\phi\circ\partial$ and it is a bigraded map of degree (g,i). We say that $\phi\colon C\to C'$ is a *bigraded R–module chain map* if it is a bigraded R–module map of some degree. We can similarly define a relative (respectively RA) $(\mathbb{G},\mathbb{Z})$–bigraded R–module chain complex and a relative bigraded R–module chain map.

We remark that if C is a $(\mathbb{G},\mathbb{Z})$–bigraded chain complex of (left) R–modules then it is not necessarily the case that any of $C_{(g,m)}$, $\bigoplus_{h\in\mathbb{G}} C_{(g,m)}$ or $\bigoplus_{m\in\mathbb{Z}} C_{(g,m)}$ is an R–module.

The primary invariant of this paper associates to each graph grid diagram a bigraded R–module chain complex. However, choosing different graph grid diagrams representing the same transverse spatial graph will lead to different chain complexes. We will show that they are all quasi-isomorphic.

Definition 4.6 A chain map $\phi\colon C\to C'$ of chain complexes is a *quasi-isomorphism* if it induces an isomorphism on homology. We say that two chain complexes C and D are *quasi-isomorphic* if there is a sequence of chain complexes $C_0,\dots,C_r$ and quasi-isomorphisms

$$\begin{tikzcd}
C_0 \arrow[dr, "\phi_1"] & & C_2 \arrow[dl, "\phi_2"'] \arrow[dr, "\phi_3"] & & \cdots & & C_{r-2} \arrow[dl, "\phi_{r-2}"'] \arrow[dr, "\phi_{r-1}"] & & C_r \arrow[dl, "\phi_r"'] \\
& C_1 & & C_3 & & C_{r-3} & & C_{r-1} &
\end{tikzcd}$$

such that $C_0 = C$, $C_r = D$. Suppose C and D are $(\mathbb{G}, \mathbb{Z})$–bigraded R–module chain complexes. We say that $\phi\colon C \to C'$ is a bigraded R–module quasi-isomorphism if ϕ is a quasi-isomorphism and a bigraded R–module homomorphism. We say that C and D are *quasi-isomorphic (as* $(\mathbb{G}, \mathbb{Z})$*–bigraded R–module chain complexes)* if they are quasi-isomorphic and all the quasi-isomorphisms are bigraded R–module chain maps. We can similarly define quasi-isomorphism for two relative (or RA) $(\mathbb{G}, \mathbb{Z})$–bigraded R–module chain complexes.

Remark 4.7 In the definition of quasi-isomorphism, it suffices to consider sequences of length $r = 2$. To see that these are equivalent, see [16, Proposition A.3.11].

4.2 The chain complex

For technical reasons, we need to restrict our definition to graphs that are both sinkless and sourceless. The graph grid diagrams representing these transverse spatial graphs have at least one X per column and row. We will need this condition to ensure that $\partial^2 = 0$.

Definition 4.8 A graph grid diagram is *saturated* if there is at least one X in each row and each column. A transverse spatial graph $f\colon G \to S^3$ is called *sinkless and sourceless* if its underlying graph G is sinkless and sourceless (ie has no vertices with only incoming edges or only outgoing edges).

Remark 4.9 (1) Suppose that g is a graph grid diagram representing the transverse spatial graph f. Then g is saturated if and only if f is sinkless and sourceless. (2) If one performs a graph grid move on a saturated graph grid diagram, then the resulting graph grid diagram is saturated.

Convention For the rest of this paper, unless otherwise mentioned, we will assume that all transverse spatial graphs are sinkless and sourceless and all graph grid diagrams are saturated.

Let $f\colon G \to S^3$ be a sinkless and sourceless transverse spatial graph, define $E(f) = S^3 \setminus N(f(G))$, where $N(f(G))$ is a regular neighborhood of $f(G)$ in S^3, let g be an $n \times n$ saturated graph grid diagram representing f, and $\mathcal{T}$ be its corresponding toroidal diagram. Now, let

$$\boldsymbol{S} = \{\{x_i\}_{i=1}^n \mid x_i = \alpha_i \cap \beta_{\sigma(i)}, \sigma \in S_n\},$$

where S_n is the symmetric group on n elements, and define $C^-(g)$ to be the free (left) R_n–module generated by $\boldsymbol{S}$, where

$$R_n = \mathbb{F}[U_1, \dots, U_n]$$

and $\mathbb{F} = \mathbb{Z}/2\mathbb{Z}$ denotes the field with two elements. When working with generators on a planar grid diagram, we use the convention that places the intersection point on the bottom leftmost grid line (as opposed to the top rightmost grid line). When we want to specify the grid, we may write $\boldsymbol{S}(g)$ instead of $\boldsymbol{S}$.

Using the toroidal grid diagram, we can view the torus $\mathcal{T}$ as a two-dimensional CW complex with n^2 0–cells (intersections of α_i and β_j), $2n^2$ 1–cells (consisting of line segments on α_i and β_j), and n^2 2–cells (squares cut out by α_i and β_j). Note that a generator $\boldsymbol{x} \in \boldsymbol{S}$ can be viewed as a 0–chain. Let $U_{\boldsymbol{\alpha}}$ be the 1–dimensional subcomplex of $\mathcal{T}$ consisting of the union of the horizontal circles. We define paths, domains, and rectangles in the same way as [12]. Given two generators $\boldsymbol{x}$ and $\boldsymbol{y}$ in $\boldsymbol{S}$, a *path* from $\boldsymbol{x}$ to $\boldsymbol{y}$ is a 1–cycle γ such that the boundary of the 1–chain obtained by intersecting γ with $U_{\boldsymbol{\alpha}}$ is $\boldsymbol{y}-\boldsymbol{x}$. A *domain* D from $\boldsymbol{x}$ to $\boldsymbol{y}$ is an 2–chain in $\mathcal{T}$ whose boundary ∂D is a path from $\boldsymbol{x}$ to $\boldsymbol{y}$. The support of D is the union of the closures of the 2–cells appearing in D (with nonzero multiplicity). We denote the set of domains from $\boldsymbol{x}$ to $\boldsymbol{y}$ by $\pi(\boldsymbol{x},\boldsymbol{y})$ and note that there is a composition of domains $*\colon \pi(\boldsymbol{x},\boldsymbol{y})\times\pi(\boldsymbol{y},\boldsymbol{z})\to\pi(\boldsymbol{x},\boldsymbol{z})$. A domain from $\boldsymbol{x}$ to $\boldsymbol{y}$ that is an embedded rectangle r is called a *rectangle* that connects $\boldsymbol{x}$ to $\boldsymbol{y}$. Let $\mathrm{Rect}(\boldsymbol{x},\boldsymbol{y})$ be the set of rectangles that connect $\boldsymbol{x}$ to $\boldsymbol{y}$. Notice if $\boldsymbol{x}$ and $\boldsymbol{y}$ agree in all but two intersection points then there are exactly two rectangles in $\mathrm{Rect}(\boldsymbol{x},\boldsymbol{y})$, otherwise $\mathrm{Rect}(\boldsymbol{x},\boldsymbol{y}) = \varnothing$. A rectangle $r \in \mathrm{Rect}(\boldsymbol{x},\boldsymbol{y})$ is *empty* if $\mathrm{Int}(r)\cap\boldsymbol{x} = \varnothing$ where $\mathrm{Int}(r)$ is the interior of the rectangle in $\mathcal{T}$. Let $\mathrm{Rect}^o(\boldsymbol{x},\boldsymbol{y})$ be the set of empty rectangles that connect $\boldsymbol{x}$ to $\boldsymbol{y}$.

We now make $C^-(g)$ into a chain complex $(C^-(g),\partial^-)$ in the usual way: by counting empty rectangles. Note that in [11; 12], the authors consider rectangles that contain both X's and O's. However, because there is no natural filtration of $H_1(E(f))$, we must restrict to rectangles without any X's and thus we get a graded object instead of a filtered object. Let $\mathbb{X}$ and $\mathbb{O}$ be the set of X's and O's in the grid. Put an ordering on each of these sets, $\mathbb{O} = \{\mathrm{O}_i\}_{i=1}^n$ and $\mathbb{X} = \{\mathrm{X}_i\}_{i=1}^m$ so that $\mathrm{O}_1,\dots,\mathrm{O}_V$ are associated to the V vertices of the graph. For a domain $D\in\pi(\boldsymbol{x},\boldsymbol{y})$, let $\mathrm{O}_i(D)$ (respectively $\mathrm{X}_i(D)$) denote the multiplicity with which O_i (respectively X_i) appear in D. More precisely, D is a domain so $D = \sum a_j r_j$, where r_j is a rectangle in $\mathcal{T}$. Thus $\mathrm{O}_i(D) = \sum a_j \mathrm{O}_i(r_j)$, where $\mathrm{O}_i(r_j)$ is 1 if $\mathrm{O}_i \in r_j$ and 0 otherwise (similarly for $\mathrm{X}_i(D)$). We note that if r is a rectangle then $\mathrm{O}_i(r) \geq 0$. Define $\partial^-\colon C^-(g)\to C^-(g)$ as follows. For $\boldsymbol{x}\in\boldsymbol{S}$, let

$$\partial^-(\boldsymbol{x}) = \sum_{\boldsymbol{y}\in\boldsymbol{S}} \sum_{\substack{r\in\mathrm{Rect}^o(\boldsymbol{x},\boldsymbol{y})\\ \mathrm{Int}(r)\cap\mathbb{X}=\varnothing}} U_1^{\mathrm{O}_1(r)}\cdots U_n^{\mathrm{O}_n(r)}\cdot\boldsymbol{y}.$$

Extend ∂^- to all of $C^-(g)$ so that it is an R_n–module homomorphism. When we want to specify the grid, we will write ∂_g^- instead of ∂^-.

Proposition 4.10 *If g is a saturated graph grid diagram then $\partial_g^- \circ \partial_g^- = 0$.*

Proof This proof follows that of [12, Proposition 2.10, page 2349] almost verbatim. The only change is that we only consider regions that do not contain any X's. Briefly, let $\boldsymbol{x} \in \boldsymbol{S}$. Then

$$\partial^- \circ \partial^-(\boldsymbol{x}) = \sum_{\boldsymbol{z}\in\boldsymbol{S}} \sum_{D\in\pi(\boldsymbol{x},\boldsymbol{z})} N(D)\cdot U_1^{\mathrm{O}_1(D)} \cdots U_n^{\mathrm{O}_n(D)}\cdot \boldsymbol{z},$$

where $N(D)$ is the number of ways one can decompose D as $D = r_1 * r_2$, where $r_1 \in \mathrm{Rect}^o(\boldsymbol{x},\boldsymbol{y})$, $r_2 \in \mathrm{Rect}^o(\boldsymbol{y},\boldsymbol{z})$ and $\mathrm{Int}(r_i)\cap\mathbb{X} = \varnothing$. When $\boldsymbol{x} \neq \boldsymbol{z}$ there are three general cases. The rectangles are either disjoint, overlapping or share a common edge. In each of these cases there are two ways that the region can be decomposed as empty rectangles. Thus the resulting $\boldsymbol{z}$ occurs in the sum twice. The case where $\boldsymbol{x} = \boldsymbol{z}$ is the result of domains $D \in \pi(\boldsymbol{x},\boldsymbol{x})$, which are width-one annuli. Such domains do not occur in the image of $\partial^- \circ \partial^-(\boldsymbol{x})$ because ∂^- only counts rectangles that do not contain X's, and we have assumed that our graph grid diagram is saturated. Thus we see that $\partial^- \circ \partial^-(\boldsymbol{x})$ vanishes. □

4.3 Gradings

We put two gradings on the $(C^-(g),\partial^-)$. The first is the homological grading, also called the Maslov grading. This will be defined exactly the same as in [12]. We quickly review the definition for completeness.

Given two finite sets of points A and B in the plane and a point $q=(q_1,q_2)$ in the plane, define $\mathcal{I}(q,B) = \#\{(b_1,b_2)\in B \mid b_1 > q_1, b_2 > q_2\}$. That is, $\mathcal{I}(q,B)$ is the number of points in B above and to the right of q. Let $\mathcal{I}(A,B) = \sum_{q\in A}\mathcal{I}(q,B)$ and $\mathcal{J}(A,B) = (\mathcal{I}(A,B)+\mathcal{I}(B,A))/2$. It will be useful to note that an equivalent definition of $\mathcal{I}(A,q)$ is the number of points in the set $\{a\in A \mid q_1 > a_1, q_2 > a_2\}$, ie the number of points in A below and to the left q. So $\mathcal{J}(q,A)$ counts with weight one half all the points in A above and to the right of q and down and to the left of q. Slightly abusing notation, we view $\mathbb{O}$ as a set of points in the grid with half-integer coordinates (the points where the O's occur). Similarly, we view $\mathbb{X}$ as a set of points in the grid with half-integer coordinates. We extend $\mathcal{J}$ bilinearly over formal sums and differences of subsets in the plane and define the Maslov grading of $\boldsymbol{x}\in\boldsymbol{S}$ to be

$$M(\boldsymbol{x}) = \mathcal{J}(\boldsymbol{x}-\mathbb{O},\boldsymbol{x}-\mathbb{O}) + 1.$$

This is consistent with the definition given in [12], and only depends on the set $\mathbb{O}$. Since, like in [12], we have exactly one O per column and row, [12, Lemmas 2.4 and 2.5] also hold for grid diagrams of transverse spatial graphs. Thus, it follows that M is a well-defined function on the toroidal grid diagram [12, Lemma 2.4]. In addition,

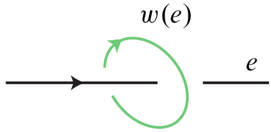

Figure 32: The weight $w(e)$ assigned to an edge $e \in E(G)$

for $x, y \in \boldsymbol{S}$, we can define the relative Maslov grading by $M(\boldsymbol{x}, \boldsymbol{y}) := M(\boldsymbol{x}) - M(\boldsymbol{y})$. By [12, Lemma 2.5],

$$M(\boldsymbol{x}, \boldsymbol{y}) = M(\boldsymbol{x}) - M(\boldsymbol{y}) = 1 - 2n_{\mathbb{O}}(r), \tag{1}$$

for any *empty*[1] rectangle r connecting $\boldsymbol{x}$ to $\boldsymbol{y}$, where $n_{\mathbb{O}}(r)$ is the number of O's in r.

Before defining the Alexander grading we first need to establish a weight system on the edges of G. Let $E(G)$ be the set of edges of the graph G. We define $w\colon E(G) \to H_1(E(f))$ by sending each edge to the meridian of the edge, with orientation given by the right-hand rule, seen as an element of $H_1(E(f))$; see Figure 32. We say that $w(e)$ is the weight of the edge e. We will denote the weight of X by $w(\mathrm{X})$ and the weight of O by $w(\mathrm{O})$, and define them based on the weight of the associated edge. If X or O appear on the interior of an edge $e \in E(G)$ in the associated transverse spatial graph, then $w(\mathrm{X}) := w(e)$ and $w(\mathrm{O}) := w(e)$. If the O is associated to the vertex v in the associated transverse spatial graph, then

$$w(\mathrm{O}) := \sum_{e \in \mathrm{In}(v)} w(e) = \sum_{e \in \mathrm{Out}(v)} w(e),$$

where $\mathrm{In}(v)$ and $\mathrm{Out}(v)$ are the sets of incoming and outgoing edges of v, respectively.

Remark 4.11 Recall that an edge of a graph G is called a *cut edge* if the number of connected components of $G \setminus e$ is greater than the number of connected components of G. Observe that $w(e) = 0$ if and only if e is a cut edge. This will be useful in the proof of Theorem 6.6.

Let the function $\epsilon\colon \mathbb{O} \cup \mathbb{X} \to \{1, -1\}$ be defined by

$$\epsilon(p) = \begin{cases} 1 & \text{if } p \in \mathbb{X}, \\ -1 & \text{if } p \in \mathbb{O}. \end{cases}$$

For a point q in the grid, define

$$A^g(q) = \sum_{p \in \mathbb{O} \cup \mathbb{X}} \mathcal{J}(q, p) w(p) \epsilon(p).$$

[1] If the rectangle r contains m points of $\boldsymbol{x}$ in its interior, then $M(\boldsymbol{x}) = M(\boldsymbol{y}) + 1 + 2(m - n_{\mathbb{O}(r)})$.

We define the *Alexander grading* of $\boldsymbol{x}$ with respect to the grid g to be

$$A^g(\boldsymbol{x}) = \sum_{p\in\mathbb{O}\cup\mathbb{X}} \mathcal{J}(\boldsymbol{x},p)w(p)\epsilon(p) = \sum_{x_i\in\boldsymbol{x}} A^g(x_i).$$

This value a priori lives in $\frac{1}{2}H_1(E(f))$; however, by Lemma 4.16, $A^g(\boldsymbol{x})\in H_1(E(f))$. Note that this definition depends on the choice of *planar* grid g, and is not a well-defined function on the toroidal grid.[2] However, the relative Alexander grading is a well-defined function on the toroidal grid diagram.

Definition 4.12 For $\boldsymbol{x},\boldsymbol{y}\in S$, let $A^{\mathrm{rel}}(\boldsymbol{x},\boldsymbol{y}) := A^g(\boldsymbol{x}) - A^g(\boldsymbol{y})$ be the *relative Alexander grading* of $\boldsymbol{x}$ and $\boldsymbol{y}$.

When it is clear, we may drop the "rel" or "g" on A. By the following lemma, A^{rel} does not depend on how you cut open the toroidal diagram $\mathcal{T}$ to give a planar grid diagram g. We first need to define some notation. For a rectangle r, we define $w_{\mathbb{O}}(r)=\sum_{q\in\mathbb{O}\cap r} w(q)$ and, similarly, $w_{\mathbb{X}}(r)=\sum_{q\in\mathbb{X}\cap r} w(q)$. If D is a domain then $D=\sum a_i D_i$, where D_i is a rectangle. We extend $w_{\mathbb{O}}$ and $w_{\mathbb{X}}$ linearly to domains, so that $w_{\mathbb{O}}(D)=\sum a_i w_{\mathbb{O}}(D_i)$ and $w_{\mathbb{X}}(D)=\sum a_i w_{\mathbb{X}}(D_i)$.

Note that a path from $\boldsymbol{x}$ to $\boldsymbol{y}$, on the toroidal grid, gives a 1–cycle in $E(f)$. To see this, recall that the transverse spatial graph associated to the graph grid diagram is constructed from vertical arcs going from an X to an O outside the torus (above the plane) and horizontal arcs going from O to X inside the torus (below the plane). Thus, the intersection of the transverse spatial graph and the torus is $\mathbb{X}\cup\mathbb{O}$. Since a path is a 1–cycle on the torus missing $\mathbb{X}\cup\mathbb{O}$, we get an element of $H_1(E(f))$. Since the α_i and β_i bound disks in $E(f)$, this is a well-defined element of $H_1(E(f))$, independent of the choice of path.

Lemma 4.13 *Let $\boldsymbol{x},\boldsymbol{y}\in \boldsymbol{S}$. If $D\in\pi(\boldsymbol{x},\boldsymbol{y})$ is a domain connecting $\boldsymbol{x}$ to $\boldsymbol{y}$ then*

$$A^g(\boldsymbol{x}) - A^g(\boldsymbol{y}) = w_{\mathbb{X}}(D) - w_{\mathbb{O}}(D). \tag{2}$$

If γ is a path connecting $\boldsymbol{x}$ to $\boldsymbol{y}$ then

$$A^g(\boldsymbol{x}) - A^g(\boldsymbol{y}) = [\gamma], \tag{3}$$

where $[\gamma]\in H_1(E(f))$ is the homology class of γ.

We note that the domain (or rectangle) in this lemma does not have to be empty.

[2] One can slightly change this definition to make it well-defined on the toroidal grid diagram. Our invariant will still only be relatively graded in the end however.

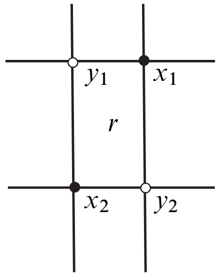

Figure 33: The rectangle r with the intersections labeled

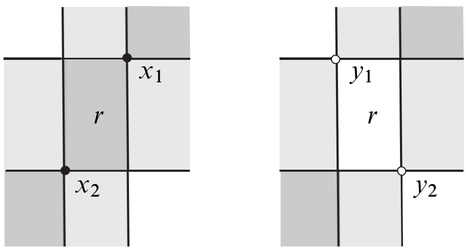

Figure 34: The lightly shaded regions are those that will be counted with weight one half in $\mathcal{J}(x_1,-)$ and $\mathcal{J}(x_2,-)$ (left), or in $\mathcal{J}(y_1,-)$ and $\mathcal{J}(y_2,-)$ (right).

Proof Let r be a rectangle connecting $\boldsymbol{x}$ to $\boldsymbol{y}$. We will first show that (2) holds for r. Consider

$$A^g(\boldsymbol{x})-A^g(\boldsymbol{y})=\sum_{q\in\mathbb{O}\cup\mathbb{X}}\mathcal{J}(\boldsymbol{x},q)w(q)\epsilon(q)-\sum_{q\in\mathbb{O}\cup\mathbb{X}}\mathcal{J}(\boldsymbol{y},q)w(q)\epsilon(q).$$

Let x_1, x_2, y_1, and y_2 be the intersection points at the corners of r, as shown in Figure 33. Since the intersection points of $\boldsymbol{x}$ and $\boldsymbol{y}$ only differ at the corners of the rectangle r this difference reduces to

$$\sum_{q\in\mathbb{O}\cup\mathbb{X}}\big[\mathcal{J}(x_1,q)+\mathcal{J}(x_2,q)-\mathcal{J}(y_1,q)-\mathcal{J}(y_2,q)\big]w(q)\epsilon(q).$$

By definition, $\mathcal{J}(x_1,\mathbb{O}\cup\mathbb{X})$ counts with weight one half all those X's and O's above and to the right of x_1 and below and to the left of x_1. In Figure 34 (left), we show which regions will have points counted in $\mathcal{J}(x_1,-)$ and $\mathcal{J}(x_2,-)$. The shading indicates if it will be counted with a weight of a half or one, this depends on whether it is counted in one or both of $\mathcal{J}(x_1,-)$ and $\mathcal{J}(x_2,-)$. Similarly, in Figure 34 (right) we show which regions will have points counted in $\mathcal{J}(y_1,-)$ and $\mathcal{J}(y_2,-)$. These counts differ by the points in r counted with weight one.

So we see that this difference is exactly

$$\sum_{q \in r \cap [\mathbb{O} \cup \mathbb{X}]} w(q)\epsilon(q) = \sum_{q \in \mathbb{X} \cap r} w(q) - \sum_{q \in \mathbb{O} \cap r} w(q).$$

Thus, (2) holds for rectangles.

Now we show that (3) holds. Let γ be a path connecting $\boldsymbol{x}$ to $\boldsymbol{y}$. Using the fact that S_n is generated by transposition, it follows that $\boldsymbol{x}, \boldsymbol{y} \in \boldsymbol{S}$ are related by a finite sequence of rectangles in $\mathcal{T}$. That is, there is a sequence $\boldsymbol{x} = \boldsymbol{x}_1, \dots, \boldsymbol{x}_l = \boldsymbol{y}$ of points in S and rectangles r_j connecting $\boldsymbol{x}_j$ to $\boldsymbol{x}_{j+1}$ for $1 \leq j \leq l-1$. Thus,

$$\begin{aligned} A^g(\boldsymbol{x}) - A^g(\boldsymbol{y}) &= \sum_j (A^g(\boldsymbol{x}_j) - A^g(\boldsymbol{x}_{j+1})) \\ &= \sum_j (w_{\mathbb{X}}(r_j) - w_{\mathbb{O}}(r_j)) = \sum_j [\partial r_j] = \Big[\sum_j \partial r_j\Big]. \end{aligned}$$

Since $\sum_j \partial r_j$ is also a path connecting $\boldsymbol{x}$ to $\boldsymbol{y}$, $\big[\sum_j \partial r_j\big] = [\gamma]$. Thus, we have proved (3).

Finally, we prove (2) for a general domain. Suppose D is a domain connecting $\boldsymbol{x}$ to $\boldsymbol{y}$. Then $D = \sum a_i D_i$ for some rectangles D_i, and ∂D is a path connecting $\boldsymbol{x}$ to $\boldsymbol{y}$. Thus $A^g(\boldsymbol{x}) - A^g(\boldsymbol{y}) = [\partial D] = \sum_i a_i[\partial D_i] = \sum_i a_i(w_{\mathbb{X}}(D_i) - w_{\mathbb{O}}(D_i)) = w_{\mathbb{X}}(D) - w_{\mathbb{O}}(D)$. □

Corollary 4.14 *The relative grading $A^{\mathrm{rel}}\colon \boldsymbol{S} \times \boldsymbol{S} \to H_1(E(f))$ is a well-defined function on the toroidal graph grid diagram.*

Proof Any two $\boldsymbol{x}, \boldsymbol{y} \in \boldsymbol{S}$ are related by a sequence of rectangles and hence there is always a path γ connecting $\boldsymbol{x}$ to $\boldsymbol{y}$. Since the homology class of the path is independent of the choice of path and $A^{\mathrm{rel}}(\boldsymbol{x}, \boldsymbol{y}) = [\gamma]$, we see that A^{rel} is independent of how you cut open the toroidal graph grid diagram to get a planar graph grid diagram. □

We now provide an easy way to compute A^g for a planar graph grid diagram g. Let $\mathcal{L}$ be the lattice points in the grid, that is, the n^2 intersections between the horizontal and vertical grid lines (ie the set of points that on the torus become $\alpha_i \cap \beta_j$). Define $h\colon \mathcal{L} \to H_1(E(f))$, the *generalized winding number*, of a point $q \in \mathcal{L}$ as follows. Place the planar graph grid diagram g on the Euclidean plane with the lower left corner at the origin (and the upper right corner at the point (n, n)). Now consider the following projection of the associated transverse spatial graph $\mathrm{pr}(f)$. Like in the last section, this is obtained by connecting the X's to O's by arcs in the columns and O's to the X's in the rows. However, we now require that the arcs do not leave the $n \times n$ planar

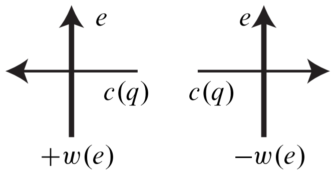

Figure 35: $\sigma(b_i) = \pm w(e)$, where the sign is given by the sign of $e \cdot c(q)$

grid (they cannot go around the torus). We also project this to the plane and ignore crossings. For $q \in \mathcal{L}$, let c be any path along the horizontal and vertical grid lines starting at the origin and ending at q. We also require that c meets $\mathrm{pr}(g)$ transversely. Then c intersects $\mathrm{pr}(g)$ in a finite number of points $b_1, \dots, b_k$, where b_i lives on the interior of some edge of the spatial graph. Suppose b_i lies on edge e. Define $\sigma(b_i)$ to be $\pm w(e)$, where the sign is given by the sign of the intersection of e with $c(q)$, with the usual orientation of the plane; see Figure 35. Using this, we set

$$h(q) = \sum_{i=1}^{k} \sigma(b_i).$$

When it is useful, we may also write h^g to specify that we are computing h in the graph grid diagram g.

Lemma 4.15 *The map h is well defined.*

Proof Consider the transverse spatial graph associated to g whose projection is $\mathrm{pr}(g)$ but which is pushed slightly above the plane. Fix a base point at infinity in S^3. It is easy to see that $h(q)$ is the homology of a loop made up of the path from infinity to the origin, then a path in the plane, from the origin to q, and finally the path from q to the point at infinity. This is independent of the choice of path from the origin to q. Therefore h is well defined. □

Lemma 4.16 *For any point q on the lattice*

$$A^g(q) = -h(q). \tag{4}$$

Proof Let g be a graph grid diagram. First we see that $h(q) = 0$ for any point on the boundary of g by definition. Notice that we have

$$\sum_{p \in \mathrm{col}_i} w(p)\epsilon(p) = 0$$

for each i, where col_i is the set of O's and X's in the i^{th} column. Similarly,

$$\sum_{p \in \mathrm{row}_i} w(p)\epsilon(p) = 0$$

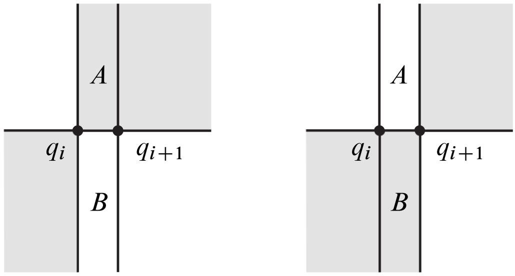

Figure 36: Here we shade the regions that will be counted with weight one half in $\mathcal{J}(q_i, -)$ (left), or $\mathcal{J}(q_{i+1}, -)$ (right).

for each i, where row_i is the set of O's and X's in the i^{th} row. Given these observations, it is immediate that $A^g(q) = \sum_{p\in\mathbb{O}\cup\mathbb{X}} \mathcal{J}(q,p)w(p)\epsilon(p)$ is also zero for any point on the boundary of g.

We will proceed by induction on the vertical grid line on which our lattice point occurs. Suppose the equality in (4) holds for q_i a lattice point on the i^{th} vertical arc, and consider q_{i+1} the point immediately to the right of q_i on the grid. Let

$$\mathrm{RHS} := \sum_{p\in\mathbb{O}\cup\mathbb{X}} \mathcal{J}(q_{i+1},p)w(p)\epsilon(p) - \sum_{p\in\mathbb{O}\cup\mathbb{X}} \mathcal{J}(q_i,p)w(p)\epsilon(p),$$

and

$$\mathrm{LHS} := -h(q_{i+1}) - (-h(q_i)).$$

Figure 36 shows the regions in which the points of $\mathbb{O}\cup\mathbb{X}$ will be counted with weight one half in $\mathcal{J}(q_i, \mathbb{O}\cup\mathbb{X})$ and $\mathcal{J}(q_{i+1}, \mathbb{O}\cup\mathbb{X})$. These differ only in what is counted in the i^{th} column. So we see that

$$\mathrm{RHS} = \frac{1}{2}\Bigg[\sum_{p\in B\cap(\mathbb{O}\cup\mathbb{X})} w(p)\epsilon(p) - \sum_{p\in A\cap(\mathbb{O}\cup\mathbb{X})} w(p)\epsilon(p)\Bigg].$$

Using the fact $\sum_{p\in\mathrm{col}_i} w(p)\epsilon(p) = 0$ again, we can simplify this to,

$$\mathrm{RHS} = -\sum_{p\in A\cap(\mathbb{O}\cup\mathbb{X})} w(p)\epsilon(p) = \sum_{p\in B\cap(\mathbb{O}\cup\mathbb{X})} w(p)\epsilon(p).$$

We now consider $\mathrm{LHS} = -h(q_i) - [-h(q_{i+1})] = h(q_{i+1}) - h(q_i)$. Suppose the O in the i^{th} column is in A. Then all the vertical arcs of $\mathrm{pr}(g)$ in the i^{th} column that intersect the arc from q_i to q_{i+1} are oriented upwards. Thus $\mathrm{LHS} = \sum_{p\in\mathbb{X}\cap B} w(p) = \sum_{p\in B\cap(\mathbb{O}\cup\mathbb{X})} w(p)\epsilon(p)$. If the O in the i^{th} column is in B, the all the vertical arcs of $\mathrm{pr}(g)$ in the i^{th} column that intersect the arc from q_i to q_{i+1} are oriented downwards. So $\mathrm{LHS} = \sum_{p\in\mathbb{X}\cap A} -w(p) = -\sum_{p\in A\cap(\mathbb{O}\cup\mathbb{X})} w(p)\epsilon(p)$. □

Corollary 4.17 *For all $\boldsymbol{x} \in \boldsymbol{S}(g)$,*

$$A^g(\boldsymbol{x}) = -\sum_{x_i \in \boldsymbol{x}} h(x_i) \in H_1(E(f)).$$

For a given saturated graph grid diagram g, the functions A^g and M make $C^-(g)$ into a well-defined $(H_1(E(f)), \mathbb{Z})$–bigraded R_n–module chain complex once we say how the grading changes when we multiply a generator by U_i. We set

$$A^g(U_i) = -w(\mathrm{O}_i), \quad M(U_i) = -2 \tag{5}$$

and define

$$A^g(U_1^{a_1} \cdots U_n^{a_n} \boldsymbol{x}) = A^g(\boldsymbol{x}) + \sum_{i=1}^{n} a_i A^g(U_i)$$

and

$$M(U_1^{a_1} \cdots U_n^{a_n} \boldsymbol{x}) = M(\boldsymbol{x}) + \sum_{i=1}^{n} a_i M(U_i).$$

We remark that since g is saturated, $A^g(U_i) \neq 0$.

For each $a \in H_1(E(f))$ and $m \in \mathbb{Z}$, let $C^-(g)_{(a,m)}$ be the (vector) subspace of $C^-(g)$ with basis $\{U_1^{a_1} \cdots U_n^{a_n} \boldsymbol{x} \mid A^g(U_1^{a_1} \cdots U_n^{a_n} \boldsymbol{x}) = a,\ M(U_1^{a_1} \cdots U_n^{a_n} \boldsymbol{x}) = m\}$. This gives a bigrading on $C^-(g) = \sum_{(a,m)} C^-(g)_{(a,m)}$.

Proposition 4.18 *The differential ∂^- drops the Maslov grading by one and respects the Alexander grading. That is, $\partial^-\colon C^-(g)_{(a,m)} \to C^-(g)_{(a,m-1)}$ for all $a \in H_1(E(f))$ and $m \in \mathbb{Z}$.*

Proof Consider $U_1^{\mathrm{O}_1(r)} \cdots U_m^{\mathrm{O}_m(r)} \cdot \boldsymbol{y}$ appearing in the boundary of $\boldsymbol{x}$. Since $\boldsymbol{x}$ and $\boldsymbol{y}$ are connected by an empty rectangle r, we see that $M(\boldsymbol{x}) = M(\boldsymbol{y}) + 1 - 2n_{\mathbb{O}(r)}$ by (1). Since each U_i drops the Maslov grading by two, $M(\boldsymbol{x}) = M(U_1^{\mathrm{O}_1(r)} \cdots U_m^{\mathrm{O}_m(r)} \cdot \boldsymbol{y}) + 1$. Thus the differential ∂^- drops the Maslov grading by one.

Next $A^g(\boldsymbol{x}) = A^g(\boldsymbol{y}) + \sum_{\mathbb{X} \cap r} w(\mathrm{X}) - \sum_{\mathbb{O} \cap r} w(\mathrm{O})$, but by definition of the differential $\mathbb{X} \cap r = \varnothing$. So $A^g(\boldsymbol{x}) = A^g(\boldsymbol{y}) - \sum_{\mathbb{O} \cap r} w(\mathrm{O}) = A^g(U_1^{\mathrm{O}_1(r)} \cdots U_m^{\mathrm{O}_m(r)} \cdot \boldsymbol{y})$. Thus the differential ∂^- respects the Alexander grading. □

We are interested in viewing $(C^-(g), \partial^-)$ as a module instead of just a vector space. Using the definition in (5), $\mathbb{F}[U_1, \dots, U_n]$ becomes an $(H_1(E(f)), \mathbb{Z})$–bigraded ring (ie $H_1(E(f)) \oplus \mathbb{Z}$–graded), and with this grading, $(C^-(g), \partial^-)$ is a $(H_1(E(f)), \mathbb{Z})$–bigraded R_n–module chain complex. We would like to define an invariant of the graph grid diagram that is unchanged under any graph grid moves, giving an invariant of the

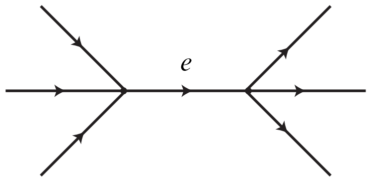

Figure 37: A singular edge e

transverse spatial graph. Since $\mathbb{F}[U_1,\dots,U_n]$ depends on the size of the grid, we need to view $C^-(g)$ as a module over a smaller ring. One choice would be to view $C^-(g)$ as a module over $\mathbb{F}[U_1,\dots,U_{V+E}]$, where $U_1,\dots,U_V$ correspond to the vertices of the graph and $U_{V+1},\dots U_{V+E}$ each correspond to a choice of O on a distinct edge of the graph. However, by Proposition 4.21, multiplication by a U_i corresponding to an edge is chain homotopic either to 0 or to multiplication by a U_j corresponding to a vertex, where $1 \le j \le V$. Thus it makes sense to view $C^-(g)$ as a module over $\mathbb{F}[U_1,\dots,U_V]$ (recall that we ordered $\mathbb{O}$ such that $\mathrm{O}_1,\dots,\mathrm{O}_V$ are vertex O's).

Let $I\colon \mathbb{F}[U_1,\dots,U_V] \to \mathbb{F}[U_1,\dots,U_n]$ be the natural inclusion of rings defined by setting $I(U_i) = U_i$ for $1 \le i \le V$. Using I, any module over $\mathbb{F}[U_1,\dots,U_n]$ naturally becomes an $\mathbb{F}[U_1,\dots,U_V]$–module. Thus, we will view $C^-(g)$ as an R_V–module, where $R_V = \mathbb{F}[U_1,\dots,U_V]$. Note that ∂^- preserves the homology, hence the homology of $(C^-(g),\partial^-)$ inherits the structure of a $(H_1(E(f)),\mathbb{Z})$–bigraded R_V–module.

Definition 4.19 Let g be a saturated graph grid diagram representing the transverse spatial graph $f\colon G \to S^3$. The *graph Floer chain complex* of g is the RA $(H_1(E(f)),\mathbb{Z})$–bigraded R_V–module chain complex $(C^-(g),\partial^-)$. The *graph Floer homology* of g, denoted $\mathrm{HFG}^-(g)$, is the homology of $(C^-(g),\partial^-)$ viewed as an RA $(H_1(E(f)),\mathbb{Z})$–bigraded R_V–module.

Before stating Proposition 4.21, we need some terminology.

Definition 4.20 We say an edge of a graph is *singular* if at each of its endpoints it is the only outgoing edge or the only incoming edge. See Figure 37 for an example.

We note that if a component of the graph is a simple closed curve, then every edge in that component is singular.

Proposition 4.21 (1) *If O_i and O_j are on the interior of the same edge, then multiplication by U_i is chain homotopic to multiplication by U_j.* (2) *If O_i is associated to a vertex with a single outgoing or incoming edge e and O_j is on the interior of e, then multiplication by U_i is chain homotopic to multiplication by U_j.* (3) *If O_i is on* *the interior of an edge that is not singular, then multiplication by U_i is null homotopic. Moreover, each of the chain homotopies is a bigraded R_n–module homomorphism of degree $(-w(\mathrm{O}_i), -1)$.*

Note that this implies that the chain homotopies are also bigraded R_V–module homomorphisms.

Proof Let $\mathrm{X}_k \in \mathbb{X}$. We define $H_k\colon C^-(g) \to C^-(g)$ by counting rectangles that contain X_k but do not contain any other X_s. Specifically,

$$H_k(\boldsymbol{x}) := \sum_{\boldsymbol{y}\in\boldsymbol{S}} \sum_{\substack{r\in\mathrm{Rect}^o(\boldsymbol{x},\boldsymbol{y}),\, \mathrm{X}_k\in r\\ \mathrm{X}_s\notin r\ \forall\, \mathrm{X}_s\in\mathbb{X}\setminus\{\mathrm{X}_k\}}} U_1^{\mathrm{O}_1(r)}\cdots U_n^{\mathrm{O}_n(r)}\cdot\boldsymbol{y}.$$

Note that $H_k\colon C^-(g)_{(a,m)} \to C^-(g)_{(a-w(\mathrm{O}_i),m-1)}$. Suppose that X_k shares a row with O_i and shares a column with O_j. There are three cases we need to consider:

(i) If X_k is the only element of $\mathbb{X}$ in its row and column then, like in the proof of [12, Lemma 2.8], we have that

$$\partial^-\circ H_k + H_k\circ\partial^- = U_i + U_j.$$

(ii) If X_k is the only element of $\mathbb{X}$ in its row but it shares its column with other elements of $\mathbb{X}$, then

$$\partial^-\circ H_k + H_k\circ\partial^- = U_i.$$

The difference here is that the vertical annulus containing X_k also includes another X_s for $s\neq k$. Thus it does not contribute to $\partial^-\circ H_k + H_k\circ\partial^-$.

(iii) Similarly, if X_k is the only element of $\mathbb{X}$ in its column but it shares its row with other elements of $\mathbb{X}$, then

$$\partial^-\circ H_k + H_k\circ\partial^- = U_j.$$

Note that we need not consider the case where X_k shares both its row and column with other elements of $\mathbb{X}$. We use the fact that $w(\mathrm{O}_i) = w(\mathrm{O}_j)$ in parts (1) and (2) and the fact that you can add two chain homotopies to get another chain homotopy to complete the proof. □

In Section 5, we show that $(C^-(g),\partial^-)$, viewed as an RA $(H_1(E(f)),\mathbb{Z})$–bigraded R_V–module chain complex, changes by a quasi-isomorphism under graph grid moves. Thus, its homology is an invariant of the spatial graph and not just the grid representative.

Theorem 4.22 *If g_1 and g_2 are saturated graph grid diagrams representing the same transverse spatial graph $f\colon G \to S^3$ then $(C^-(g_1), \partial^-)$ is quasi-isomorphic to $(C^-(g_2), \partial^-)$ as RA $(H_1(E(f)), \mathbb{Z})$–bigraded R_V–modules. In particular,* $\mathrm{HFG}^-(g_1)$ *is isomorphic to* $\mathrm{HFG}^-(g_2)$ *as RA $(H_1(E(f)), \mathbb{Z})$–bigraded R_V–modules.*

Proof Suppose g_1 and g_2 are saturated graph grid diagrams that are related by a cyclic permutation move. Then they have the same toroidal grid $\mathcal{T}$. Note that there is a natural identification of $\boldsymbol{S}$ for both graph grid diagrams so that $C(g_1) = C(g_2)$ as abelian groups. Let $\boldsymbol{x}, \boldsymbol{y} \in \boldsymbol{S}$. By Corollary 4.14, $A^{g_1}(\boldsymbol{x}) - A^{g_1}(\boldsymbol{y}) = A^{g_2}(\boldsymbol{x}) - A^{g_2}(\boldsymbol{y})$. Hence $A^{g_1}(\boldsymbol{x}) - A^{g_2}(\boldsymbol{x}) = A^{g_1}(\boldsymbol{y}) - A^{g_2}(\boldsymbol{y})$ is a constant a that is independent of element of $\boldsymbol{S}$. By [12, Lemma 2.4], $M(\boldsymbol{x})$ gives the same value for both g_1 and g_2. Thus the identity map id: $C^-(g_1) \to C^-(g_2)$ is an $(H_1(E(f)), \mathbb{Z})$–bigraded R_V–module chain map of degree $(a, 0)$. Thus $(C^-(g_1), \partial^-)$ is quasi-isomorphic to $(C^-(g_1), \partial^-)$ as RA $(H_1(E(f)), \mathbb{Z})$–bigraded R_V–modules. If g_1 and g_2 are saturated graph grid diagrams that are related by a commutation$'$ or stabilization$'$ moves then by Propositions 5.1 and 5.5, $(C^-(g_1), \partial^-)$ is quasi-isomorphic to $(C^-(g_1), \partial^-)$ as RA $(H_1(E(f)), \mathbb{Z})$–bigraded R_V–modules. By Theorem 3.6, g_1 and g_2 are related by a finite sequence of graph grid moves, which completes the proof. □

By Theorem 4.22, the following definitions of $\mathrm{QI}^-(f)$ and $\mathrm{HFG}^-(f)$ are well defined and independent of choice of grid diagram.

Definition 4.23 Let $f\colon G \to S^3$ be a sinkless and sourceless transverse spatial graph. We define $\mathrm{QI}^-(f)$ to be the quasi-isomorphism class of the RA $(H_1(E(f)), \mathbb{Z})$–bigraded R_V–module chain complex $(C^-(g), \partial^-)$, for any saturated graph grid diagram g representing f. The *graph Floer homology* of f, denoted $\mathrm{HFG}^-(f)$, is the homology of $(C^-(g), \partial^-)$ viewed as an RA $(H_1(E(f)), \mathbb{Z})$–bigraded R_V–module, for any saturated graph grid diagram g representing f.

We note that $C^-(g)$ is a finitely generated R_n–module. However, as an R_V–module, it is not finitely generated, but, using Proposition 4.21, we can show that $\mathrm{HFG}^-(f)$ is.

Proposition 4.24 $\mathrm{HFG}^-(f)$ *is a finitely generated R_V–module for any sinkless and sourceless transverse spatial graph $f\colon G \to S^3$.*

Proof The proof is similar to [12, Lemma 2.13]. Let g be a saturated graph grid diagram representing f. We first note that $C^-(g)$ is a finitely generated R_n–module, so $H_*(C^-(g))$ is finitely generated as an R_n–module. Let $[z_1], \dots, [z_r]$ be the generators of $H_*(C^-(g))$ as a finitely generated R_n–module. Let $[c] \in H_*(C^-(g))$. Then we can write $[c] = \sum p_i[z_i]$ for some $p_i \in R_n$. Let $V + 1 \le j \le n$ and $[b] \in \mathrm{HFG}^-(f)$. Then by Proposition 4.21, $U_j[b]$ is either 0 or equal to $U_i[b]$ for some $1 \le i \le V$. Using this repeatedly, it follows that $p_i[z_i] = q_i[z_i]$ for some $q_i \in R_V$. □

4.4 Tilde and hat variants

For a saturated graph grid diagram g, we can define two other variants of $(C^-(g), \partial^-)$. First we define the hat theory. Let $\mathcal{U}_V$ be the $\mathbb{F}$–vector subspace of $C^-(g)$ spanned by $U_1C^-(g) \cup \cdots \cup U_VC^-(g)$. Define $\widehat{C}(g)$ to be the quotient $C^-(g)/\mathcal{U}_V$. Since $\partial^-(\mathcal{U}_V) \subset \mathcal{U}_V$, it follows that ∂^- descends to an R_V–module homomorphism

$$\widehat{\partial}\colon \widehat{C}(g) \to \widehat{C}(g).$$

Since $C^-(g)$ has a basis of homogeneous elements $\{b_i\}_{i\in I}$ as an $\mathbb{F}$–vector space, with respect to the $(H_1(E(f)), \mathbb{Z})$–grading on $C^-(g)$, and $\mathcal{U}_V$ has a basis that is a subbasis of $\{b_i\}_{i\in I}$, the $(H_1(E(f)), \mathbb{Z})$–bigrading on $C^-(g)$ descends to a well-defined $(H_1(E(f)), \mathbb{Z})$–bigrading on $\widehat{C}(g)$.

Definition 4.25 Let g be saturated graph grid diagram representing the sinkless and sourceless transverse spatial graph $f\colon G \to S^3$. The *graph Floer hat chain complex* of g is the $(H_1(E(f)), \mathbb{Z})$–bigraded chain complex $(\widehat{C}(g), \widehat{\partial})$. The *graph Floer hat homology* of g, denoted $\widehat{\mathrm{HFG}}(g)$, is the homology of $(\widehat{C}(g), \widehat{\partial})$ viewed as an $(H_1(E(f)), \mathbb{Z})$–bigraded vector space over $\mathbb{F}$.

For a given sinkless and sourceless transverse spatial graph f, we can use Theorem 4.22 to show that the quasi-isomorphism class (and hence homology) of $(\widehat{C}(g), \widehat{\partial})$ does not depend on the choice of graph grid diagram representing f. The following lemma is well-known but we include it for completeness.

Lemma 4.26 *Let C and D be $\mathbb{F}[U_1, \dots, U_V]$–module chain complexes and let $\phi\colon C \to D$ be an $\mathbb{F}[U_1, \dots, U_V]$–module quasi-isomorphism. Then ϕ descends to a quasi-isomorphism $\widehat{\phi}\colon \widehat{C} \to \widehat{D}$ of $\mathbb{F}$–vector spaces, where $\widehat{C} = C/\mathcal{U}_V$ and $\widehat{D} = D/\mathcal{U}_V$.*

Proof We prove this by induction on V. Suppose $V = 1$. Then ϕ is an $\mathbb{F}[U_1]$–module homomorphism, and ϕ descends to a well-defined chain map $\widehat{\phi}\colon \widehat{C} \to \widehat{D}$. The following diagram commutes and the horizontal sequences are exact:

$$\begin{tikzcd}
0 \arrow[r] & C \arrow[r, "U_1"] \arrow[d, "\phi"] & C \arrow[r, "q"] \arrow[d, "\phi"] & \widehat{C} \arrow[r] \arrow[d, "\widehat{\phi}"] & 0 \\
0 \arrow[r] & D \arrow[r, "U_1"] & D \arrow[r, "q"] & \widehat{D} \arrow[r] & 0
\end{tikzcd}$$

Here U_1 indicates the map that is multiplication by U_1 and q is the quotient map. Thus on homology, we get the following commutative diagram with horizontal long exact sequences:

$$\begin{tikzcd} H_*(C) \arrow[r, "(U_1)_*"] \arrow[d, "\phi_*"'] & H_*(C) \arrow[r, "q_*"] \arrow[d, "\phi_*"'] & H_*(\widehat{C}) \arrow[r] \arrow[d, "\widehat{\phi}_*"'] & H_*(C) \arrow[r, "(U_1)_*"] \arrow[d, "\phi_*"'] & H_*(C) \arrow[d, "\phi_*"'] \\ H_*(D) \arrow[r, "(U_1)_*"] & H_*(D) \arrow[r, "q_*"] & H_*(\widehat{D}) \arrow[r] & H_*(D) \arrow[r, "(U_1)_*"] & H_*(D) \end{tikzcd}$$

Since ϕ_* is an isomorphism, by the five lemma, so is $\widehat{\phi}_*$.

Now suppose the lemma is true for V and let C and D be $\mathbb{F}[U_1,\dots,U_{V+1}]$–module chain complexes and $\phi\colon C \to D$ be an $\mathbb{F}[U_1,\dots,U_{V+1}]$–module quasi-isomorphism. Consider C and D as $\mathbb{F}[U_1,\dots,U_V]$–modules. Then by the inductive hypothesis, $\phi'\colon C/\mathcal{U}_V \to D/\mathcal{U}_V$ is a quasi-isomorphism, where ϕ' is induced from ϕ (which we called $\widehat{\phi}$ before). Moreover, note that ϕ' is an $\mathbb{F}[U_{V+1}]$–module homomorphism. Let $C' = C/\mathcal{U}_V$ and $D' = D/\mathcal{U}_V$. Using the proof from the case when $V=1$, we can show that the induced map $\widehat{\phi}'\colon C'/U_{V+1}C' \to D'/U_{V+1}D'$ is a quasi-isomorphism. It is straightforward to show that the natural map $C/\mathcal{U}_{V+1} \to C'/U_{V+1}C'$ is a chain isomorphism (similarly for D), which completes the proof. □

Corollary 4.27 *If g_1 and g_2 are saturated graph grid diagrams that represent the same transverse spatial graph $f\colon G \to S^3$, then $(\widehat{C}(g_1),\widehat{\partial})$ and $(\widehat{C}(g_2),\widehat{\partial})$ are quasi-isomorphic as RA $(H_1(E(f)),\mathbb{Z})$–bigraded vector spaces. In particular, $\widehat{\mathrm{HFG}}(g_1)$ is isomorphic to $\widehat{\mathrm{HFG}}(g_2)$ as RA $(H_1(E(f)),\mathbb{Z})$–bigraded vector spaces.*

As a result, the following definitions of $\widehat{\mathrm{QI}}(f)$ and $\widehat{\mathrm{HFG}}(f)$ are well-defined and independent of choice of graph grid diagram.

Definition 4.28 Let $f\colon G \to S^3$ be a sinkless and sourceless transverse spatial graph. We define $\widehat{\mathrm{QI}}(f)$ to be the quasi-isomorphism class of the RA $(H_1(E(f)),\mathbb{Z})$–bigraded chain complex $(\widehat{C}(g),\widehat{\partial})$, for any saturated graph grid diagram g representing f. The *graph Floer hat homology* of f, denoted $\widehat{\mathrm{HFG}}(f)$, is the homology of $(\widehat{C}(g),\widehat{\partial})$ viewed as an RA $(H_1(E(f)),\mathbb{Z})$–bigraded vector space over $\mathbb{F}$, for any saturated graph grid diagram g representing f.

Note that $(\widehat{C}(g),\widehat{\partial})$ is an infinitely generated vector space, but in the same way as Proposition 4.24 one can show that its homology is finitely generated.

Proposition 4.29 *$\widehat{\mathrm{HFG}}(f)$ is a finitely generated vector space over $\mathbb{F}$ for any sinkless and sourceless transverse spatial graph $f\colon G \to S^3$.*

Proof Choose a saturated graph grid diagram g representing f. Let j be such that $V+1 \le j \le n$. Then by Proposition 4.21, there is a chain homotopy $H\colon C^-(g) \to C^-(g)$

(H is H_k for some k) that is an R_V–module homomorphism and satisfies one of the following conditions: (i) $\partial^- \circ H + H \circ \partial^- = U_j$ or (ii) there exists an $1 \le i \le V$ such that $\partial^- \circ H + H \circ \partial^- = U_i + U_j$. Since H is an R_V–module homomorphism, H descends to a well-defined $\widehat{H}\colon \widehat{C}(g) \to \widehat{C}(g)$ satisfying

$$\widehat{\partial} \circ \widehat{H} + \widehat{H} \circ \widehat{\partial} = U_j.$$

Therefore $U_j[b] = 0$ for all $[b] \in \widehat{\mathrm{HFG}}(g)$. The rest of the proof is similar to the proof of Proposition 4.24. □

We now define the tilde theory. The tilde theory will be the easiest theory to compute. However, it narrowly fails to be an invariant of the spatial graph since it will depend on the grid size. On the other hand, one can recover the hat theory from it, which makes it quite useful. It will also be easier to compute the bigraded Euler characteristic (Alexander polynomial) of the hat theory using tilde theory; for more details, see Section 6.

Let $\mathcal{U}_n$ be the $\mathbb{F}$–vector subspace of $C^-(g)$ spanned by $U_1 C^-(g) \cup \cdots \cup U_n C^-(g)$. Define $\widetilde{C}(g)$ to be the quotient $C^-(g)/\mathcal{U}_n$. Since $\partial^-(\mathcal{U}_n) \subset \mathcal{U}_n$, it follows that ∂^- descends to a linear map

$$\widetilde{\partial}\colon \widetilde{C}(g) \to \widetilde{C}(g)$$

of vector spaces over $\mathbb{F}$. Since $C^-(g)$ has a basis of homogeneous elements $\{b_i\}_{i \in I}$ as an $\mathbb{F}$–vector space, with respect to the $(H_1(E(f)), \mathbb{Z})$ grading on $C^-(g)$, and $\mathcal{U}_n$ has a basis that is a subbasis of $\{b_i\}_{i \in I}$, the $(H_1(E(f)), \mathbb{Z})$–bigrading on $C^-(g)$ descends to a well-defined $(H_1(E(f)), \mathbb{Z})$–bigrading on $\widetilde{C}(g)$. Thus $(\widetilde{C}(g), \widetilde{\partial})$ is a $(H_1(E(f)), \mathbb{Z})$–bigraded chain complex.

Definition 4.30 Let g be a saturated graph grid diagram representing the sinkless and sourceless transverse spatial graph $f\colon G \to S^3$. The *graph Floer tilde chain complex* of g is the $(H_1(E(f)), \mathbb{Z})$–bigraded chain complex $(\widetilde{C}(g), \widetilde{\partial})$. The *graph Floer tilde homology* of g, denoted $\widetilde{\mathrm{HFG}}(g)$, is the homology of $(\widetilde{C}(g), \widetilde{\partial})$ viewed as an $(H_1(E(f)), \mathbb{Z})$–bigraded vector space over $\mathbb{F}$.

We will relate $\widetilde{\mathrm{HFG}}(g)$ and $\widehat{\mathrm{HFG}}(g)$ for a given graph grid diagram g. First, we recall the (bigraded) mapping cone which we will use in the next lemma.

Let (A, ∂^A) and (B, ∂^B) be $(\mathbb{G}, \mathbb{Z})$–bigraded chain complexes and let $\phi\colon A \to B$ be a bigraded chain map of degree (g, m) for some $g \in \mathbb{G}$ and $m \in \mathbb{Z}$. Define the *(bigraded) mapping cone complex* of ϕ, denoted $(\mathrm{cone}(\phi), \partial)$, as follows:

$$\mathrm{cone}(\phi) = \bigoplus_{(h,n) \in \mathbb{G} \oplus \mathbb{Z}} \mathrm{cone}(\phi)_{(h,n)},$$

where

$$\mathrm{cone}(\phi)_{(h,n)} = A_{(h-g,n-m-1)} \oplus B_{(h,n)}$$

and the boundary map is defined as

$$\partial(a,b) = (-\partial^A(a), -\phi(a) + \partial^B(b))$$

for all $a \in A$ and $b \in B$. Checking the definitions, we see that ∂ is a bigraded map of degree $(0,-1)$. We also note that if A and B are $(\mathbb{G},\mathbb{Z})$–bigraded R–module chain complexes and ϕ is a bigraded R–module chain map then $(\mathrm{cone}(\phi), \partial)$ is an $(\mathbb{G},\mathbb{Z})$–bigraded R–module chain complex.

The following lemma is similar to [12, Lemma 2.14] except now we have bigraded chain complexes instead of filtered graded chain complexes. For $g \in \mathbb{G}$ and $m \in \mathbb{Z}$, let $W(-g,-m+1)$ be the two dimensional $(\mathbb{G},\mathbb{Z})$–bigraded vector space over $\mathbb{F}$ spanned by one generator in degree $(0,0)$ and the other in degree $(-g,-m+1)$. If (C,∂) is any bigraded $(\mathbb{G},\mathbb{Z})$–chain complex over $\mathbb{F}$, then $C \otimes W(-g,-m+1)$ becomes a bigraded chain complex with boundary $\partial \otimes \mathrm{id}$ in the usual way. That is,

$$(C \otimes W(-g,-m+1))_{(h,l)} = \bigoplus_{(h,l)=(h_1+h_2,l_1+l_2)} C_{(h_1,l_1)} \otimes W(-g,-m+1)_{(h_2,l_2)}.$$

Lemma 4.31 *Let (C,∂) be a $(\mathbb{G},\mathbb{Z})$–bigraded $\mathbb{F}[U_1,\dots,U_s]$–module chain complex and $g \in \mathbb{G}$ and $m \in \mathbb{Z}$ be fixed group elements. Suppose that for each $i \geq 2$, multiplication by U_i (which we denote by U_i) is a bigraded $\mathbb{F}[U_1,\dots,U_s]$–module chain map of degree $(-g,-m)$ and that*

(1) *U_i is chain homotopic to U_1 or*
(2) *U_i is null-homotopic (where the chain homotopy is an $\mathbb{F}[U_1,\dots,U_s]$–module homomorphism).*

Then $(C/\mathcal{U}_s, \partial)$ is quasi-isomorphic to $(C/\mathcal{U}_1 \otimes W(-g,-m+1)^{\otimes s-1}, \partial \otimes \mathrm{id})$ and hence

$$H_*(C/\mathcal{U}_s) \cong H_*(C/\mathcal{U}_1) \otimes W(-g,-m+1)^{\otimes s-1}.$$

Note that by $H_*(C/\mathcal{U}_1)$ (respectively $H_*(C/\mathcal{U}_s)$), we mean the homology of the chain complex whose chain group is $C/\mathcal{U}_1$ (respectively $C/\mathcal{U}_s$) and whose boundary map is induced by ∂.

Proof Let $D = C/\mathcal{U}_1 = C/U_1C$ and $\partial^D\colon D \to D$ be induced by ∂. Consider multiplication by U_2 on D, $\widehat{U}_2\colon D \to D$. Since U_1 and U_2 commute, this is a well-defined bigraded map. There is a long exact sequence

$$0 \to D \xrightarrow{\widehat{U}_2} D \xrightarrow{\mathrm{pr}} D/\widehat{U}_2 D \to 0,$$

where pr is the natural projection to the quotient. Let $F\colon \mathrm{cone}(\widehat{U}_2) \to D/\widehat{U}_2 D$ be defined by $F(c_1, c_2) = \mathrm{pr}(c_2)$. By [23, Section 1.5.8], the map F is a quasi-isomorphism. Moreover, F is a bigraded map of degree $(0,0)$.

If U_2 is chain homotopic to U_1 via a chain homotopy H that is an $\mathbb{F}[U_1, \dots, U_s]$–module homomorphism, then H induces a well-defined map $\widehat{H}\colon D \to D$ such that

$$\partial^D \circ \widehat{H} + \widehat{H} \circ \partial^D = \widehat{U}_2.$$

This also holds if U_2 is null-homotopic. Since $\widehat{U}_2$ is null-homotopic, there is a bigraded chain isomorphism from $\mathrm{cone}(\widehat{U}_2)$ to $\mathrm{cone}(0\colon D \to D)$ of degree $(0,0)$. Hence $\mathrm{cone}(\widehat{U}_2)$ is isomorphic to $D \oplus D[g, m-1]$ as bigraded chain complexes, where $D[g, m-1]$ is the bigraded vector space defined by $D[g, m-1]_{(h,n)} = D_{h+g,n+m-1}$ and the boundary map on $D \oplus D[g, m-1]$ is $\partial^D \oplus \partial^D$. Moreover, this is isomorphic, as bigraded chain complexes, to $D \otimes W(-g, -m+1)$. The proof for $n = 2$ is complete after noting that the obvious map $C/\mathcal{U}_2$ to $D/\widehat{U}_2 D$ is a bigraded chain isomorphism. To complete this proof, continue this type of argument, one by one for each U_i. □

We can use this to relate the tilde and hat chain complexes.

Proposition 4.32 *Let g be a saturated graph grid diagram representing the sinkless and sourceless transverse spatial graph $f\colon G \to S^3$. Then*

$$\widetilde{\mathrm{HFG}}(g) \cong \widehat{\mathrm{HFG}}(g) \otimes \bigotimes_{e \in E(G)} W(-w(e), -1)^{\otimes n_e}$$

as $(H_1(E(f)), \mathbb{Z})$–bigraded $\mathbb{F}$–vector spaces, where n_e is the number of O's in g associated to the interior of e (not including the vertices).

Proof We note that if O_i is on the interior of edge e then multiplication by U_i is a graded map of degree $(-w(e), -2)$. In addition, U_i is either null homotopic or homotopic to some U_j with $j \leq V$, where O_j is a vertex. Use Lemma 4.31 repeatedly to complete the proof. □

5 Invariance of $\mathrm{HFG}^-(f)$

In this section we will complete the necessary steps to prove that $\mathrm{HFG}^-(f)$ is an invariant of a sinkless and sourceless transverse spatial graph; see Theorem 4.22 and its proof for more details. That is, we will show that $\mathrm{HFG}^-(g)$ is invariant under each of the graph grid moves: commutation$'$ and stabilization$'$. The proofs will be similar to the proofs found in [12]. There are two major differences though. The first is that we are working with more general commutation and stabilization moves, commutation$'$ and stabilization$'$. The second difference is the Alexander grading.

5.1 Commutation$'$ invariance

Proposition 5.1 *Suppose g and $\bar{g}$ are saturated graph grid diagrams that differ by a commutation$'$ move. Let $f\colon G \to S^3$ be the transverse graph associated to g and $\bar{g}$, and V be the number of vertices of G. Then there is an $(H_1(E(f)), \mathbb{Z})$–bigraded R_V–module quasi-isomorphism $(C(g), \partial_g^-) \to (C(\bar{g}), \partial_{\bar{g}}^-)$ of degree $(\delta(g, \bar{g}), 0)$ for some $\delta(g, \bar{g}) \in H_1(E(f))$.*

We remark that the quasi-isomorphism above will be a bigraded map for some degree (that depends on g and $\bar{g}$), but will not necessarily be of degree $(0, 0)$.

The proof of Proposition 5.1 will take up the rest of this subsection. We will prove the case when $\bar{g}$ is obtained from g by a commutation$'$ move of columns. The case where you exchange rows is similar.

As in [12], we draw both graph grid diagrams on a single $n \times n$ grid (respectively torus when the sides are identified), which we will call the combined grid diagram, as follows. Let the vertical line segment (respectively circle) between the columns that are exchanged be labeled β in g and γ in $\bar{g}$ and call the other vertical circles $\beta_1, \dots, \beta_{n-1}$, where n is the size of the grid for g. Let γ be a simple closed curve on the graph grid diagram g such that the following conditions are held: (1) γ is homotopic to β, (2) γ hits each of the horizontal curves, α_i, precisely once, (3) γ does not intersect β_i for $i \le n-1$, (4) after removing the β curve, one obtains $\bar{g}$, (5) γ and β intersect transversely exactly twice, and (6) the intersections of γ and β do not lie on the horizontal curves. It is easy to use the line segments LS_1 and LS_2 in the definition of commutation$'$ to see that such a curve exists. First, note that we can assume the endpoints of the line segments do not lie on α curves by slightly changing them. Now, take pushoffs of the line segments LS_1 and LS_2 to the left or right as needed, and connect them up so that they satisfy the requirements above. Let a and b be the intersections of β and γ. See Figures 38 and 39 for examples. We still let $\mathcal{T}$ be the torus of the combined grid diagram obtained by gluing the top/bottom and sides.

We will define a chain map $\Phi_{\beta\gamma}\colon C^-(g) \to C^-(\bar{g})$ and show that it is a chain homotopy equivalence. This will show that $\Phi_{\beta\gamma}$ is a quasi-isomorphism. For $\boldsymbol{x} \in \boldsymbol{S}(g)$ and $\boldsymbol{y} \in \boldsymbol{S}(\bar{g})$, we let $\mathrm{Pent}_{\beta\gamma}(\boldsymbol{x}, \boldsymbol{y})$ be the set of embedded pentagons with the following

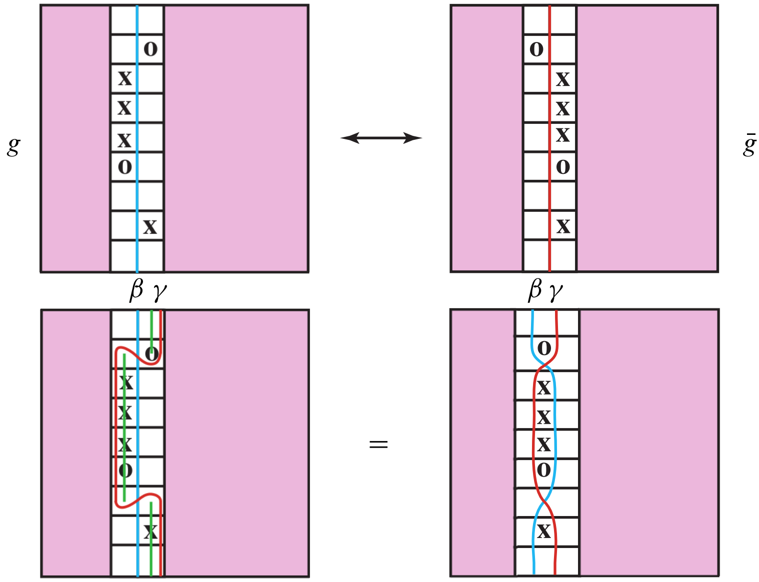

Figure 38: Commutation′ move between g and $\bar{g}$ (top), and the corresponding combined grid diagram, where we show the line segments in the definition of commutation′ on the left (bottom)

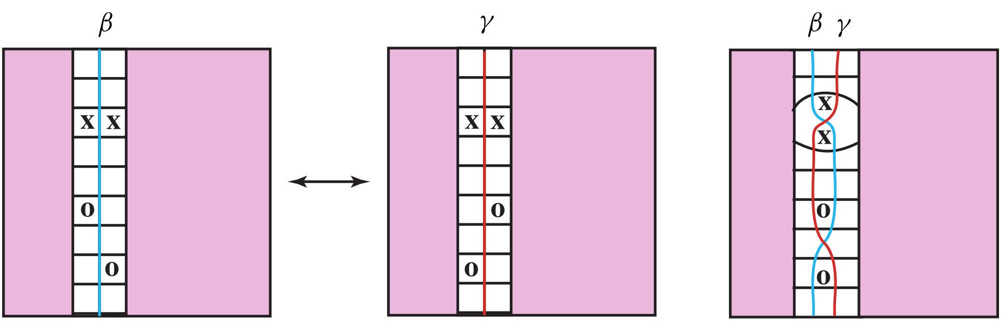

Figure 39: Another example of a commutation′ move, in which the X's appear in the same row; from left to right we have g, $\bar{g}$ and the combined grid diagram

properties. If $\boldsymbol{x}$ and $\boldsymbol{y}$ do not coincide at $n-2$ points, then we let $\mathrm{Pent}_{\beta\gamma}(\boldsymbol{x},\boldsymbol{y})=\varnothing$. Suppose that $\boldsymbol{x}$ and $\boldsymbol{y}$ coincide at $n-2$ points (say $x_3=y_3,\dots,x_n=y_n$). Without loss of generality, let $x_2=\boldsymbol{x}\cap\beta$ and $y_2=\boldsymbol{y}\cap\gamma$. An element $p\in\mathrm{Pent}_{\beta\gamma}(\boldsymbol{x},\boldsymbol{y})$ is an embedded disk in $\mathcal{T}$, whose boundary consists of five arcs, each of which are contained in the circles β_i, α_i, β or γ and satisfies the following conditions. The intersections of the arcs lie on the points x_1, x_2, y_1, y_2 and a. The point a is in $\beta\cap\gamma$ and locally looks like the top intersection in Figure 40 (b is the one that locally looks the bottom

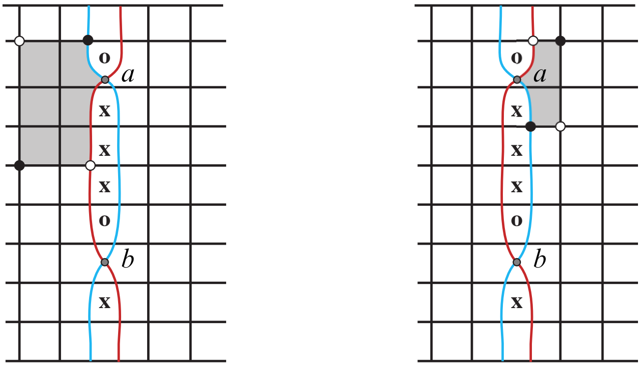

Figure 40: Examples of pentagons in $\mathrm{Pent}^o_{\beta\gamma}(\boldsymbol{x},\boldsymbol{y})$

intersection point in $\beta \cap \gamma$). Moreover, start at the point in x_2 and transverse the boundary of p, using the orientation given by p. The condition to be in $\mathrm{Pent}_{\beta\gamma}(\boldsymbol{x},\boldsymbol{y})$ is that you will first travel along a horizontal circle, meet y_1, proceed along a vertical circle β_i, meet x_1, continue along another horizontal circle, meet y_2, proceed though an arc in γ until you meet a, and finally traverse an arc in β until arriving back at x_2. Finally, all angles are required to be less than straight.

The set of empty pentagons, $\mathrm{Pent}^o_{\beta\gamma}(\boldsymbol{x},\boldsymbol{y})$, are those pentagons $p \in \mathrm{Pent}_{\beta\gamma}(\boldsymbol{x},\boldsymbol{y})$ such that $\boldsymbol{x} \cap \mathrm{Int}(p) = \varnothing$. The map $\Phi_{\beta\gamma}\colon C^-(g) \to C^-(\bar{g})$ is defined by counting empty pentagons, that do not contain X's in the combined grid diagram as follows. For $\boldsymbol{x} \in \boldsymbol{S}(g)$, define

$$\Phi_{\beta\gamma}(\boldsymbol{x}) = \sum_{\boldsymbol{y}\in\boldsymbol{S}(\bar{g})} \sum_{\substack{p\in\mathrm{Pent}^o_{\beta\gamma}(\boldsymbol{x},\boldsymbol{y}) \\ \mathrm{Int}(p)\cap\mathbb{X}=\varnothing}} U_1^{O_1(p)} \cdots U_n^{O_n(p)} \cdot \boldsymbol{y} \in C^-(\bar{g}).$$

Extend $\Phi_{\beta\gamma}$ to $C^-(g)$ so that it is an R_n–module homomorphism. In particular, it is also an R_V–module homomorphism.

Lemma 5.2 *$\Phi_{\beta\gamma}$ is an $(H_1(E(f)),\mathbb{Z})$–bigraded R_V–module chain map of some degree.*

Proof Since $\Phi_{\beta\gamma}$ is an R_V–module homomorphism, the proof is broken into three parts: checking that each grading is preserved, and showing that

$$\partial^- \circ \Phi_{\beta\gamma} = \Phi_{\beta\gamma} \circ \partial^-.$$

The map $\Phi_{\beta\gamma}$ preserves the Maslov grading Since the definition of the Maslov grading only depends on the set $\mathbb{O}$, and we consider a subset of the pentagons considered

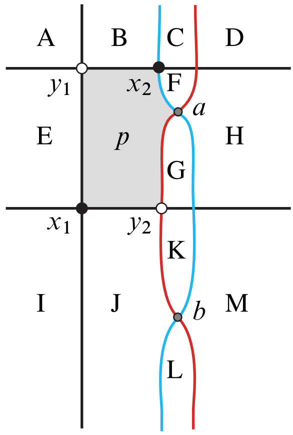

Figure 41: The combined grid diagram, with regions A, ..., M labeled and the pentagon p shaded

in the proof of commutation in [12, Section 3.1], this technically follows from [12, Lemma 3.1]. However, since they do not include a proof that the Maslov grading is preserved (this is left to the reader), we will include a sketch of the proof here.

We will go though the details of this computation for the case pictured in Figure 41, other cases follow similarly. Consider a $U_1^{O_1(p)} \cdots U_n^{O_n(p)} \cdot \boldsymbol{y}$ in the sum of $\Phi_{\beta\gamma}(\boldsymbol{x})$. Recall that

$$M(\boldsymbol{x}) = \mathcal{J}(\boldsymbol{x}, \boldsymbol{x}) - 2\mathcal{J}(\boldsymbol{x}, \mathbb{O}) + \mathcal{J}(\mathbb{O}, \mathbb{O}) + 1.$$

To compare the Maslov grading we interpret each of these terms for $\boldsymbol{x}$ in the grid g in relation to $\boldsymbol{y}$ in the grid $\bar{g}$. Let the intersection points of $\boldsymbol{x}$ be $x_1, \dots, x_n$ and the intersection points of $\boldsymbol{y}$ be $y_1, \dots, y_n$, with the same subscript where they coincide. Label the intersection points where $\boldsymbol{x}$ and $\boldsymbol{y}$ differ as x_1, x_2, y_1 and y_2 and break the combined grid diagram into 14 regions labeled A, ..., M, and p, as shown in Figure 41.

Notice that the count for x_i is the same as y_i for $i \neq 1, 2$. The number of points in $\mathbb{O}$ up and to the right, and down and to the left are not changed, since this could only be changed for an intersection between the commuted edges (ie x_2 or y_2). So $\mathcal{J}(x_i, \mathbb{O}) = \mathcal{J}(y_i, \mathbb{O})$. The number of points in $\boldsymbol{x}$ and $\boldsymbol{y}$ up and to the right and down and to the left are the same, this can be checked region by region. If an intersection point is in region E then x_2 will be counted in the points up and to the right; this is replaced by the point y_1 which is also up and to the right. Similarly, for all of the regions, since $x_i = y_i \in \{\mathrm{A}, \mathrm{B}, \dots, \mathrm{M}\}$, we have $\mathcal{J}(x_i, \boldsymbol{x}) = \mathcal{J}(y_i, \boldsymbol{y})$ for all $i \neq 1, 2$.

Now for the points where $\boldsymbol{x}$ and $\boldsymbol{y}$ differ, Figure 42 (left) shows the regions that are counted for x_1 and x_2, and Figure 42 (right) shows the regions that are counted for

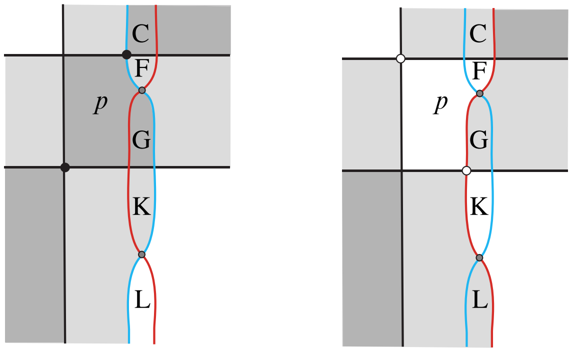

Figure 42: The lightly shaded regions are those that will be counted with weight one half in $\mathcal{J}(x_1, -)$ and $\mathcal{J}(x_2, -)$ (left), or in $\mathcal{J}(y_1, -)$ and $\mathcal{J}(y_2, -)$ (right).

y_1 and y_2. So we see that the regions C, F, G and K are counted with weight $\frac{1}{2}$ more for x_1 and x_2, and the region p is counted with weight 1 more for x_1 and x_2 and, lastly, region L is counted with weight $\frac{1}{2}$ less for x_1 and x_2. So,

$$\mathcal{J}(\boldsymbol{x}, \boldsymbol{x}) = \mathcal{J}(\boldsymbol{y}, \boldsymbol{y}) + 1,$$

because x_1 will count x_2 with weight $\frac{1}{2}$ and vice versa, but y_1 and y_2 do not count each other. Next, $\boldsymbol{x}$ will count all of the points in $\mathbb{O}$ that $\boldsymbol{y}$ will count and, additionally, will count those O's in the region p with weight 1, those O's in the regions C, F, G, and K with weight $\frac{1}{2}$ and those O's in the region L with weight $-\frac{1}{2}$. Notice that the region made up of G and K must contain exactly one O. Thus,

$$\mathcal{J}(\boldsymbol{x}, \mathbb{O}) = \mathcal{J}(\boldsymbol{y}, \mathbb{O}) + \mathrm{O}_1(p) + \cdots + \mathrm{O}_n(p) + \tfrac{1}{2}(\mathrm{O}(C) + \mathrm{O}(F) + 1) - \tfrac{1}{2}\mathrm{O}(L),$$

where $\mathrm{O}(C)$, $\mathrm{O}(F)$, and $\mathrm{O}(L)$ are the number of O's in the respective regions.

Lastly, if we look at what happens for the different diagrams with the sets of $\mathbb{O}$, the only difference is for the O's in the columns that are changed. Again we know that there is exactly one O in the regions G and K. So we have

$$\mathcal{J}(\mathbb{O}, \mathbb{O})_g = \mathcal{J}(\mathbb{O}, \mathbb{O})_{\bar{g}} + \mathrm{O}(C) + \mathrm{O}(F) - \mathrm{O}(L).$$

Putting this all together, we have

$$\begin{aligned} M(\boldsymbol{x}) = [\mathcal{J}(\boldsymbol{y}, \boldsymbol{y}) + 1]& \\ &- 2[\mathcal{J}(\boldsymbol{y}, \mathbb{O}) + \mathrm{O}_1(p) + \cdots + \mathrm{O}_n(p) + \tfrac{1}{2}(\mathrm{O}(C) + \mathrm{O}(F) + 1) - \tfrac{1}{2}\mathrm{O}(L)] \\ &+ [\mathcal{J}(\mathbb{O}, \mathbb{O})_{\bar{g}} + \mathrm{O}(C) + \mathrm{O}(F) - \mathrm{O}(L)] + 1 \\ = \mathcal{J}(\boldsymbol{y}, \boldsymbol{y})& - 2\mathcal{J}(\boldsymbol{y}, \mathbb{O}) + \mathcal{J}(\mathbb{O}, \mathbb{O})_{\bar{g}} - 2[\mathrm{O}_1(p) + \cdots + \mathrm{O}_n(p)] + 1 \\ = \mathcal{J}(\boldsymbol{y} - \mathbb{O}&, \boldsymbol{y} - \mathbb{O}) + 1 - 2[\mathrm{O}_1(p) + \cdots + \mathrm{O}_n(p)]. \end{aligned}$$

Thus we see that the Maslov grading is unchanged.

The map $\Phi_{\beta\gamma}$ preserves the Alexander grading up to a shift Now, consider the $H_1(E(f))$–grading on $C^-(g)$, $C^-(g)=\bigoplus_{a\in H_1(E(f))}C^-(g)_a$ (similarly for $C^-(\bar{g})$). We will show that there is an element $\delta(g,\bar{g})$ that only depends on g and $\bar{g}$ (not on $\boldsymbol{x}$) such that $\Phi_{\beta\gamma}(C^-(g)_a)\subset C^-(\bar{g})_{a+\delta(g,\bar{g})}$. We will work with the second definition of the Alexander grading, $A^g(\boldsymbol{x})=\sum_{x_i\in\boldsymbol{x}}[-h^g(x_i)]$ to prove this.

Let $\boldsymbol{x}\in\boldsymbol{S}(g)$ and $p\in\mathrm{Pent}^o_{\beta\gamma}(\boldsymbol{x},\boldsymbol{y})$ such that $p\cap\mathbb{X}=\varnothing$ and $\mathrm{Pent}^o_{\beta\gamma}(\boldsymbol{x},\boldsymbol{y})\neq\varnothing$. Then $U_1^{\mathrm{O}_1(p)}\cdots U_n^{\mathrm{O}_n(p)}\cdot\boldsymbol{y}$ is a term in $\Phi_{\beta\gamma}(\boldsymbol{x})$. We use the convention as before that $x_i=y_i$ for $i\geq 3$, $x_2\in\beta$, and $y_2\in\gamma$. We note that $h^g(x_i)=h^{\bar{g}}(y_i)$ for $i\geq 3$. So we need to show that

$$h^g(x_1)+h^g(x_2)-h^{\bar{g}}(y_1)-h^{\bar{g}}(y_2)-\sum_{i=1}^{n}w(\mathrm{O}_i)\mathrm{O}_i(p)=\delta(g,\bar{g}) \tag{6}$$

for some fixed $\delta(g,\bar{g})\in H_1(E(f))$.

We will prove the case when a is the topmost intersection of β and γ and p is a pentagon lying to the left of a. See two examples of these pentagons in Figure 43. Note that the boundary of the pentagon can contain b, and p can contain an O that lies between β and γ. The other three cases are similar. Let β_{n-1} be the vertical line segment/circle in g directly to the left of β, and β_1 be the vertical line segment/circle in g directly to the right of β. We will label the α_i in the usual way so that α_i is height $i-1$. Let α_l be the horizontal line segment/circle directly below b, α_{l+1} be the horizontal line segment/circle directly above b, α_k be the horizontal circle directly below a, and α_{k+1} be the horizontal line segment/circle directly above a. Finally, let u_1 be the point on β_{n-1} that is at the same height as x_1 and let u_2 be the point on β_{n-1} that is at the same height as x_2. See Figures 43 and 44 for our conventions.

We will say that the pentagon p is narrow if $y_1\in\beta_{n-1}$. If p is not narrow, then there is a rectangle in g that is contained in p. Let r be the largest such rectangle. Then p decomposes into r and a narrow pentagon p'. Note that $r\in\mathrm{Rect}^o(\{x_1,u_2\},\{u_1,y_1\})$ and $p'\in\mathrm{Pent}^o(\{x_2,u_1\},\{y_2,u_2\})$. Moreover, $r\cap\mathbb{X}=p\cap\mathbb{X}=\varnothing$. Since the boundary map on $C^-(g)$ preserves the Alexander grading, we see that

$$h^g(x_1)+h^g(u_2)=\sum_{i=1}^{n}w(\mathrm{O}_i)\mathrm{O}_i(r)+h^g(y_1)+h^g(u_1).$$

We consider $h^g(x_2)-h^g(u_2)$ and $h^{\bar{g}}(y_2)-h^{\bar{g}}(u_1)=h^{\bar{g}}(y_2)-h^g(u_1)$.

In order to compute h^g or $h^{\bar{g}}$, draw the transverse spatial graph for g and g' so that the horizontal and vertical arcs connecting the X's and O's are inside the grid, and

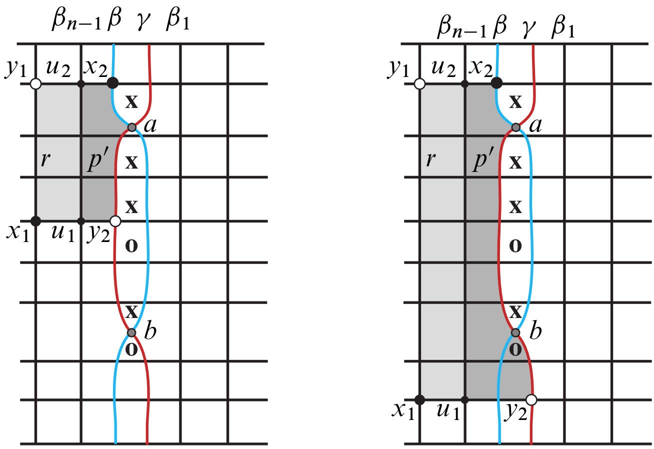

Figure 43: Decomposing p into a narrow pentagon p' and a rectangle r

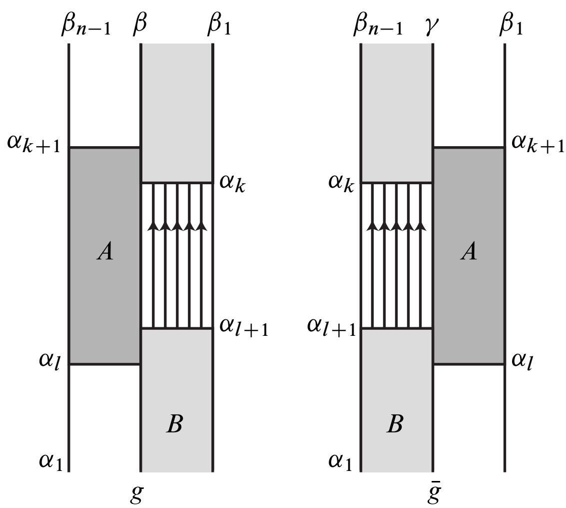

Figure 44: A commutation$'$ move; regions A and B contain X's and O's

consider their projections $\mathrm{pr}(g)$ and $\mathrm{pr}(g')$. We will think of column $n-1$ as the column with β_{n-1} on the left and column n as the column with β or γ on the left. Assume that LS_1 lies inside column $n-1$ and LS_2 lies in column n. Let A be the union of rectangles containing LS_1 and B be the union of rectangles containing LS_2 (recall, we are assuming the ends of LS_i do not lie on an α curve). Then the X's and O's in columns $n-1$ and n are contained in $A \cup B$ and projections of A and B intersect in the two rows that contain a and b. Since there are no X's or O's in $\mathrm{col}_n \backslash B$, the vertical arcs in $\mathrm{pr}(g) \cap (\mathrm{col}_n \setminus B)$ form a collection of parallel arcs starting and stopping at α_k and α_{k+1} which are all oriented in the same direction (all upwards or all downwards). In addition, $\mathrm{pr}(g) \cap (\mathrm{col}_{n-1} \setminus A)$ is empty. See Figure 44.

Let O' be the O in column $n-1$ of g and let O'' be the O in column $n-1$ of $\bar{g}$. Note that p' either contains O' or O'' or both or is empty (in particular, it never contains an element of $\mathbb{X}$). We first consider $h^g(x_2)-h^g(u_2)$. There are three cases. First suppose $x_2\in\alpha_i$ for $i\geq k+1$ or $i\leq l$. Then $h^g(x_2)-h^g(u_2)=0$ since the region above and below A in g contains no vertical arcs in $\mathrm{pr}(g)$. In addition, we see that p' cannot contain O' so that $h^g(x_2)-h^g(u_2)=0=\mathrm{O}'(p')w(\mathrm{O}')$ where by $\mathrm{O}'(p')$, we mean the number of O's in p'. Now suppose $x_2\in\alpha_i$ for $l+1\leq i\leq k$. If p' does not contain O' then $h^g(x_2)-h^g(u_2)=0=\mathrm{O}'(p')w(\mathrm{O}')$. If p' contains O' then the arc going from u_2 to x_2 crosses all the vertical strands emanating from this O, all oriented downwards, since p' does not contain any X's. Thus, $h^g(x_2)-h^g(u_2)=\mathrm{O}'(p')w(\mathrm{O}')$. Thus, in all cases, we see that $h^g(x_2)-h^g(u_2)=\mathrm{O}'(p')w(\mathrm{O}')$.

Now consider $h^{\bar{g}}(y_2)-h^{\bar{g}}(u_1)$. We again have three cases to consider. First suppose that $y_2\in\alpha_j$ for $l+1\leq j\leq k$. Then the arc from u_1 to y_2 crosses m vertical arcs, all oriented in the same direction so $h^{\bar{g}}(y_2)-h^{\bar{g}}(u_1)=\eta$ for some $\eta\in H_1(E(f))$. In addition, $\mathrm{O}''(p)=0$ so that $h^{\bar{g}}(y_2)-h^{\bar{g}}(u_1)=\eta-\mathrm{O}''(p')w(p')$. Now suppose that $x_2\in\alpha_i$ for $i\geq k+1$ or $i\leq l$. If p' does not contain O'' then $h^{\bar{g}}(y_2)-h^{\bar{g}}(1_2)=\eta=\eta-\mathrm{O}''(p')w(p')$. If p' contains O'', $h^{\bar{g}}(y_2)-h^{\bar{g}}(u_1)=\eta-w(\mathrm{O}'')$. Thus, in all cases, $h^{\bar{g}}(y_2)-h^{\bar{g}}(u_1)=\eta-\mathrm{O}''(p')w(p')$.

Putting this together and using that $h^{\bar{g}}(y_1)=h^g(y_1)$ and $h^{\bar{g}}(u_1)=h^g(u_1)$, we have

$$\begin{aligned}
&h^g(x_1)+h^g(x_2)-h^{\bar{g}}(y_1)-h^{\bar{g}}(y_2)\\
&\qquad=(h^g(x_1)\ +h^g(u_2))-(h^g(y_1)+h^g(u_1))\\
&\qquad\qquad+(h^g(x_2)-h^g(u_2))-(h^{\bar{g}}(y_2)-h^{\bar{g}}(u_1))\\
&\qquad=\sum_{i=1}^n w(\mathrm{O}_i)\mathrm{O}_i(r)+\mathrm{O}'(p')w(\mathrm{O}')-(\eta-\mathrm{O}''(p')w(p'))\\
&\qquad=\sum_{i=1}^n w(\mathrm{O}_i)\mathrm{O}_i(p)-\eta.
\end{aligned}$$

Thus, (6) holds with $\delta(g,\bar{g})=-\eta$ which completes the proof that $\Phi_{\beta\gamma}$ is a graded map (with respect to the Alexander grading).

$\Phi_{\beta\gamma}$ is a chain map The remaining portion of the proof that $\Phi_{\beta\gamma}$ is a chain map follows almost immediately from the proof of [12, Lemma 3.1]. However, our pentagons and rectangles cannot count X's so we need to be a little more careful.

For $\boldsymbol{x}\in\boldsymbol{S}(g)$, there is a unique element $c(\boldsymbol{x})$ of $\boldsymbol{S}(\bar{g})$, called the canonical closest generator of $\boldsymbol{x}$, defined as follows. Let t be such that $\boldsymbol{x}\cap\beta\in\alpha_t$ and let x' be the point in $\alpha_t\cap\gamma$. Define

$$c(\boldsymbol{x}):=\{x_i\in\boldsymbol{x}\mid x_i\notin\beta\}\cup\{x'\}\in\boldsymbol{S}(\bar{g}).$$

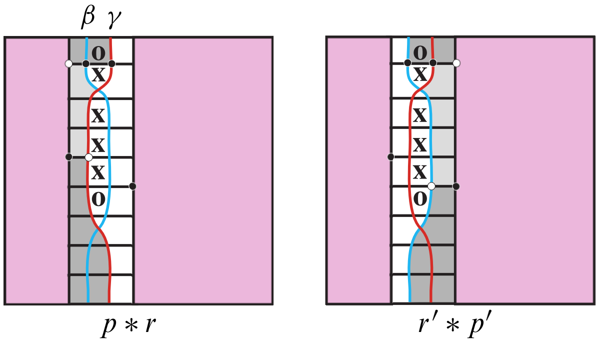

Figure 45: An example of two domains connecting $\boldsymbol{x}$ to $c(\boldsymbol{x})$. The generators $\boldsymbol{x}$ and $c(\boldsymbol{x})$ are both in black circles; they only disagree on one row.

Suppose D is a domain of the form $p * r$ representing a term in $\partial^- \circ \Phi_{\beta,\gamma}(\boldsymbol{x})$ and D connects $\boldsymbol{x}$ to $\boldsymbol{y}$ with $\boldsymbol{y} \neq c(\boldsymbol{x})$. By this, we mean to consider the juxtaposition of the pentagon p connecting $\boldsymbol{x}$ to $\boldsymbol{z}$ and the rectangle r connecting $\boldsymbol{z}$ to $\boldsymbol{y}$, in the combined grid diagram. Note that the domain does not contain any element of $\mathbb{X}$. Then there is exactly one other empty rectangle r' (in g or $\bar{g}$) and empty pentagon p' such that $r' * p'$ or $p' * r'$ gives a decomposition of D. Note that most of the time the other decomposition is of the form $r' * p'$. To see this, one just needs to draw every possible domain of the form $p * r$ and $r * p$, where r is an empty rectangle (in g or $\bar{g}$) and p is an empty pentagon. In addition since p' and r' will be contained in D, they will not contain any element of $\mathbb{X}$ so $r' * p'$ or $p' * r'$ will represent an element of $\Phi_{\beta,\gamma} \circ \partial^-$ or $\partial^- \circ \Phi_{\beta,\gamma}$. The same statement is true if you start with a domain D of the form $r * p$ representing a term in $\partial^- \circ \Phi_{\beta,\gamma}(\boldsymbol{x})$ as long as D connects $\boldsymbol{x}$ to $\boldsymbol{y}$ with $\boldsymbol{y} \neq c(\boldsymbol{x})$.

Suppose D is a domain of the form $p * r$ representing a term in $\partial^- \circ \Phi_{\beta,\gamma}(\boldsymbol{x})$ and D connects $\boldsymbol{x}$ to $c(\boldsymbol{x})$. Then D consists of two regions C and E, where C is the region that lies to the left of both γ and β and to the right of β_{n-1}, and E is a subset of the region that lies to the right of β and to the left of γ. Note that the $C \cap \mathbb{O} = C \cap \mathbb{X} = E \cap \mathbb{X} = \varnothing$. There is exactly one other domain D' connecting $\boldsymbol{x}$ to $c(\boldsymbol{x})$ of the form $p' * r'$ or $r' * p'$. See Figure 45 for an example. This domain consists of a region C' and E, where C' is the region that lies to the right of both γ and β and to the left of β_1. Note that $C' \cap \mathbb{X} = C' \cap \mathbb{X} = \varnothing$ and so $\mathrm{O}_i(D) = \mathrm{O}_i(D')$ and $D' \cap \mathbb{X} = \varnothing$. Thus D' represents an element of $\Phi_{\beta,\gamma} \circ \partial^-(\boldsymbol{x})$ or $\partial^- \circ \Phi_{\beta,\gamma}(\boldsymbol{x})$. A similar statement holds for domain of the form $p * r$ representing a term in $\partial^- \circ \Phi_{\beta,\gamma}(\boldsymbol{x})$ and connecting $\boldsymbol{x}$ to $c(\boldsymbol{x})$. Thus, every term is canceled by another. So $\partial^- \circ \Phi_{\beta\gamma}(\boldsymbol{x}) = \Phi_{\beta\gamma} \circ \partial^-(\boldsymbol{x})$. $\square$

In order to prove that $\Phi_{\beta\gamma}$ is a chain homotopy equivalence we define a similar map $H_{\beta\gamma\beta}$ which counts hexagons in the combined grid diagram. These hexagons are just like the ones in [12] except they don't contain elements of $\mathbb{X}$. We recall the definition. For $\boldsymbol{x}, \boldsymbol{y} \in \boldsymbol{S}(g)$, let $\mathrm{Hex}_{\beta\gamma\beta}(\boldsymbol{x}, \boldsymbol{y})$ be the set of embedded hexagons defined as follows. If $\boldsymbol{x}$ and $\boldsymbol{y}$ don't coincide at $n-2$ points then $\mathrm{Hex}_{\beta\gamma\beta}(\boldsymbol{x}, \boldsymbol{y})$ is the empty set. Suppose that $\boldsymbol{x}$ and $\boldsymbol{y}$ coincide at $n-2$ points (say $x_3 = y_3, \cdots, x_n = y_n$). Without loss of generality, let $x_2 = \boldsymbol{x} \cap \beta$ and $y_2 = \boldsymbol{y} \cap \gamma$. An element $\mathcal{H} \in \mathrm{Hex}_{\beta\gamma\beta}(\boldsymbol{x}, \boldsymbol{y})$ is an embedded disk in the combined grid diagram, whose boundary consists of six arcs, each of which are contained in the circles β_i, α_i, β or γ and satisfies the following conditions. The intersections of the arcs lie on the points of x_1, x_2, y_1, y_2, a and b. Moreover, start at the point in x_2 and transverse the boundary of $\mathcal{H}$, using the orientation given by $\mathcal{H}$. The condition to be in $\mathrm{Hex}_{\beta\gamma\beta}(\boldsymbol{x}, \boldsymbol{y})$ is that you will first travel along a horizontal circle, meet y_1, proceed along a vertical circle β_i, meet x_1, continue along another horizontal circle, meet y_2, proceed though an arc in β until you meet b, then travel along an arc in γ until you hit a and finally travel along an arc in β until arriving back at x_2. Finally, all angles are required to be less than straight. For $\boldsymbol{x}, \boldsymbol{y} \in \boldsymbol{S}(\bar{g})$, there is a corresponding set of hexagons $\mathrm{Hex}_{\gamma\beta\gamma}(\boldsymbol{x}, \boldsymbol{y})$. The set of empty pentagons $\mathrm{Hex}^o_{\beta\gamma\beta}$ are those hexagons $q \in \mathrm{Hex}_{\beta\gamma\beta}(\boldsymbol{x}, \boldsymbol{y})$ where $\boldsymbol{x} \cap \mathrm{Int}(q) = \varnothing$. Define $H_{\beta\gamma\beta}\colon C^-(g) \to C^-(g)$ by

$$H_{\beta\gamma\beta}(\boldsymbol{x}) = \sum_{\boldsymbol{y} \in \boldsymbol{S}(g)} \sum_{\substack{q \in \mathrm{Hex}^o_{\beta\gamma\beta}(\boldsymbol{x}, \boldsymbol{y}) \\ \mathrm{Int}(q) \cap \mathbb{X} = \varnothing}} U_1^{O_1(q)} \cdots U_n^{O_n(q)} \cdot \boldsymbol{y}.$$

Proposition 5.3 *The map $\Phi_{\beta\gamma}\colon C^-(g) \to C^-(\bar{g})$ is a chain homotopy equivalence.*

Proof To prove this, we show that

$$\mathrm{Id} + \Phi_{\gamma\beta} \circ \Phi_{\beta\gamma} + \partial^- \circ H_{\beta\gamma\beta} + H_{\beta\gamma\beta} \circ \partial^- = 0$$

and

$$\mathrm{Id} + \Phi_{\beta\gamma} \circ \Phi_{\gamma\beta} + \partial^- \circ H_{\gamma\beta\gamma} + H_{\gamma\beta\gamma} \circ \partial^- = 0.$$

The proof is similar to the proof of [12, Proposition 3.2]. Let $\boldsymbol{x} \in S(g)$. Typically, every domain that arises as the composition of two empty pentagons or an empty hexagon and an empty rectangle representing terms from $\Phi_{\gamma\beta} \circ \Phi_{\beta\gamma}(\boldsymbol{x})$, $\partial^- \circ H_{\beta\gamma\beta}(\boldsymbol{x})$ or $H_{\beta\gamma\beta} \circ \partial^-(\boldsymbol{x})$ can be decomposed in exactly two ways representing terms from $\Phi_{\gamma\beta} \circ \Phi_{\beta\gamma}(\boldsymbol{x})$, $\partial^- \circ H_{\beta\gamma\beta}(\boldsymbol{x})$ or $H_{\beta\gamma\beta} \circ \partial^-(\boldsymbol{x})$. The only case when this does not happen is when the domain connects $\boldsymbol{x}$ to $\boldsymbol{x}$. In this case, the domain consists of the region that is either (1) to the left of both γ and β and to the right of β_{n-1} or (2) to the right of both γ and β and to the left of β_1. Such a domain can be decomposed in three ways representing terms in $\Phi_{\gamma\beta} \circ \Phi_{\beta\gamma}(\boldsymbol{x})$, $\partial^- \circ H_{\beta\gamma\beta}(\boldsymbol{x})$ or $H_{\beta\gamma\beta} \circ \partial^-(\boldsymbol{x})$. The other case follows similarly. □

Remark 5.4 $H_{\beta\gamma\beta}$ is a $(H_1(E(f)),\mathbb{Z})$–bigraded R_V–module homomorphism of degree $(0,1)$. Therefore $(C(g),\partial)$ and $(C(\bar{g}),\partial)$ are chain homotopy equivalent as bigraded R_V–module chain complexes.

5.2 Stabilization′ invariance

Proposition 5.5 *Suppose g and $\bar{g}$ are saturated graph grid diagrams that differ by a stabilization′ move. Let $f\colon G\to S^3$ be the transverse graph associated to g and $\bar{g}$ and V be the number of vertices of G. Then there is an $(H_1(E(f)),\mathbb{Z})$–bigraded R_V–module quasi-isomorphism $(C(g),\partial_g^-)\to(C(\bar{g}),\partial_{\bar{g}}^-)$ of degree $(\delta(g,\bar{g}),0)$ for some $\delta(g,\bar{g})\in H_1(E(f))$.*

The proof of Proposition 5.5 will take up the rest of this section. The proof of stabilization′ is similar to the proof of stabilization in [12]. However, because of the fact that we only have a graded theory instead of a filtered theory, the proof becomes drastically simplified. We also fill in some of the details and clarify some of the arguments in the proof of [12]. We will only prove the case for row stabilization′. The proof of column stabilization′ is similar.

Let g be a graph grid diagram and $\bar{g}$ be obtained from g by a row stabilization′ move. An example of a row stabilization′ move is shown in Figure 46. To get $\bar{g}$, we take some row $\boldsymbol{R}$ in g with l X's, delete it and replace it with two new rows and then add a new column. We place $\mathrm{O}_k,\mathrm{X}_{j_2},\dots,\mathrm{X}_{j_l}$ into one of the new rows (and in the same columns as before) and X_{j_1} into the other new row (and in the same column as before). We place decorations O_n and X_m into the new column so that O_n occupies the same row as X_{j_1}, and X_m occupies the same row as O_k. By Remark 3.4, we may assume that X_{j_1}, X_m and O_n share a corner, called $\star$, where X_{j_1} is directly to the left of O_n, and O_n is directly above X_m; see Figure 46. Let β_n be the vertical grid circle directly to the left of O_n and let β_1 be the vertical grid circle directly to the right of O_n. Let α_n be the horizontal grid circle to between O_n and X_m.

Let $(B,\partial_B)=(C^-(g),\partial_g^-)$ and $(C,\partial_C)=(C^-(\bar{g}),\partial_{\bar{g}}^-)$. Let $(B[U_n],\partial_B)$ be the chain complex obtained as follows. $B[U_n]$ is the free (left) R_n–module generated by $\boldsymbol{S}(g)$, and ∂_B is the unique extension of ∂_g to $B[U_n]$ so that ∂_B is an R_n–module homomorphism. We note that $(B[U_n],\partial_B)$ is isomorphic to the chain complex whose group is $B\otimes_{R_{n-1}}R_n$ and whose boundary map is $\partial_B\otimes\mathrm{id}$. $(B[U_n],\partial_B)$ becomes an $(H_1(E(f)),\mathbb{Z})$–bigraded R_n–module chain complex by setting the $H_1(E(f))$–grading of U_n to be $w(\mathrm{X}_{j_1})$ and the $\mathbb{Z}$–grading of U_n to be -2.

Definition 5.6 Let

$$\zeta=\begin{cases}U_n+U_k & \text{if } l=1,\\ U_n & \text{if } l\geq 2,\end{cases}$$

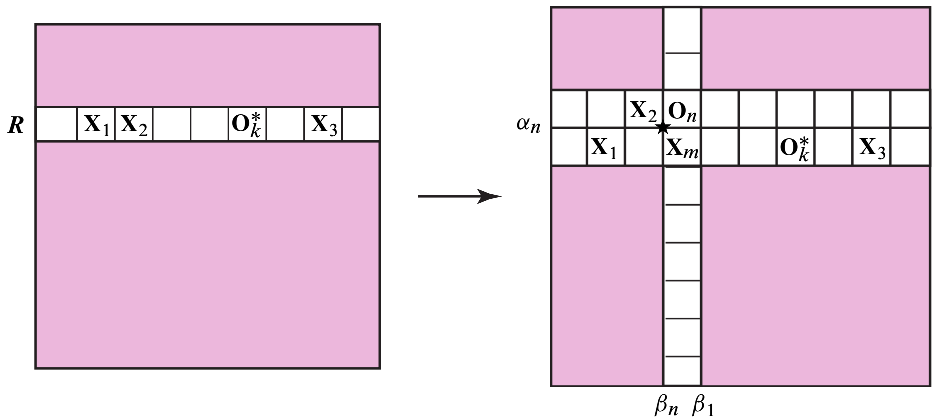

Figure 46: An example of stabilization$'$

so that $\zeta\colon B[U_n] \to B[U_n]$ is a bigraded R_n–module chain map of degree $(-w(\mathrm{O}_n), -2)$. Let (C', ∂') be the mapping cone complex of ζ. Since $(B[U_n], \partial_B)$ is a $(H_1(E(f)), \mathbb{Z})$–bigraded R_n–module chain complexes, the $(\mathrm{cone}(\zeta), \partial')$ is a $(H_1(E(f)), \mathbb{Z})$–bigraded R_n–module chain complex. See page 1490 for the definition of the mapping cone and its grading.

We will first show that C' is quasi-isomorphic to B and then we will show that C is quasi-isomorphic to C'. The first step follows from basic facts from homological algebra. Consider the cokernel of ζ, $B[U_n]/\mathrm{im}(\zeta)$. The $(H_1(E(f)), \mathbb{Z})$–bigrading on $C^-(g)$ descends to a well-defined $(H_1(E(f)), \mathbb{Z})$–bigrading on $B[U_n]/\mathrm{im}(\zeta)$ and so $(B[U_n]/\mathrm{im}(\zeta), \partial_B)$ is an $(H_1(E(f)), \mathbb{Z})$–bigraded R_n–module chain complex. In addition, using the inclusion $R_{n-1} \subset R_n$, it is also naturally an $(H_1(E(f)), \mathbb{Z})$–bigraded R_{n-1}–module chain complex. Moreover the map

$$B \xrightarrow{\cong} B[U_n]/\mathrm{im}(\zeta),$$

which sends $b \in B$ to the equivalence class of itself, is a bigraded R_{n-1}–module chain isomorphism of degree $(0,0)$. Thus, we just need to show that C' is quasi-isomorphic to $B/\mathrm{im}(\zeta)$.

Lemma 5.7 *Let* $\mathrm{pr}\colon B[U_n] \to B[U_n]/\mathrm{im}(\zeta)$ *be the quotient map. The map from* C' *to* $B[U_n]/\mathrm{im}(\zeta)$ *that sends* (a,b) *to* $\mathrm{pr}(b)$ *is a bigraded* R_n*–module quasi-isomorphism of degree* $(0,0)$.

Proof There is a short exact sequence of chain complexes

$$0 \to B[U_n] \xrightarrow{\zeta} B[U_n] \xrightarrow{\mathrm{pr}} B[U_n]/\mathrm{im}(\zeta) \to 0.$$

Therefore, by [23, Section 1.5.8], the map $\mathrm{cone}(\zeta) \to B[U_n]/\mathrm{im}(\zeta)$ sending (a, b) to $\mathrm{pr}(b)$ is a quasi-isomorphism. This map is bigraded of degree $(0, 0)$ and an R_n–module homomorphism. □

We now define a quasi-isomorphism $F\colon C \to C'$ similar to the one in [12]. However, since we are only considering a bigraded chain complex instead of a filtered chain complex and we only need to consider one of the four stabilization′s, our map becomes very simple. We first consider some notation.

Let $\boldsymbol{I} \subset \boldsymbol{S}(\bar{g})$ be the set of $\boldsymbol{x} \in \boldsymbol{S}(\bar{g})$ that contain $\star$: the intersection of the new grid lines/circles α_n and β_n. There is a natural one-to-one correspondence between $\boldsymbol{I}$ and $\boldsymbol{S}(g)$. For $\boldsymbol{x} \in \boldsymbol{S}(g)$ let $\psi(\boldsymbol{x})$ be the point in $\boldsymbol{I}$ defined by $\boldsymbol{x} \cup \star$. Note that if $\boldsymbol{x} \in \boldsymbol{I}$ then $\boldsymbol{x} = \{x_1, x_2, \ldots, x_{n-1}, \star\}$ so $\psi^{-1}(\boldsymbol{x}) = \{x_1, \ldots, x_{n-1}\}$ is the generator of B obtained by removing $\star$. The gradings of $\boldsymbol{x} \in \boldsymbol{S}(g)$ and $\psi(\boldsymbol{x})$ are related as follows:

$$M^g(\boldsymbol{x}) = M^{C'}(\boldsymbol{x}, 0) + 1 = M^{C'}(0, \boldsymbol{x}) = M^{\bar{g}}(\psi(\boldsymbol{x})) + 1, \tag{7}$$

$$A^g(\boldsymbol{x}) = A^{C'}(\boldsymbol{x}, 0) + w(\mathrm{O}_n) = A^{C'}(0, \boldsymbol{x}) = A^{\bar{g}}(\psi(\boldsymbol{x})) - A^{\bar{g}}(\star). \tag{8}$$

Define $F_L\colon C \to B[U_n]$ by

$$F_L(\boldsymbol{x}) = \begin{cases} 0 & \text{if } \boldsymbol{x} \notin \boldsymbol{I} \\ \psi^{-1}(\boldsymbol{x}) & \text{if } \boldsymbol{x} \in \boldsymbol{I} \end{cases}$$

and extend it to C so that it is an R_n–module homomorphism. The reason for this choice of map is that the trivial region is the only type-L region in [12] that doesn't contain X_{j_1} when X_{j_1} is directly to the left of O_n. For the definition of an type-L region, see [12, Definition 3.4 and Figure 13].

There is one type-R region that does not contain X_{j_1}: the rectangle with $\star$ in its upper left corner. For $\boldsymbol{x} \in S(\bar{g})$ and $\boldsymbol{y} \in S(g)$, let $\pi_R(\boldsymbol{x}, \psi(\boldsymbol{y}))$ be the set of $p \in \mathrm{Rect}^o(\boldsymbol{x}, \psi(\boldsymbol{y}))$ whose upper left corner is $\star$; see Figure 47. We will call such a domain an *R–domain*. Define $F_R\colon C \to B[U_n]$ by

$$F_R(\boldsymbol{x}) = \sum_{\boldsymbol{y} \in S(g)} \sum_{\substack{p \in \pi_R(\boldsymbol{x}, \psi(\boldsymbol{y})) \\ (\mathbb{X} \setminus \mathrm{X}_m) \cap \mathrm{Int}(p) = \varnothing}} U_1^{\mathrm{O}_1(p)} \cdots U_{n-1}^{\mathrm{O}_{n-1}(p)} \boldsymbol{y}.$$

Note that we are counting domains in $\bar{g}$ that cannot contain $\mathrm{X}_1, \ldots, \mathrm{X}_{m-1}$ but can contain X_m. Also, there is no factor of U_n in the terms of $F_R(\boldsymbol{x})$. Using these, we define $F\colon C \to C'$ by

$$F(\boldsymbol{x}) = (F_L(\boldsymbol{x}), F_R(\boldsymbol{x})).$$

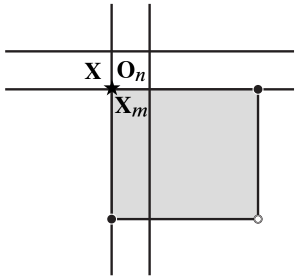

Figure 47: A domain in $\pi_R(\boldsymbol{x}, \psi(\boldsymbol{y}))$; the points of $\boldsymbol{x}$ are in black, the points of $\boldsymbol{y}$ are in white, the domain is shaded

Lemma 5.8 *$F\colon C \to C'$ is a $(H_1(E(f)), \mathbb{Z})$–bigraded R_n–module chain map of degree $(-w(\mathrm{X}_m) - A^{\bar{g}}(\star), 0)$.*

Proof F is an R_n–module homomorphism by definition. It follows from [12, Lemma 3.5] that the Maslov grading is preserved.

***F* is an $H_1(E(f))$–graded map of degree $-A^{\bar{g}}(\star) - w(\mathrm{O}_n)$** Let $\boldsymbol{x} \in \boldsymbol{S}(\bar{g})$. We first consider the grading of $(F_L(\boldsymbol{x}), 0)$. $F_L(\boldsymbol{x})$ is either 0 or is $\psi^{-1}(\boldsymbol{x})$. Suppose $F_L(\boldsymbol{x}) \neq 0$. Then $F_L(\boldsymbol{x}) = \psi^{-1}(\boldsymbol{x})$, so by (8),

$$A^{C'}(F_L(\boldsymbol{x}), 0) = A^{g}(\psi^{-1}(\boldsymbol{x})) - w(\mathrm{O}_n) = A^{\bar{g}}(\boldsymbol{x}) - A^{\bar{g}}(\star) - w(\mathrm{O}_n).$$

We now consider the grading of $(0, F_R(\boldsymbol{x}))$. Let $U_1^{\mathrm{O}_1(p)} \cdots U_{n-1}^{\mathrm{O}_{n-1}(p)} \boldsymbol{y}$ be a term in $F_R(\boldsymbol{x})$. Then p is a rectangle connecting $\boldsymbol{x}$ to $\psi(y)$ that doesn't contain any elements of $\mathbb{X}$ except X_m. Moreover, p does not contain O_n and contains X_m exactly once. So by Lemma 4.13,

$$A^{\bar{g}}(\boldsymbol{x}) - A^{\bar{g}}(\psi(\boldsymbol{y})) = w_{\mathbb{X}}(p) - w_{\mathbb{O}}(p) = w(\mathrm{X}_m) - \sum_{i=1}^{n-1} \mathrm{O}_i(p) w(\mathrm{O}_i).$$

Therefore, by (8), we have

$$\begin{aligned}
A^{C'}(0, U_1^{\mathrm{O}_1(p)} \cdots U_{n-1}^{\mathrm{O}_{n-1}(p)} \boldsymbol{y}) &= A^{C'}(0, \boldsymbol{y}) - \sum_{i=1}^{n-1} \mathrm{O}_i(p) w(\mathrm{O}_i) \\
&= A^{\bar{g}}(\psi(\boldsymbol{y})) - A^{\bar{g}}(\star) - \sum_{i=1}^{n-1} \mathrm{O}_i(p) w(\mathrm{O}_i) \\
&= A^{\bar{g}}(\boldsymbol{x}) - w(\mathrm{X}_m) - A^{\bar{g}}(\star) \\
&= A^{\bar{g}}(\boldsymbol{x}) - w(\mathrm{O}_n) - A^{\bar{g}}(\star).
\end{aligned}$$

***F* is a chain map** Let $\boldsymbol{x} \in \boldsymbol{S}(\bar{g})$. Recall that

$$\partial'(F(\boldsymbol{x})) = (\partial_B(F_L(\boldsymbol{x})), 0) + (0, \zeta(\boldsymbol{x})) + (0, \partial_B(F_R(\boldsymbol{x}))$$

and

$$F(\partial_C(\boldsymbol{x})) = (F_L(\partial_C(\boldsymbol{x})), 0) + (0, F_{\boldsymbol{R}}(\partial_C(\boldsymbol{x})).$$

The proof that F is a chain map is similar to the proof that the commutation$'$ map $\Phi_{\beta,\gamma}$ is a chain map.

For this proof, whenever we have an empty rectangle r in g (contributing to a term in $\partial_{\boldsymbol{B}}$), we will view it as living in $\bar{g}$ in the obvious way. Note that such a rectangle cannot have a boundary on α_n or β_n and hence cannot have $\star$ on its boundary. Usually (in a filtered theory), such a rectangle could contain the point $\star$ in its interior. However, since r cannot contain X_{j_1}, it also cannot contain $\star$ in its interior.

We first show that $\partial_{\boldsymbol{B}}(F_L(\boldsymbol{x})) = F_L(\partial_C(\boldsymbol{x}))$. Suppose D is a domain of the form $p * r$ representing a nontrivial term in $\partial_{\boldsymbol{B}} \circ F_L(\boldsymbol{x})$. Then p is a trivial domain connecting a point in $\boldsymbol{I}$ to itself and r is an empty rectangle in g. We will think of p as a point at $\star$. Since $\star$ cannot be on the corner of r or in its interior, r and p must be disjoint. Suppose D is a domain of the form $r' * p'$ representing a term in $F_L \circ \partial_C(\boldsymbol{x})$. Then p' is a trivial domain connecting a point in $\boldsymbol{I}$ to itself and r is an empty rectangle in $\bar{g}$. Since r' is empty, $\star$ is not in the interior of p'. Since r' cannot contain X_m or X_{j_1}, it cannot have $\star$ as one of its corners. Thus r' and p' are disjoint. Therefore the terms in $(\partial_{\boldsymbol{B}}(F_L(\boldsymbol{x})), 0)$ and $(F_L(\partial_C(\boldsymbol{x})), 0)$ cancel each other out.

We now wish to show that $\partial_{\boldsymbol{B}}(F_{\boldsymbol{R}}(\boldsymbol{x})) + \zeta(\boldsymbol{x}) = F_{\boldsymbol{R}}(\partial_C(\boldsymbol{x})$. Suppose D is a domain of the form $p * r$ representing a nontrivial term in $\partial_{\boldsymbol{B}} \circ F_{\boldsymbol{R}}(\boldsymbol{x})$. Then p is an empty rectangle in $\bar{g}$ with $\star$ on its upper left corner and r is an empty rectangle in g. If p and r share zero corners or share one corner then there is exactly one empty rectangle r' in $\bar{g}$ and R–domain p such that $r' * p'$ gives a decomposition of D (p' and r' will also share zero corners or share one corner). These represent terms in $F_{\boldsymbol{R}} \circ \partial_C(\boldsymbol{x})$. Note that p and r cannot share two or three corners. Conversely, suppose D is a domain of the form $p' * r'$ representing a nontrivial term in $F_{\boldsymbol{R}} \circ \partial_C(\boldsymbol{x})$. Then p' is an empty rectangle in $\bar{g}$ with $\star$ on its upper left corner and r' is an empty rectangle in $\bar{g}$. If p' and r' share no corners or share one corner then there is exactly one other empty rectangle r'' (in g or $\bar{g}$) and R–domain p'' such that $r'' * p''$ or $p'' * r''$ gives a decomposition of D. Here p'' and r'' will also share zero corners or share one corner. These will represent terms in $\partial_{\boldsymbol{B}} \circ F_{\boldsymbol{R}}(\boldsymbol{x})$ or $F_{\boldsymbol{R}} \circ \partial_C(\boldsymbol{x})$. Note that p' and r' cannot share two or three corners. Thus, these terms cancel one another out.

First note that if D is a domain of the form $p * r$ representing a nontrivial term in $\partial_{\boldsymbol{B}} \circ F_{\boldsymbol{R}}(\boldsymbol{x})$, then p and r cannot share more than one corner (hence cannot share four corners). Suppose D is a domain of the form $p' * r'$ representing a nontrivial term in $F_{\boldsymbol{R}} \circ \partial_C(\boldsymbol{x})$ where p' and r' share four corners. Then D is either the width-one horizontal annulus containing X_m or the width-one vertical annulus containing O_n.

The width-one vertical annulus always contributes $U_n\boldsymbol{x}$. If there is more than one element of $\mathbb{X}$ in row $\boldsymbol{R}$ ($l \geq 2$) then the width-one horizontal annulus contains an element of $\mathbb{X}$ that is not X_m, so is not counted. If there is exactly one element of $\mathbb{X}$ in row $\boldsymbol{R}$ ($l = 1$) then the width-one horizontal annulus containing X_m contributes $U_k\boldsymbol{x}$. Thus these terms cancel with $\zeta(\boldsymbol{x})$. □

To show that F is a quasi-isomorphism, we will first show that $\widetilde{F}\colon \widetilde{C} \to \widetilde{C}'$ is a quasi-isomorphism, where $\widetilde{C}$ is the quotient $C/\mathcal{U}_n$ defined in Section 4.4. To do this, we introduce a filtration on $\widetilde{C}$ and $\widetilde{C}'$ so that $\widetilde{F}$ is a filtered map, and show $\widetilde{F}$ induces a quasi-isomorphism on its associated graded object. The rest of the proof will follow from the following well-known lemma.

Lemma 5.9 [14, Theorem 3.2] *Suppose that $F\colon C \to C'$ is a filtered chain map that induces an isomorphism on the homology of the associated graded object. Then F is a filtered quasi-isomorphism.*

The definition of the filtration and the proof that $\widetilde{F}$ induces a quasi-isomorphism on its associated graded object is essentially the same as in [12]. However, there is a small mistake in their definition of the filtration which we fix. We also give more details which we believe clarifies their proof.

For any $\mathbb{F}[U_1,\ldots,U_n]$–module chain complex (C,∂), one can define the chain complex $(\widetilde{C},\widetilde{\partial})$ like we did in Section 4.4. Let $\mathcal{U}_V$ be the $\mathbb{F}$–vector subspace of C spanned by $U_1C \cup \cdots \cup U_nC$. Define $\widetilde{C}$ to be the quotient $C/\mathcal{U}_n$. Since $\partial^-(\mathcal{U}_n) \subset \mathcal{U}_n$, it follows that ∂ descends to a linear map

$$\widetilde{\partial}\colon \widetilde{C} \to \widetilde{C}$$

of vector spaces over $\mathbb{F}$.

Define the Q–filtration $\mathcal{F}_k^Q(C)$ on (C,∂_C), where $C = C^-(g)$, as follows. Let Q be the collection of $(n-1)^2$ dots in $\bar{g}$, with one dot placed in each square which does not appear in the row or column containing O_n. For a domain $p \in \pi(\boldsymbol{x},\boldsymbol{y})$, let $\mathbb{O}(p)$ be the total number of O's in p counted with sign. That is, $\mathbb{O}(p) = \sum_{i=1}^n \mathrm{O}_i(p)$. Similarly, we define $Q(p)$ to be the total number of dots in p counted with sign. Here, we are viewing the points in $\mathbb{O}$ and Q as having positive orientation. Note with this convention, if r is a rectangle connecting $\boldsymbol{x}$ to $\boldsymbol{y}$, then $Q(r) \geq 0$ and $\mathbb{O}(r) \geq 0$.

Lemma 5.10 *Let p and p' be domains in $\bar{g}$ connecting $\boldsymbol{x}$ to $\boldsymbol{y}$ such that*

$$\mathrm{O}_n(p) = \mathrm{O}_n(p') = 0 = \mathbb{O}(p) = \mathbb{O}(p').$$

Then $Q(p) = Q(p')$.

Proof For $1 \le i \le n$, let $\boldsymbol{R}_i \in \pi(\boldsymbol{x},\boldsymbol{x})$ (respectively $\mathbb{C}_i$) be the domain that is the positively oriented row (respectively column) contain O_i. Note that $\mathrm{O}_k(\boldsymbol{R}_i) = \mathrm{O}_k(\boldsymbol{C}_i) = \delta_{ik}$. Suppose $p, p' \in \pi(\boldsymbol{x},\boldsymbol{y})$ then p and p' differ by a domain in $\pi(\boldsymbol{x},\boldsymbol{x})$ so that

$$p' = p + \sum_{i=1}^{n} (a_i \boldsymbol{R}_i + b_i \boldsymbol{C}_i). \tag{9}$$

This follows from the fact that the space of domains on the torus of the form $\pi(\boldsymbol{x},\boldsymbol{x})$ is generated by $\boldsymbol{R}_i$ and $\boldsymbol{C}_i$ with the relation that $\sum_{i=1}^{n}(\boldsymbol{R}_i - \boldsymbol{C}_i) = 0$.

Now, we note that $Q(\boldsymbol{R}_i) = Q(\boldsymbol{C}_i) = n-1$ for $i \neq n$ and $Q(\boldsymbol{R}_n) = Q(\boldsymbol{C}_n) = 0$. Thus

$$Q(p') = Q(p) + (n-1)\sum_{i=1}^{n-1}(a_i + b_i).$$

Since $\mathrm{O}_n(p) = \mathrm{O}_n(p') = 0$ by hypothesis, using (9) we get

$$0 = \mathrm{O}_n(p') = \mathrm{O}_n(p) + \mathrm{O}_n\biggl(\sum_{i=1}^{n}(a_i \boldsymbol{R}_i + b_i \boldsymbol{C}_i)\biggr) = a_n + b_n.$$

Similarly since $\mathbb{O}(p) = \mathbb{O}(p') = 0$,

$$0 = \mathbb{O}\biggl(\sum_{i=1}^{n}(a_i \boldsymbol{R}_i + b_i \boldsymbol{C}_i)\biggr) = \sum_{i=1}^{n}(a_i + b_i).$$

Using these three equalities, we have that $Q(p) = Q(p')$. □

Lemma 5.11 *Let $\boldsymbol{x},\boldsymbol{y} \in \boldsymbol{S}(\bar{g})$, then there is a domain $p \in \pi(\boldsymbol{x},\boldsymbol{y})$ with $\mathrm{O}_n(p) = \mathbb{O}(p) = 0$.*

Proof Let $\boldsymbol{x},\boldsymbol{y} \in \boldsymbol{S}(\bar{g})$. First we note that there is domain connecting $\boldsymbol{x}$ to $\boldsymbol{y}$. Since S_n is generated by transpositions, there is a sequence of rectangles connecting $\boldsymbol{x}$ to $\boldsymbol{y}$ (not necessarily empty). The sum of these rectangles is a domain p_0 connecting $\boldsymbol{x}$ to $\boldsymbol{y}$.

Let $m_0 = \mathrm{O}_n(p)$, which is not necessarily zero. We replace each rectangle containing O_n with the other rectangle connecting its corners as follows. Let

$$p_1 = p_0 - m_0\biggl(\boldsymbol{R}_n + \sum_{i=1}^{n-1} C_i\biggr).$$

Then p_1 connects $\boldsymbol{x}$ to $\boldsymbol{y}$ since $\boldsymbol{R}_n + \sum_{i=1}^{n-1} \boldsymbol{C}_i$ is periodic. Moreover, we have $\mathrm{O}_n(\boldsymbol{R}_n + \sum_{i=1}^{n-1} \boldsymbol{C}_i) = 1$ so that $\mathrm{O}_n(p_1) = 0$. (We could also let $p_1 = p_0 - m_0 \boldsymbol{R}_n$ or $p_1 = p_0 - m_0 \boldsymbol{C}_n$.) Now let $m_1 = \mathbb{O}(p_1)$ and define $p_2 = p_1 - m_1 \boldsymbol{R}_1$. Then p_2 connects $\boldsymbol{x}$ to $\boldsymbol{y}$ and as $\mathrm{O}_n(\boldsymbol{R}_1) = 0$ and $\mathbb{O}(\boldsymbol{R}_1) = 1$, $\mathrm{O}_n(p_2) = \mathbb{O}(p_2) = 0$. □

We use this to define a function $\boldsymbol{F}^Q \colon \boldsymbol{S}(\bar{g}) \to \mathbb{Z}$ by first defining $\boldsymbol{F}^Q(\boldsymbol{x}_0) = 0$, where $\boldsymbol{x}_0$ is the lower left corner of the O's. (It doesn't really matter what value we choose.) Then for $\boldsymbol{x} \in \boldsymbol{S}(\bar{g})$, use Lemma 5.11 to pick a domain $p_{\boldsymbol{x}}$ connecting $\boldsymbol{x}$ to $\boldsymbol{x}_0$ with $\mathrm{O}_n(p_{\boldsymbol{x}}) = \mathbb{O}(p_{\boldsymbol{x}}) = 0$. Define

$$\boldsymbol{F}^Q(\boldsymbol{x}) = \boldsymbol{F}^Q(x_0) + Q(p_{\boldsymbol{x}}) = Q(p_{\boldsymbol{x}}).$$

This is well defined by Lemma 5.10.

Lemma 5.12 *Suppose that $\boldsymbol{x}, \boldsymbol{y} \in \boldsymbol{S}(\bar{g})$ and p is any domain connecting $\boldsymbol{x}$ to $\boldsymbol{y}$ with $\mathrm{O}_n(p) = \mathbb{O}(p) = 0$. Then*

$$\boldsymbol{F}^Q(\boldsymbol{x}) - \boldsymbol{F}^Q(\boldsymbol{y}) = Q(p).$$

Proof Let $p_{\boldsymbol{x}}$ be a domain connecting $\boldsymbol{x}$ to $\boldsymbol{x}_0$ with $\mathrm{O}_n(p_{\boldsymbol{x}}) = \mathbb{O}(p_{\boldsymbol{x}}) = 0$. Define $p_{\boldsymbol{y}}$ similarly. Then $p_{\boldsymbol{x}} - p_{\boldsymbol{y}}$ is a domain connecting $\boldsymbol{x}$ to $\boldsymbol{y}$ with $\mathrm{O}_n(p_{\boldsymbol{x}} - p_{\boldsymbol{y}}) = \mathbb{O}(p_{\boldsymbol{x}} - p_{\boldsymbol{y}}) = 0$. So by Lemma 5.10, $\boldsymbol{F}^Q(\boldsymbol{x}) - \boldsymbol{F}^Q(\boldsymbol{y}) = Q(p_{\boldsymbol{x}}) - Q(p_{\boldsymbol{y}}) = Q(p_{\boldsymbol{x}} - p_{\boldsymbol{y}}) = Q(p)$. □

We now use $\boldsymbol{F}^Q$ to define the Q–filtration on $\widetilde{C}$ by

$$\mathcal{F}_p^Q(\widetilde{C}) = \Big\{ \sum b(\boldsymbol{x})\boldsymbol{x} \in \widetilde{C} \;\Big|\; \boldsymbol{F}^Q(\boldsymbol{x}) \le p \text{ whenever } b(\boldsymbol{x}) \neq 0 \Big\}.$$

By Lemma 5.12, $\widetilde{\partial}_C \colon \mathcal{F}_p^Q(\widetilde{C}) \to \mathcal{F}_p^Q(\widetilde{C})$ so that $(\widetilde{C}, \widetilde{\partial}_C)$ becomes a $\mathbb{Z}$–filtered chain complex.

Note that we have already shown that F is a $(H_1(E(f)), \mathbb{Z})$–bigraded R_n–module chain map. Thus, the following proposition will complete the proof that two grids that differ by a stabilization$'$ move are quasi-isomorphic as $(H_1(E(f)), \mathbb{Z})$–bigraded R_n–module chain complexes.

Proposition 5.13 *$F \colon C \to C'$ is a quasi-isomorphism.*

Proof Since C' is an R_n–module chain complex, we can consider the chain complex $(\widetilde{C}', \widetilde{\partial}')$ obtained by setting all the U_i equal to zero as explained above, $\widetilde{C}' = C'/\mathcal{U}_n C'$. Since F is an R_n–module homomorphism and a chain map, it descends to a well-defined chain map $\widetilde{F} \colon \widetilde{C} \to \widetilde{C}'$.

Now we can define a Q–filtration on $\widetilde{C}'$ using the Q–filtration on $\widetilde{C}$. Specifically, we define $\boldsymbol{F}^Q\colon \widetilde{B} \to \mathbb{Z}$ by $\boldsymbol{F}^Q(\boldsymbol{x}) = \boldsymbol{F}^Q(\psi(\boldsymbol{x}))$ for all $\boldsymbol{x} \in \boldsymbol{S}(g)$. From this we have

$$\mathcal{F}_p^Q(\widetilde{B}) = \Big\{\sum b(\boldsymbol{x})\boldsymbol{x} \in \widetilde{B} \;\Big|\; \boldsymbol{F}^Q(\boldsymbol{x}) \le p \text{ whenever } b(\boldsymbol{x}) \neq 0\Big\}.$$

One can identify $(\widetilde{C}', \widetilde{\partial}')$ with the mapping cone of $\widetilde{\zeta}\colon \widetilde{B} \to \widetilde{B}$ (this is the direct sum because $\widetilde{\zeta}$ is the zero map). Then we can define the Q–filtration on C' by $\mathcal{F}_p^Q(\widetilde{C}') = \mathcal{F}_p^Q(\widetilde{B}) \oplus \mathcal{F}_p^Q(\widetilde{B})$. It is easy to check that $\widetilde{F}$ preserves this filtration.

Consider the map induced on their associated graded complexes

$$\widetilde{F}_Q\colon \widetilde{C}_Q \to \widetilde{C}'_Q.$$

The first chain complex $\widetilde{C}_Q$ is the $\mathbb{F}$ vector space generated by $\boldsymbol{S}(\bar{g})$ whose boundary map counts rectangles supported in the column and row through O_n that do not contain O_n, X_m or X_{j_1}. Since the column and row through O_n look exactly the same as the column and row through O_1 in [12] (after renumbering), this chain complex is the same as it is for links. In particular, [12, Lemma 3.7] holds in our case. Similarly, like in [12], $\widetilde{C}'_Q$ is the chain complex whose underlying group is $\widetilde{B} \oplus \widetilde{B}$ and whose boundary maps are trivial. Moreover, the map $\widetilde{F}_Q$ is exactly the same as in [12]. Thus, their proof holds in our case to show that $\widetilde{F}_Q$ is a quasi-isomorphism. Now by Lemma 5.9, $\widetilde{F}$ is a quasi-isomorphism.

We remark that one can define a filtration on C so that $(\widetilde{C}, \widetilde{\partial}_C)$ is its associated graded object. Define

$$\mathcal{F}_p^U(C) = \Big\{\sum b(\boldsymbol{x}) U_1^{a_1(\boldsymbol{x})} \cdots U_n^{a_n(\boldsymbol{x})} \boldsymbol{x} \in C \;\Big|\; \sum a_i(\boldsymbol{x}) \ge p \text{ whenever } b(\boldsymbol{x}) \neq 0\Big\}.$$

The boundary preserves the filtration making (C, ∂_C) into a filtered chain complex. We can do the same with B, making (B, ∂_B) into a filtered chain complex. Since ζ is a filtered map, we can define a filtration on the mapping cone as before: $\mathcal{F}_p^U(C') = \mathcal{F}_p^U(B) \oplus \mathcal{F}_p^U(B)$. It is easy to see that F is a filtered map. Moreover, the map on the associated graded objects of C and C' induced by F, $F_U\colon C_U \to C'_U$, can be identified with $\widetilde{F}\colon \widetilde{C} \to \widetilde{C}'$. Since $\widetilde{F}$ is a quasi-isomorphism, so is F_U. Therefore, F is a quasi-isomorphism by Lemma 5.9. □

6 The Alexander polynomial and sutured Floer homology

In this section, we will define the Alexander polynomial of a transverse spatial graph $f\colon G \to S^3$ as a torsion invariant of a balanced sutured manifold associated to f and show that it agrees with the graded Euler characteristic of $\widehat{\mathrm{HFG}}(f)$ (when f is sourceless and sinkless and G has no cut edges). In addition, we will relate the sutured

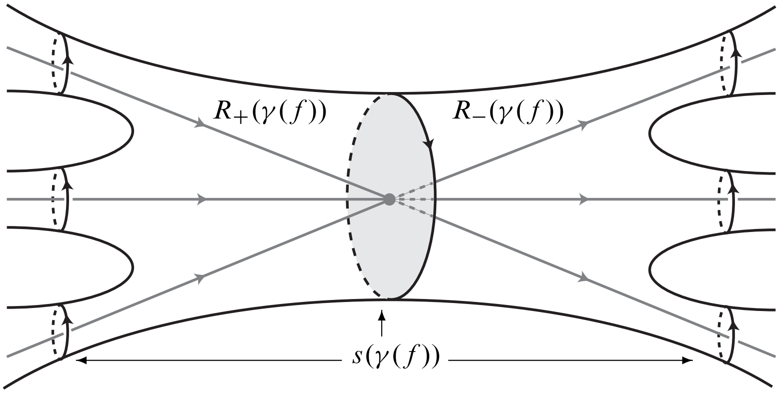

Figure 48: The sutured manifold $(E(f), \gamma(f))$

Floer homology of this balanced sutured manifold to $\widehat{\mathrm{HFG}}(f)$ (when f is sourceless and sinkless and G has no cut edges).

6.1 The Alexander polynomial of a spatial graph

Let $f\colon G \to S^3$ be a transverse spatial graph, and $E(f) = S^3 \setminus N(f(G))$, where $N(f(G))$ is a regular neighborhood of $f(G)$ in S^3. Then $E(f)$ has the structure of a (strongly) balanced sutured manifold $(E(f), \gamma(f))$ which is defined as follows. There will be one suture per edge and one suture per vertex. The suture associated to a vertex is the boundary of the transverse disk at that vertex and the suture associated to an edge is the boundary of a disk transverse to that edge of f. The sutures, denoted by $s(\gamma(f))$, are oriented as shown in Figure 48. This $\gamma(f)$ is a collection of annuli that are small neighborhoods of the sutures in $\partial E(f)$. Recall that $R(\gamma) = \partial E(f) \setminus \mathrm{int}(\gamma)$ is the oriented surface where the orientation of $R(\gamma)$ is such that the induced orientation on each component of $\partial R(\gamma)$ agrees with the orientation of the corresponding suture. Then $R_+(\gamma)$ (respectively $R_-(\gamma)$) is the set of components of $R(\gamma)$ whose normal vectors point out of (respectively into) $E(f)$. Note that $R_+(\gamma)$ is the set of components of $\partial E(f)$ that have the same orientation as $\partial E(f)$. It is easy to check that for each component Σ of $\partial E(f)$, $\chi(\Sigma \cap R_-(\gamma(f))) = \chi(\Sigma \cap R_+(\gamma(f)))$ so that $(E(f), \gamma(f))$ is strongly balanced (in particular, it is balanced). In addition, we note that $\gamma(f)$ contains no toroidal components. Note that we do not need f to be sourceless and sinkless to define this. See [7, Sections 2–3] for the definition of a balanced and strongly balanced sutured manifold.

In [4], S Friedl, A Juhász, and J Rasmussen assign to each balanced sutured manifold (M, γ), a torsion invariant $T(M, \gamma) \in \mathbb{Z}[H_1(M)]$ that is well defined up to $\pm h$ for $h \in H_1(M)$. This invariant is essentially the maximal abelian torsion for the pair

$(M, R_-(\gamma))$. See [4, Sections 3–4] for details. Using their torsion invariant and the sutured manifold associated to a transverse spatial graph defined above, we can define our Alexander polynomial.

Definition 6.1 Let $f\colon G \to S^3$ be a transverse spatial graph. The *(refined) Alexander polynomial* of f, denoted by Δ_f, is defined to be $T(E(f), \gamma(f))$ considered as an element of $\mathbb{Z}[H_1(E(f))]$ modulo units.

Remark 6.2 Others have considered Alexander polynomials of spatial graphs in the past.

(1) The first place this seems to appear is in a 1958 paper by Kinoshita [9]. In this paper, Kinoshita defines the Alexander polynomial of a spatial graph as the Alexander polynomial of its exterior. However, this can be computed using $\pi_1(S^3 \setminus f(G))$ and cannot differentiate between graphs with the same exterior. Our definition depends on more than just the exterior, so it gives more information about the graph than the polynomial defined by Kinoshita.

(2) In 1989, Litherland defined an Alexander polynomial for an embedding of a generalized theta graph that is not determined by its exterior [10]; see also [13]. He considers the Alexander polynomial associated to the torsion free abelian cover of the pair $(S^3 \setminus f(G), R_-)$, where R_- is half of the boundary obtained by cutting open $\partial(S^3 \setminus f(G))$ along the meridians of the edges and throwing away one of the components. We note that, for theta graphs, Litherland's definition and ours are very similar; the main difference is how we decompose $\partial(S^3 \setminus f(G))$. In our case the sutures depend on the orientation of the edges. We note that if all the edges are oriented in the same direction, Δ_f will be zero since $R_-(\gamma)$ will contain a disjoint disk.

(3) If G contains a vertex all of whose edges are incoming or outgoing, then for any transverse spatial graph $f\colon G \to S^3$, $R_-(\gamma)$ will contain a disjoint disk and hence $\Delta_f = 0$.

(4) Like in Litherland's paper, instead of just studying the Alexander polynomial of a transverse spatial graph, one could study the entire Alexander module $\mathbb{Z}[H_1(E(f))]$–module $H_1(E(f), R_-(\gamma(f)))$.

6.2 The sutured Floer homology of a spatial graph

In the preceding subsection, we defined a balanced sutured manifold $(E(f), \gamma(f))$, associated to a transverse spatial graph f. Instead of just considering the torsion of this sutured manifold, we can consider the sutured Floer homology of it. We will describe this in more detail in this subsection. We will also show that this homology theory coincides with our hat theory. We begin with more definitions and background.

X	**O**
O	**X**

Figure 49: A graph grid diagram g for the unknot

Associated to each $n \times n$ graph grid diagram g representing f, there is another sutured manifold $(E(f), \gamma(g))$ which is defined as follows. For each X and O on the torus, remove an (open) disk. Then one obtains an oriented torus with $n+r$ disks removed, where n is the size of the grid and r is the number of X's in the grid; call this surface $\Sigma(g)$. Note that the orientation of the torus comes from the standard counterclockwise orientation of the plane. Recall that the horizontal circles of g are called α_i, the vertical circles are called β_j, $\boldsymbol{\alpha} = \{\alpha_1, \dots, \alpha_n\}$ and $\boldsymbol{\beta} = \{\beta_1, \dots, \beta_n\}$. Thus $(\Sigma(g), \boldsymbol{\alpha}, \boldsymbol{\beta})$ gives a sutured Heegaard decomposition associated to g whose underlying manifold is $E(f)$. Let $(E(f), \gamma(g))$ be the sutured manifold associated to $(\Sigma(g), \boldsymbol{\alpha}, \boldsymbol{\beta})$. Recall that $E(f)$ is obtained by from $(\Sigma(g), \boldsymbol{\alpha}, \boldsymbol{\beta})$ by attaching 3–dimensional 2–handles to $\Sigma(g) \times I$ along the curves $\alpha_i \times \{0\}$ and $\beta_j \times \{1\}$ for $i, j \in \{1, \dots, n\}$. The sutures are defined by taking $s(\gamma(g)) = \partial\Sigma(g) \times \left\{\frac{1}{2}\right\}$ and $\gamma(g) = \partial\Sigma(g) \times I$. Here, we are using the outward normal first convention for the induced orientation on the boundary and we are viewing I with the usual orientation (oriented from 0 to 1). Thus, the induced orientation on the boundary would give $\Sigma(g) \times \{1\}$ the same orientation as $\Sigma(g)$, and $\Sigma(g) \times \{0\}$ the opposite. Note that $(E(f), \gamma(g))$ is a strongly balanced sutured manifold with one suture for each X and O. An example for the trivial knot is shown in Figures 49 and 50. Here, we are viewing one of the O's as being associated with a vertex. In Figure 50, one needs to attach 2–handles to $\alpha_i \times \{0\}$ and $\beta_i \times \{1\}$ to obtain $E(f)$.

The sutured manifold $(E(f), \gamma(g))$ is similar to the sutured manifold $(E(f), \gamma(f))$ except that there are an extra $2n_e$ sutures per edge (all parallel and alternating in orientation), where n_e is the number of O's associated to the edge e (this does not count the O's associated to the vertices at the boundary of the edge). Since $(E(f), \gamma(f))$ and $(E(f), \gamma(g))$ are balanced sutured manifolds, we can consider their sutured Floer homologies

$$\mathrm{SFH}(E(f), \gamma(f)) \quad \text{and} \quad \mathrm{SFH}(E(f), \gamma(g)),$$

respectively. See [6] for the definition of sutured Floer homology. We note that the former group is an invariant of the spatial graph while the latter group $\mathrm{SFH}(E(f), \gamma(g))$ depends on the grid g. Each of these groups has two (relative) gradings, an $H_1(M)$ (or equivalently Spin^c) and a homological grading, which we discuss below.

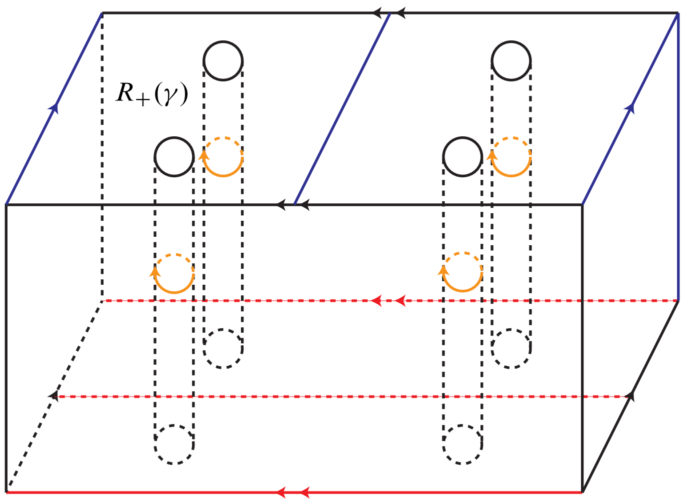

Figure 50: The sutured manifold $(E(f), \gamma(g))$ corresponding to the graph grid diagram g in Figure 49

Let (M, γ) be a balanced sutured manifold. We first discuss the homological grading on $\mathrm{SFH}(M, \gamma)$. Let $(\Sigma, \boldsymbol{\alpha}, \boldsymbol{\beta})$ be a balanced and admissible diagram for (M, γ), where $\boldsymbol{\alpha}$ and $\boldsymbol{\beta}$ each contain d disjointly embedded curves. Admissible means that every nontrivial periodic domain has both positive and negative coefficients. Recall that $\mathrm{SFH}(M, \gamma)$ is defined as the homology of a chain complex $\mathrm{CFH}(\Sigma, \boldsymbol{\alpha}, \boldsymbol{\beta})$ which is an $\mathbb{F}$–vector space and is roughly defined as follows. Consider $\mathbb{T}_{\boldsymbol{\alpha}} = \alpha_1 \times \cdots \times \alpha_d$ and $\mathbb{T}_{\boldsymbol{\beta}} = \beta_1 \times \cdots \times \beta_d$, the d–dimensional tori in $\mathrm{Sym}^d(\Sigma)$. The set of generators of $\mathrm{CFH}(\Sigma, \boldsymbol{\alpha}, \boldsymbol{\beta})$ is $\boldsymbol{x} \in \mathbb{T}_{\boldsymbol{\alpha}} \cap \mathbb{T}_{\boldsymbol{\beta}}$ and the differential is defined by counting rigid holomorphic disks in $\mathrm{Sym}^d(\Sigma)$ connecting two points in $\mathbb{T}_{\boldsymbol{\alpha}} \cap \mathbb{T}_{\boldsymbol{\beta}}$. Choose orientations on $\mathbb{T}_{\boldsymbol{\alpha}}$, $\mathbb{T}_{\boldsymbol{\beta}}$ and $\mathrm{Sym}^d(\Sigma)$, and define $\boldsymbol{m}(\boldsymbol{x})$ to be the intersection sign of $\mathbb{T}_{\boldsymbol{\alpha}}$ and $\mathbb{T}_{\boldsymbol{\beta}}$ in $\mathrm{Sym}^d(\Sigma)$. This depends on the choice of orientations but the difference $\boldsymbol{m}(\boldsymbol{x})\boldsymbol{m}(\boldsymbol{y})^{-1}$ between $\boldsymbol{m}(\boldsymbol{x})$ and $\boldsymbol{m}(\boldsymbol{y})$ is independent of the choice of orientations. So $\boldsymbol{m}$ gives a well-defined relative $\{\pm 1\}$–grading on $\mathrm{CFH}(\Sigma, \boldsymbol{\alpha}, \boldsymbol{\beta})$. Let $\mathbb{Z}_2 = \{0, 1\}$ be the group with 2 elements and let $\exp\colon \mathbb{Z}_2 \to \{\pm 1\}$ be the isomorphism sending l to $(-1)^l$. Using $e\boldsymbol{m} := \exp^{-1} \circ \boldsymbol{m}$ (instead of just $\boldsymbol{m}$), we get a relative $\mathbb{Z}_2$–grading on $\mathrm{CFH}(\Sigma, \boldsymbol{\alpha}, \boldsymbol{\beta})$. Since the parity of the Maslov index of a holomorphic disk connecting $\boldsymbol{x}$ to $\boldsymbol{y}$ is equal to $\exp^{-1}(\boldsymbol{m}(\boldsymbol{x})\boldsymbol{m}(\boldsymbol{y})^{-1})$, the differential reduces the homological grading by $1 \pmod 2$.

We now briefly review the Spin^c–grading. See [7, Section 3] for details. Recall that for any balanced sutured manifold (M, γ), one can define $\mathrm{Spin}^c(M, \gamma)$, the set of Spin^c structures of (M, γ), as the set of homology classes of nowhere-zero vector fields on M that restrict to a special vector field v_0 on ∂M. The vector field v_0 depends on the sutures. One can use obstruction theory to see that $\mathrm{Spin}^c(M, \gamma)$

forms an affine space over $H^2(M, \partial M)$ which we will identify with $H_1(M)$ via the Poincaré duality isomorphism (PD: $H^2(M, \partial M) \to H_1(M)$). Thus, once we pick a fixed $\mathfrak{s}_0 \in \mathrm{Spin}^c(M, \gamma)$, there is a unique bijective correspondence $\xi_{\mathfrak{s}_0}\colon H_1(M) \to \mathrm{Spin}^c(M, \gamma)$, $v \mapsto v + \mathfrak{s}_0$, making $\mathrm{Spin}^c(M, \gamma)$ into an abelian group. Moreover, for any $\mathfrak{s}, \mathfrak{t} \in \mathrm{Spin}^c(M, \gamma)$, there is a well-defined difference, denoted $\mathfrak{s} - \mathfrak{t} \in H_1(M)$, that is defined as the unique element in $H_1(M)$ such that $(\mathfrak{s} - \mathfrak{t}) + \mathfrak{t} = \mathfrak{s}$. Note that the difference does not depend on any choices. Indeed, it is easy to see that for any $\mathfrak{s}_0 \in \mathrm{Spin}^c(M, \gamma)$ and $v, w \in H_1(M)$, $(v + \mathfrak{s}_0) - (w + \mathfrak{s}_0) = v - w$.

To each $\boldsymbol{x} \in \mathbb{T}_{\boldsymbol{\alpha}} \cap \mathbb{T}_{\boldsymbol{\beta}}$, one can assign an element of $\mathrm{Spin}^c(M, \gamma)$, denoted $\mathfrak{s}(\boldsymbol{x})$, making $\mathrm{CFH}(\Sigma, \boldsymbol{\alpha}, \boldsymbol{\beta})$ into a graded vector space over $\mathrm{Spin}^c(M, \gamma)$. The differential on $\mathrm{CFH}(\Sigma, \boldsymbol{\alpha}, \boldsymbol{\beta})$ preserves the $\mathrm{Spin}^c(M, \gamma)$–grading, giving a $\mathrm{Spin}^c(M, \gamma)$–grading to $\mathrm{SFH}(M, \gamma)$. Using the bijection $\xi_{\mathfrak{s}_0}\colon H_1(M) \to \mathrm{Spin}^c(M, \gamma)$ as described above, $\mathrm{SFH}(M, \gamma)$ becomes a relatively graded vector space over $H_1(M)$. We can easily compute the relative grading as follows. Let $\boldsymbol{x}, \boldsymbol{y} \in \mathbb{T}_{\boldsymbol{\alpha}} \cap \mathbb{T}_{\boldsymbol{\beta}}$ and choose paths $a\colon I \to \mathbb{T}_{\boldsymbol{\alpha}}$ and $b\colon I \to \mathbb{T}_{\boldsymbol{\beta}}$ with $\partial a = \partial b = \boldsymbol{y} - \boldsymbol{x}$. Then $a - b$ can be viewed as a 1–cycle in Σ. Using the inclusion map of Σ into M, we can view this as a cycle in M. Let $\varepsilon(\boldsymbol{y}, \boldsymbol{x}) \in H_1(M)$ be the homology class of $a-b$. By [6, Lemma 4.7], $\varepsilon(\boldsymbol{y}, \boldsymbol{x})$ is the relative grading in $H_1(M)$ associated to the $\mathrm{Spin}^c(M)$–grading on (M, γ). That is,

$$\mathfrak{s}(\boldsymbol{y}) - \mathfrak{s}(\boldsymbol{x}) = \varepsilon(\boldsymbol{y}, \boldsymbol{x}). \tag{10}$$

Note that [6] actually says that $\mathrm{PD}(\mathfrak{s}(\boldsymbol{y}) - \mathfrak{s}(\boldsymbol{x})) = \varepsilon(\boldsymbol{y}, \boldsymbol{x})$, but we have already identified $\mathfrak{s}(\boldsymbol{y}) - \mathfrak{s}(\boldsymbol{x})$ with an element of $H_1(M)$ using Poincaré duality. Using the map $(\xi_{\mathfrak{s}_0}^{-1} \circ \mathfrak{s}) \oplus m\colon \mathbb{T}_{\boldsymbol{\alpha}} \cap \mathbb{T}_{\boldsymbol{\beta}} \to H_1(M) \oplus \mathbb{Z}_2$, we see that $\mathrm{CFH}(\Sigma, \boldsymbol{\alpha}, \boldsymbol{\beta})$ is a well-defined relatively $(H_1(M), \mathbb{Z}_2)$–bigraded chain complex and $\mathrm{SFH}(M, \gamma)$ is a well-defined relatively $(H_1(M), \mathbb{Z}_2)$–bigraded $\mathbb{F}$–vector space. Even though $\mathrm{CFH}(\Sigma, \boldsymbol{\alpha}, \boldsymbol{\beta})$ depends on the choice of Heegaard diagram for (M, γ), by [6], the isomorphism class of $\mathrm{SFH}(M, \gamma)$ as a relatively $(H_1(M), \mathbb{Z}_2)$–bigraded vector space only depends on the sutured manifold.

Definition 6.3 For a transverse spatial graph $f\colon G \to S^3$, the *sutured graph Floer homology* is $\mathrm{SFH}(E(f), \gamma(f))$ considered as a relatively $(H_1(E(f)), \mathbb{Z}_2)$–bigraded $\mathbb{F}$–vector space.

Unless otherwise stated, when we refer to $\mathrm{SFH}(E(f), \gamma(f))$ and $\mathrm{SFH}(E(f), \gamma(g))$, we will be considering them as relatively bigraded vector spaces.

6.3 Relating $\widetilde{\mathrm{HFG}}(f)$ and $\mathrm{SFH}(E(f), \gamma(f))$

The main result of this section is that the graph Floer homology of a sinkless and sourceless transverse spatial graph is isomorphic to its sutured Floer homology (after a slight change of the Alexander grading). To prove this, we first notice that the sutured Floer homology of a grid is the same as $\widetilde{\mathrm{HFG}}(g)$. First we need to discuss how the grading is changed.

Let $\mathbb{G}$ be an abelian group and C be a $(\mathbb{G},\mathbb{Z}_2)$–bigraded chain complex or $\mathbb{F}$–vector space with bigrading $C=\bigoplus_{(g,m)\in\mathbb{G}\oplus\mathbb{Z}_2}C_{(g,m)}$. Let $(\mathrm{r}C)_{(g,m)}=C_{(-g,m)}$ for each $g\in\mathbb{G}$ and $m\in\mathbb{Z}_2$. Then C has a $(\mathbb{G},\mathbb{Z}_2)$–bigrading given by $C=\bigoplus_{(g,m)\in\mathbb{G}\oplus\mathbb{Z}_2}(\mathrm{r}C)_{(g,m)}$, which we call the *reverse bigrading* on C. We denote by $\mathrm{r}C$ the underlying vector space C with its reverse bigrading. If C is a chain complex, then $\partial\colon(\mathrm{r}C)_{(g,m)}\to(\mathrm{r}C)_{(g,m-1)}$. So ∂ is a degree $(0,-1)$ map on $\mathrm{r}C$ and $\mathrm{r}C$ is a $(\mathbb{G},\mathbb{Z}_2)$–bigraded chain complex. If C has a relative $(\mathbb{G},\mathbb{Z}_2)$–bigrading then $\mathrm{r}C$ has a well-defined relative $(\mathbb{G},\mathbb{Z}_2)$–bigrading. Note that we are only "reversing" the $\mathbb{G}$–grading.

We note that using the natural projection of $\mathbb{Z}$ to $\mathbb{Z}_2$, $\widehat{\mathrm{HFG}}(f)$, $\widetilde{\mathrm{HFG}}(f)$, $\widehat{\mathrm{HFG}}(g)$ and $\widetilde{\mathrm{HFG}}(g)$ become relatively $(H_1(E(f)),\mathbb{Z}_2)$–bigraded $\mathbb{F}$–vector spaces (similarly for the chain complexes defining them).

Lemma 6.4 *Let $f\colon G\to S^3$ be a sinkless and sourceless transverse spatial graph and g be a graph grid diagram representing f. Then*

$$\widetilde{\mathrm{HFG}}(g)\cong\mathrm{rSHF}(E(f),\gamma(g))$$

as relatively $(H_1(E(f)),\mathbb{Z}_2)$–bigraded $\mathbb{F}$–vector spaces.

Proof Let $(\Sigma(g),\boldsymbol{\alpha},\boldsymbol{\beta})$ be the specific Heegaard decomposition for $E(f)$ associated to the graph grid g as defined beforehand. Both $\mathrm{CFH}(\Sigma(g),\boldsymbol{\alpha},\boldsymbol{\beta})$ and $\widetilde{C}(g)$ are $\mathbb{F}$–vector spaces with the same generating set. One can check that the boundary maps are the same, giving an identification of the two chain complexes. Thus, we just need to compare their (relative) gradings.

Let $\boldsymbol{x}$ and $\boldsymbol{y}$ be generators (in either chain complex). If there is a rectangle connecting $\boldsymbol{x}$ and $\boldsymbol{y}$, then by (1), $M(\boldsymbol{x})-M(\boldsymbol{y})=1\pmod 2$. Moreover, using the definition of $\boldsymbol{m}$ as described in the previous subsection, it is straightforward to check that $\boldsymbol{m}(\boldsymbol{x})\boldsymbol{m}(\boldsymbol{y})^{-1}=-1\in\{\pm1\}$. Now, for any $\boldsymbol{x}$ and $\boldsymbol{y}$, there is a sequence of rectangles $r_1,\dots,r_k$ connecting $\boldsymbol{x}$ and $\boldsymbol{y}$. Thus, $M(\boldsymbol{x})-M(\boldsymbol{y})=k\pmod 2$ and $\boldsymbol{m}(\boldsymbol{x})\boldsymbol{m}(\boldsymbol{y})^{-1}=(-1)^k\in\{\pm1\}$. Hence

$$(-1)^{M(\boldsymbol{x})-M(\boldsymbol{y})}=\boldsymbol{m}(\boldsymbol{x})\boldsymbol{m}(\boldsymbol{y})^{-1}.$$

By Lemma 4.13 and Equation (10), we see that

$$A(\boldsymbol{x})-A(\boldsymbol{y})=\varepsilon(\boldsymbol{y},\boldsymbol{x})=-(\mathfrak{s}(\boldsymbol{x})-\mathfrak{s}(\boldsymbol{y})).\qquad\square$$

Using [7, Proposition 5.4], we can relate $\mathrm{SFH}(E(f),\gamma(f))$ and $\mathrm{SFH}(E(f),\gamma(g))$. For $g\in\mathbb{G}$ and $m\in\mathbb{Z}_2$, let $W(-g,-1)$ (which equals $W(-g,1)$) be the 2–dimensional $(\mathbb{G},\mathbb{Z}_2)$–bigraded vector space over $\mathbb{F}$ spanned by one generator in degree $(0,0)$ and the other in degree $(-g,-1)$. (Note that we are slightly abusing notation since, in Section 4, we defined $W(-g,-1)$ to be the $(\mathbb{G},\mathbb{Z})$–bigraded vector space over $\mathbb{F}$ spanned by one generator in degree $(0,0)$ and the other in degree $(-g,-1)$.) If (C,∂) is a relatively bigraded $(\mathbb{G},\mathbb{Z}_2)$–chain complex over $\mathbb{F}$, then $C\otimes W(-g,-1)$ becomes a relatively bigraded $(\mathbb{G},\mathbb{Z}_2)$ chain complex with boundary $\partial\otimes\mathrm{id}$ in the usual way.

Proposition 6.5 *Let $f\colon G\to S^3$ be a sinkless and sourceless transverse spatial graph and let g be a graph grid diagram representing f. Then*

$$\mathrm{SFH}(E(f),\gamma(g))\cong\mathrm{SFH}(E(f),\gamma(f))\otimes\bigotimes_{e\in E(G)}W(w(e),1)^{\otimes n_e}$$

as relatively $(H_1(E(f)),\mathbb{Z}_2)$–bigraded $\mathbb{F}$–vector spaces, where n_e is the number of O's in g associated to the interior of e (not including the vertices).

Proof Recall that $(E(f),\gamma(g))$ is a sutured manifold with $2n_e+1$ sutures associated to each edge e (n_e sutures are associated to O's on the interior of e and the other n_e+1 sutures are associated to X's on the interior of e). Pick an edge e. If $n_e=0$, leave the sutures on that edge alone. If $n_e\geq 1$, then there are at least three sutures associated to the edge that are parallel and have alternating orientations. Let S be the properly embedded surface in $E(f)$ as pictured in Figure 51 with either orientation. In this figure, the inner annulus is part of the boundary of the neighborhood of the edge of the graph. It contains the three parallel sutures with alternating orientations. Since G is sinkless and sourceless, no component of ∂S will bound a disk in $R(\gamma)$. Thus, one can verify that S is a decomposing surface and hence it defines a sutured manifold decomposition

$$(E(f),\gamma(g))\overset{S}{\rightsquigarrow}(E(f)',\gamma(g)').$$

See [7, Definition 2.5] for the definition of a decomposing surface and a sutured manifold decomposition. The resulting manifold $E(f)'$ is defined as $E(f)\setminus\mathrm{int}(N(S))$, where $N(S)$ is a neighborhood of S in $E(f)$ and hence is homeomorphic to the disjoint union of $E(f)$ and $S^1\times D^2$. To get the sutures on $E(f)\subset E(f)'$, we remove two of the three aforementioned sutures associated to e with opposite orientations. There are four sutures on $S^1\times D^2\subset E(f)'$; they are all parallel to $S^1\times\{p\}$ for $p\in\partial D^2$ and have alternating orientations. Let (M_1,γ_1) be the component of $(E(f)',\gamma(g)')$ with M_1 homeomorphic to $E(f)$ and (M_2,γ_2) be the component of $(E(f)',\gamma(g)')$ with M_2 homeomorphic to $S^1\times D^2$.

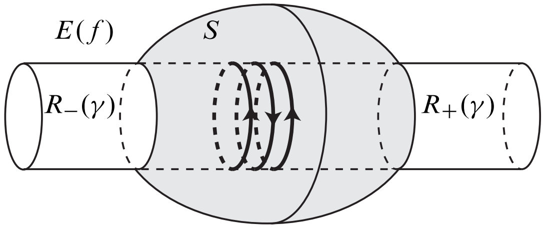

Figure 51: The decomposing surface S (shaded) properly embedded in $E(f)$

Since S is a nice decomposing surface (see [7, Definition 3.22] for the definition of nice), we can use [7, Proposition 5.4] to compute $\mathrm{SFH}(E(f)', \gamma(g)')$. First we need some notation. Let $i\colon E(f)' \to E(f)$ be the inclusion map and $i_*\colon H_1(E(f)') \to H_1(E(f))$ be the induced map on $H_1(-)$. For $\mathfrak{s} \in \mathrm{Spin}^c(E(f), \gamma(g))$, $\mathrm{CFH}(\Sigma, \boldsymbol{\alpha}, \boldsymbol{\beta}, \mathfrak{s})$ is defined as the chain complex generated by $\boldsymbol{x} \in \mathbb{T}_{\boldsymbol{\alpha}} \cap \mathbb{T}_{\boldsymbol{\beta}}$ with $\mathfrak{s}(\boldsymbol{x}) = \mathfrak{s}$, where $(\Sigma, \boldsymbol{\alpha}, \boldsymbol{\beta})$ is a balanced admissible diagram for $(E(f), \gamma(g))$. $\mathrm{SFH}(E(f), \gamma(g), \mathfrak{s})$ is the homology of $\mathrm{CFH}(\Sigma, \boldsymbol{\alpha}, \boldsymbol{\beta}, \mathfrak{s})$ (similarly for $(E(f)', \gamma(g)')$). By [7, Proposition 5.4], there is an affine map

$$f_S\colon \mathrm{Spin}^c(E(f)', \gamma(g)') \to \mathrm{Spin}^c(E(f), \gamma(g))$$

satisfying the following two conditions:

(1) There is an isomorphism

$$\widehat{p}\colon \mathrm{SFH}(E(f)', \gamma(g)') \xrightarrow{\cong} \bigoplus_{\mathfrak{s} \in \mathfrak{I}(f_S)} \mathrm{SFH}(E(f), \gamma(g), \mathfrak{s})$$

such that for every $\mathfrak{s}' \in \mathrm{Spin}^c(E(f)', \gamma(g)')$ we have

$$\widehat{p}(\mathrm{SFH}(E(f)', \gamma(g)', \mathfrak{s}')) \subset \mathrm{SFH}(E(f), \gamma(g), f_S(\mathfrak{s}')).$$

(2) If $\mathfrak{s}_1', \mathfrak{s}_2' \in \mathrm{Spin}^c(E(f)', \gamma(g)')$, then

$$i_*(\mathfrak{s}_1' - \mathfrak{s}_2') = f_S(\mathfrak{s}_1') - f_S(\mathfrak{s}_2') \in H_1(E(f)).$$

Note that in [6], Juhász identifies $\mathrm{Spin}^c(E(f), \gamma(g))$ with $H^2(E(f), \partial E(f))$, so the statement looks slightly different. Since $i_{|M_1}\colon M_1 \to E(f)$ is a homotopy equivalence, $i_*\colon H_1(E(f)') \to H_1(E_f)$ is surjective. Fix an $\mathfrak{s}_0' \in \mathrm{Spin}^c(E(f)', \gamma(g)')$ and let $\mathfrak{s}_0 := f_S(\mathfrak{s}_0')$. Use $\mathfrak{s}_0$ to identify $H_1(E(f))$ and $\mathrm{Spin}^c(E(f), \gamma(g))$. This identifies $v \in H_1(E(f))$ with $v + \mathfrak{s}_0 \in \mathrm{Spin}^c(E(f), \gamma(g))$. Let $\mathfrak{s} \in \mathrm{Spin}^c(E(f), \partial E(f))$. Then $\mathfrak{s} = v + \mathfrak{s}_0$ for some $v \in H_1(E(f))$. Since i_* is surjective, there is a $v' \in H_1(E(f)')$ with $i_*(v') = v$. The second statement above implies that

$$i_*(v') = i_*((v' + \mathfrak{s}_0') - \mathfrak{s}_0') = f_S(v' + \mathfrak{s}_0') - f_S(\mathfrak{s}_0') = f_S(v' + \mathfrak{s}_0') - \mathfrak{s}_0.$$

Therefore, $\mathfrak{s} = v + \mathfrak{s}_0 = i_*(v') + \mathfrak{s}_0 = f_S(v' + \mathfrak{s}_0')$, so f_S is surjective.

Choose an orientation on Σ, α_i and β_j for all i, j. Then we have an absolute $\mathbb{Z}_2$–grading on $\mathrm{SFH}(E(f), \gamma(g))$ given by $\mathrm{e}\boldsymbol{m} = \exp^{-1} \circ \boldsymbol{m}$. It can be shown that, as a relative grading, it agrees with $gr \pmod 2$. For a definition of gr see [6, Definition 8.1]. However, gr is only defined for two generators that have the same Spin^c class. Thus, we will need to consider the proof [7, Proposition 5.4], in order to show that $\mathrm{e}\boldsymbol{m}$ is preserved under $\widehat{p}$. In this proof, he considers a balanced diagram $(\Sigma, \boldsymbol{\alpha}, \boldsymbol{\beta}, P)$ adapted to the surface S in $(E(f), \gamma(g))$. Here $(\Sigma, \boldsymbol{\alpha}, \boldsymbol{\beta})$ is a Heegaard diagram for $(E(f), \gamma(g))$ and $P \subset \Sigma$ is a quasipolygon. Using P, he then constructs a Heegaard diagram $(\Sigma', \boldsymbol{\alpha}', \boldsymbol{\beta}')$ for $(E(f)', \gamma(g)')$ and a map

$$p\colon \Sigma' \to \Sigma$$

such that p sends α_i' to α_i and β_j' to β_j and

$$p_{|\Sigma' \setminus p^{-1}(P)}\colon \Sigma' \setminus p^{-1}(P) \to \Sigma \setminus P$$

is a diffeomorphism. Moreover, since f_S is onto in our case, it follows that all the intersections of α_i and β_j lie in $\Sigma \setminus P$ and all the intersections of α_i' and β_j' lie in $\Sigma' \setminus p^{-1}(P)$. The map p induces a bijection $\widehat{p}\colon \mathbb{T}_{\boldsymbol{\alpha}'} \cap \mathbb{T}_{\boldsymbol{\beta}'} \to \mathbb{T}_{\boldsymbol{\alpha}} \cap \mathbb{T}_{\boldsymbol{\beta}}$. This gives the isomorphism $\widehat{p}\colon \mathrm{SFH}(E(f)', \gamma(g)') \to \mathrm{SFH}(E(f), \gamma(g))$. Choose the orientations of Σ', α_i' and β_j' coming from Σ, α_i and β_j so that p preserves all the orientations. It then follows that if $\boldsymbol{x}' \in \mathbb{T}_{\boldsymbol{\alpha}'} \cap \mathbb{T}_{\boldsymbol{\beta}'}$ then

$$\boldsymbol{m}(\widehat{p}(\boldsymbol{x}')) = \boldsymbol{m}(\boldsymbol{x}'). \tag{11}$$

Using f_S and using the above identification of $H_1(E(f))$ and $\mathrm{Spin}^c(E(f), \gamma(g))$, $\mathrm{SFH}(E(f)', \gamma(g)')$ inherits an $H_1(E(f))$–grading. This makes $\mathrm{SFH}(E(f), \gamma(g))$ and $\mathrm{SFH}(E(f)', \gamma(g)')$ into $(H_1(E(f)), \mathbb{Z}_2)$–bigraded $\mathbb{F}$–vector spaces. We can now show that $\widehat{p}\colon \mathrm{SFH}(E(f)', \gamma(g)') \to \mathrm{SFH}(E(f), \gamma(g))$ is an $(H_1(E(f)), \mathbb{Z}_2)$–bigraded map. Let $x' \in \mathrm{SFH}(E(f)', \gamma(g)')_{(v,i)}$, where $(v, i) \in H_1(E(f)) \oplus \mathbb{Z}_2$. Since

$$f_S(v' + \mathfrak{s}_0') = i_*(v') + \mathfrak{s}_0,$$

x' is in $\mathrm{SFH}(E(f)', \gamma(g)', v' + \mathfrak{s}_0')$ for some $v' \in H_1(E(f)')$ with $i_*(v') = v$. So by [7, Proposition 5.4(1)],

$$\widehat{p}(\mathrm{SFH}(E(f)', \gamma(g)', v' + \mathfrak{s}_0')) \subset \mathrm{SFH}(E(f), \gamma(g), v + \mathfrak{s}_0).$$

Using this and (11), it follows that $\widehat{p}(x') \in \mathrm{SFH}(E(f), \gamma(g))_{(v,i)}$.

We show that

$$\mathrm{SFH}(E(f)', \gamma(g)') \cong \mathrm{SFH}(M_1, \gamma_1) \otimes W(w(e), 1).$$

To see this, note that $(E(f)', \gamma(g'))$ is the disjoint union of (M_1, γ_1) and (M_2, γ_2). Moreover, it is easy to see that

$$\mathrm{SFH}(M_2, \gamma_2) \cong W(e(g), 1)$$

as a relatively $(H_1(E(f)), \mathbb{Z}_2)$–bigraded $\mathbb{F}$–vector space. To complete the proof, we keep removing pairs of sutures on each edge until we are left with $(E(f), \gamma(f))$. □

We can use this to complete the relationship between $\widehat{\mathrm{HFG}}(f)$ and $\mathrm{rSHF}(E(f), \gamma(f))$.

Theorem 6.6 *Let $f\colon G \to S^3$ be a sinkless and sourceless transverse spatial graph where G has no cut edges. Then*

$$\widehat{\mathrm{HFG}}(f) \cong \mathrm{rSHF}(E(f), \gamma(f))$$

as relatively $(H_1(E(f)), \mathbb{Z}_2)$–bigraded $\mathbb{F}$–vector spaces.

Proof Let g be a graph grid diagram representing f. By Proposition 4.32, Lemma 6.4, and Proposition 6.5, we have that

$$\begin{aligned}
\widehat{\mathrm{HFG}}(f) \otimes \bigotimes_{e\in E(G)} W(-w(e), -1)^{\otimes n_e} &\cong \widetilde{\mathrm{HFG}}(g) \\
&\cong \mathrm{rSHF}(E(f), \gamma(g)) \\
&\cong \mathrm{r}\Big(\mathrm{SFH}(E(f), \gamma(f)) \otimes \bigotimes_{e\in E(G)} W(w(e), 1)^{\otimes n_e}\Big) \\
&\cong \mathrm{rSHF}(E(f), \gamma(f)) \otimes \bigotimes_{e\in E(G)} W(-w(e), -1)^{\otimes n_e}
\end{aligned}$$

as relatively $(H_1(E(f)), \mathbb{Z}_2)$–bigraded $\mathbb{F}$–vector spaces.

The result follows from a slight generalization of [22, Lemma 3.18] (replace $\mathbb{Z}^2$ with $H_1(E(f)) \oplus \mathbb{Z}_2 \cong \mathbb{Z}^l \oplus \mathbb{Z}_2$ in the proof) that $\widehat{\mathrm{HFG}}(f) \cong \mathrm{rSHF}(E(f), \gamma(f))$ as relatively $(H_1(E(f)), \mathbb{Z}_2)$–bigraded $\mathbb{F}$–vector spaces. We will sketch of proof of this. Let $V = \bigotimes_{e\in E(G)} W(-w(e), -1)^{\otimes n_e}$. After shifting by an element of $H_1(E(f)) \oplus \mathbb{Z}_2$, we can assume that $\mathrm{rSHF}(E(f), \gamma(f))$ is (absolutely) bigraded and that $\widehat{\mathrm{HFG}}(f) \otimes V \cong \mathrm{rSHF}(E(f), \gamma(f)) \otimes V$ as $(H_1(E(f)), \mathbb{Z}_2)$ (absolutely) bigraded $\mathbb{F}$–vector spaces. Since G has no cut edges, $w(e) \neq 0$ for all $e \in E(G)$.

Suppose $V_1 \otimes W(a, m) \cong V_2 \otimes W(a, m)$ as $(H_1(E(f)), \mathbb{Z}_2)$–bigraded $\mathbb{F}$–vector spaces, where $(a, m) \in H_1(E(f)) \oplus \mathbb{Z}_2$, $a \neq 0$ and V_i is a finitely generated $\mathbb{F}$–vector space. V_i can be represented as a function $f_i\colon H_1(E(f)) \oplus \mathbb{Z}_2 \to \mathbb{Z}_{\geq 0}$, where $f_i(h, n) = \dim_{\mathbb{F}}(V_i)_{(h,n)}$. Since V_i is finitely generated, $f_i(h, n) = 0$ for all but finitely many pairs $(h,n) \in H_1(E(f)) \oplus \mathbb{Z}_2$. Then $V_i \otimes W(h,-1)$ can be represented by the function $g_i\colon H_1(E(f)) \oplus \mathbb{Z}_2 \to \mathbb{Z}_{\geq 0}$ where

$$g_i(h,n) = f_i(h,n) + f_i(h-a,n-m).$$

Since $V_1 \otimes W(a,m) \cong V_2 \otimes W(a,m)$, we have that $g_1 = g_2$. We now note that since $f_i(h,n) = 0$ for all but finitely many pairs (h,n) that $g_i(h,n) = 0$ for all but finitely many pairs. In addition, since $a \neq 0$ and $H_1(E(f)) \cong \mathbb{Z}^l$, $(h-ja,n-jm) \neq (h-j'a,n-j'm)$ whenever $j \neq j'$. Hence $\sum_{j=0}^{\infty} g_i(h-ja,n-jm)$ is a well-defined function and

$$f_i(h,n) = \sum_{j=0}^{\infty} g_i(h-ja,n-jm)$$

for all $(h,n) \in H_1(E(f)) \oplus \mathbb{Z}_2$. Since $g_1 = g_2$, it follows that $f_1 = f_2$ and hence $V_1 \cong V_2$ as $(H_1(E(f)),\mathbb{Z}_2)$–bigraded $\mathbb{F}$–vector spaces. □

As a result we see that the decategorification of $\widehat{\mathrm{HFG}}(f)$ is essentially the torsion invariant $T(E(f),\gamma(f))$ associated to sutured manifold $(E(f),\gamma(f))$.

Definition 6.7 Let $f\colon G \to S^3$ be a sinkless and sourceless transverse spatial graph. Define

$$\chi(\widehat{\mathrm{HFG}}(f)) = \sum_{(h,i)\in(H_1(E(f)),\mathbb{Z})} (-1)^i \operatorname{rank}_{\mathbb{F}} \widehat{\mathrm{HFG}}(f)_{(h,i)} h$$

considered as an element of $\mathbb{Z}[H_1(E(f)]$ modulo positive units; ie as an element of $H_1(E(f))$.

If $r \in \mathbb{Z}[H_1(E(f))]$ then $r = \sum_i a_i h_i$, where $a_i \in \mathbb{Z}$ and $h_i \in H_1(E(f))$. Define $\bar{r} := \sum_i a_i h_i^{-1}$, where here we are viewing $H_1(E(f))$ as a multiplicative group.

Corollary 6.8 *If $f\colon G \to S^3$ is a sinkless and sourceless transverse spatial graph where G has no cut edges then*

$$\chi(\widehat{\mathrm{HFG}}(f)) \doteq \bar{\Delta}_f.$$

That is, they are the same up to multiplication by units in $\mathbb{Z}[H_1(E(f))]$.

Proof Choose an $\mathfrak{s}_0 \in \mathrm{Spin}^c(E(f),\gamma(f))$. By [4, Theorem 1.1], we have that $\chi(\mathrm{SFH}(E(f),\gamma(g))) \doteq \Delta_f$, where

$$\chi(\mathrm{SFH}(E(f),\gamma(g))) = \sum_{\boldsymbol{x}\in\mathbb{T}_{\boldsymbol{\alpha}}\cap\mathbb{T}_{\boldsymbol{\beta}}} \boldsymbol{m}(\boldsymbol{x})\xi_{\mathfrak{s}_0}^{-1}(\mathfrak{s}(\boldsymbol{x}))$$

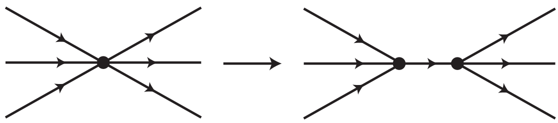

Figure 52: Transverse spatial graph to balanced bipartite graph with balanced orientation

for any admissible balanced Heegaard diagram $(\Sigma, \boldsymbol{\alpha}, \boldsymbol{\beta})$ for $(E(f), \gamma(f))$. By a standard argument,

$$\sum_{\boldsymbol{x} \in \mathbb{T}_{\boldsymbol{\alpha}} \cap \mathbb{T}_{\boldsymbol{\beta}}} \boldsymbol{m}(\boldsymbol{x}) \xi_{\mathfrak{s}_0}^{-1}(\mathfrak{s}(\boldsymbol{x})) = \sum_{(h,i) \in (H_1(E(f)), \mathbb{Z})} (-1)^i \operatorname{rank}_{\mathbb{F}} \widehat{\mathrm{SFH}}(E(f), \gamma(g))_{(h,i)} h.$$

Hence, the result follows from Theorem 6.6. □

We now relate Bao's theory for balanced bipartite spatial graph with balanced orientations to ours. Given a transverse spatial graph, one can get a balanced bipartite spatial graph with balanced orientation by replacing each vertex with an edge; see Figure 52.

Conversely, suppose one has a balanced bipartite spatial graph $F\colon G_{V_1,V_2} \to S^3$ with balanced orientation. This means that $V_1 \cup V_2$ is the set of vertices, $|V_1| = |V_2|$ and each edge connects a vertex in V_1 with one in V_2. Moreover, since this has a balanced orientation, there are precisely $|V_1|$ edges that are oriented from V_1 to V_2, and these edges give a bijection between V_1 and V_2; see [1] for the precise definitions. Thus, we can isotope F so that all of these edges are very short straight arcs like on the right-hand side of Figure 52. We can collapse this edge to obtain a transverse spatial graph. Moreover, Bao constructs a sutured manifold which is the same as $(E(f), \gamma(f))$ for a transverse spatial graph f, and points out in [1, Proposition 4.11] that her hat version is the same as the sutured Floer homology of her sutured manifold. Thus, by Theorem 6.6 and Corollary 6.8, our hat theory (and decategorification) is the same as her hat theory (and decategorification), up to reversing the bigrading, as long as the underlying graph for the transverse graph has no sinks, sources or cut edges.

References

[1] **Y Bao**, *Heegaard Floer homology for embedded bipartite graphs*, preprint (2014) arXiv

[2] **P R Cromwell**, *Embedding knots and links in an open book, I: Basic properties*, Topology Appl. 64 (1995) 37–58 MR

[3] **I A Dynnikov**, *Arc-presentations of links: monotonic simplification*, Fund. Math. 190 (2006) 29–76 MR

[4] **S Friedl**, **A Juhász**, **J Rasmussen**, *The decategorification of sutured Floer homology*, J. Topol. 4 (2011) 431–478 MR

[5] **P Ghiggini**, *Knot Floer homology detects genus-one fibred knots*, Amer. J. Math. 130 (2008) 1151–1169 MR

[6] **A Juhász**, *Holomorphic discs and sutured manifolds*, Algebr. Geom. Topol. 6 (2006) 1429–1457 MR

[7] **A Juhász**, *The sutured Floer homology polytope*, Geom. Topol. 14 (2010) 1303–1354 MR

[8] **L H Kauffman**, *Invariants of graphs in three-space*, Trans. Amer. Math. Soc. 311 (1989) 697–710 MR

[9] **S Kinoshita**, *Alexander polynomials as isotopy invariants, I*, Osaka Math. J. 10 (1958) 263–271 MR

[10] **R Litherland**, *The Alexander module of a knotted theta-curve*, Math. Proc. Cambridge Philos. Soc. 106 (1989) 95–106 MR

[11] **C Manolescu**, **P Ozsváth**, **S Sarkar**, *A combinatorial description of knot Floer homology*, Ann. of Math. 169 (2009) 633–660 MR

[12] **C Manolescu**, **P Ozsváth**, **Z Szabó**, **D Thurston**, *On combinatorial link Floer homology*, Geom. Topol. 11 (2007) 2339–2412 MR

[13] **J McAtee**, **D S Silver**, **S G Williams**, *Coloring spatial graphs*, J. Knot Theory Ramifications 10 (2001) 109–120 MR

[14] **J McCleary**, *User's guide to spectral sequences*, Mathematics Lecture Series 12, Publish or Perish, Wilmington, DE (1985) MR

[15] **Y Ni**, *Link Floer homology detects the Thurston norm*, Geom. Topol. 13 (2009) 2991–3019 MR

[16] **P S Ozsváth**, **A I Stipsicz**, **Z Szabó**, *Grid homology for knots and links*, Mathematical Surveys and Monographs 208, Amer. Math. Soc., Providence, RI (2015) MR

[17] **P Ozsváth**, **Z Szabó**, *Holomorphic disks and genus bounds*, Geom. Topol. 8 (2004) 311–334 MR

[18] **P Ozsváth**, **Z Szabó**, *Holomorphic disks and knot invariants*, Adv. Math. 186 (2004) 58–116 MR

[19] **P Ozsváth**, **Z Szabó**, *Holomorphic disks, link invariants and the multivariable Alexander polynomial*, Algebr. Geom. Topol. 8 (2008) 615–692 MR

[20] **J A Rasmussen**, *Floer homology and knot complements*, PhD thesis, Harvard University (2003) MR Available at `http://search.proquest.com/docview/305332635`

[21] **S Sarkar**, *Grid diagrams and the Ozsváth–Szabó tau-invariant*, Math. Res. Lett. 18 (2011) 1239–1257 MR

[22] **E Tweedy**, *The antidiagonal filtration: reduced theory and applications*, Int. Math. Res. Not. 2015 (2015) 7979–8035 MR

[23] **C A Weibel**, *An introduction to homological algebra*, Cambridge Studies in Advanced Mathematics 38, Cambridge University Press (1994) MR

Department of Mathematics, Rice University
MS 136, PO Box 1892, Houston, TX 77251-1892, United States

Department of Mathematics, Indiana University
Rawles Hall, 831 E 3rd St, Bloomington, IN 47505, United States

shelly@rice.edu, odonnol@indiana.edu

Received: 23 September 2015 Revised: 11 October 2016